PETROLOGY AND STRUCTURE
OF
PRECAMBRIAN GNEISSES AT BIG FALLS,
EAU CLAIRE COUNTY, WISCONSIN

A THESIS
SUBMITTED TO THE FACULTY OF THE GRADUATE SCHOOL
OF THE UNIVERSITY OF MINNESOTA

BY
MICHAEL LEVI CUMMINGS

IN PARTIAL FULFILLMENT OF THE REQUIREMENTS
FOR THE DEGREE OF
MASTER OF SCIENCE

FEBRUARY 1975

Abstract

Precambrian amphibolite gneisses and schists at Big Falls County Park in Eau Claire County, Wisconsin, include four main lithologic units: banded amphibolite gneiss, amphibolite schist, transition gneisses and feldspathic gneiss. Structural and petrologic investigation indicate three deformational phases accompanied by recrystallization.

The first deformational phase is represented by coarse garnet porphyroblasts that were shattered and flattened in the plane of younger schistosity. Rootless intrafolial folds of compositionally banded rocks are relics of this first deformational phase. Inferred medium pressures and temperatures suggest metamorphism in the amphibolite facies.

The second deformational phase resulted in folding of the banded amphibolite gneiss into open folds whose isogon pattern and layer geometry suggest formation as flattened flexural slip folds that were later deformed by inhomogeneous strain. Fold axial plunges are to the north and are coincident with the plunge of the earliest definable lineation. Folds in the amphibolite schist are tight, often isoclinal, isogon patterns suggest formation by inhomogeneous compressive strain.

Mineral lineations cross-cut the south plunging fold axes. Folds in both units developed between subparallel slip planes with folding occurring between the slip surfaces. Faults, with apparent left-lateral displacements, developed in the banded amphibolite gneiss prior to final recrystallization. Garnet, hornblende and plagioclase were the main phases crystallized under medium temperatures and pressures in the amphibolite facies.

The third deformational phase resulted in development of shear zones and cataclastic deformation. A major fault developed between the banded amphibolite gneiss either prior to, or during the third deformational phase. A second schistosity cross-cuts the schistosity formed during the second deformational phase. Crystallization of epidote, cummingtonite, and sphene as well as blue-green hornblende and plagioclase indicate low load pressures and low to medium temperatures. The third recrystallization resulted in disequilibrium textures and incomplete mineral reactions and represents retrograde metamorphism in the epidote-amphibolite facies.

Late faulting and jointing were not accompanied by major recrystallization, however alteration is associated with one of three fault sets.

Whole rock chemical analyses and individual phase chemistry indicate that the amphibolite schist is more magnesian than the banded amphibolite gneiss. High weight percent of Al_2O_3 is typical of the banded amphibolite gneiss and the feldspathic gneiss. The chemistry of the rocks indicate the protolith to be a differentiated mafic intrusive. The banded amphibolite gneiss represents a plagioclase cumulate while the amphibolite schist and feldspathic gneiss represent a gabbro grading to an anorthosite or anorthositic gabbro. Traces of vanadium, nickel and chromium in hornblende further suggest a mafic igneous protolith.

Isotopic age dates on zircons from an intrusion one mile east of Big Falls were 1900 m.y.. The main structural elements of the region are considered coincident with this intrusion. The 1900 m.y. date is interpreted as the age of the second deformation at Big Falls, suggesting intrusion of the Big Falls rocks into the "Chippewa Amphibolite Complex" in early to middle Precambrian time.

Acknowledgments

The author would like to thank Dr. James A. Grant for his guidance in the preparation of materials presented in this study and for serving as advisor and chairman of the author's thesis committee. Dr. Donald M. Davidson Jr. and Dr. James C. Nichol also served on the thesis committee and are acknowledged for their help in this area. Dr. Davidson also contributed to the interpretation of structural data from the area.

Appreciation is extended to Dr. Paul E. Myers at the University of Wisconsin-Eau Claire for his help, encouragement and enthusiasm for the study of the Precambrian in western Wisconsin.

Dr. Paul Weiblen, Mr. Robert Stevenson, and Mr. Klaus Schulz helped in obtaining results from the electron microprobe at the University of Minnesota-Minneapolis.

Mr. Nile Ostenso of Eau Claire, Wisconsin is acknowledged for the air photographs of the Big Falls area used for a base map.

Chemical analyses were made possible by a grant from the Bear Creek Mining Company Ore Discovery Field Research Scholarship.

Twenty five thin sections were purchased by the Department of Geology, University of Minnesota-Duluth for use in this study.

Table of Contents

List of Tables and Figures

Tables

Introduction

Investigation of the Precambrian geology of western Wisconsin has been minimal with many unsolved problems remaining. The present work is an attempt to unravel the geologic history of the Precambrian gneisses exposed at Big Falls County Park in Eau Claire County, with the hope of gaining insight into the geology of the region. In particular, the relation between the deformational and metamorphic histories are considered on the basis of field and petrologic evidence.

Previous Work and Geologic Setting

The earliest work in western Wisconsin was done by the State as part of the Mineral Lands Survey with location of outcrops and dip needle surveys, but no detailed systematic study of the geology. Work in the Big Falls area was started by the author for the Third Annual Wisconsin State University Geologic Field Conference (Cummings, 1971) held at Eau Claire in 1971. At that time, preliminary maps of the western part of the area and general petrologic data was presented. In 1972 a regional mapping and petrologic study of Eau Claire and Chippewa counties was started by Paul Myers and students (In preparation) at the University of Wisconsin-Eau Claire. The deformational history of the Jim Falls area was worked out by Maercklein (1974) as a masters thesis at the University of Wisconsin-Milwaukee. In the Fall of 1974 the 38th Annual Tri-State Geologic Field Conference (Myers et al., 1974) was held at Eau Claire with field trips into the Precambrian, Paleozoic and Pleistocene geology of the region.

The Precambrian gneisses at Big Falls County Park are part of an extensive terrain of amphibolite and biotite amphibolite gneisses and schists associated with granites and granite gneisses. The Precambrian rocks of the region are unconformably overlain by Upper Cambrian sandstones, which in turn are overlain unconformably by unconsolidated till and alluvium of Quaternary Age.

Precambrian Gneisses and Granites

The oldest Precambrian rocks of Eau Claire and Chippewa counties are part of a terrain of considerable extent (figure 1) composed of amphibolitic gneisses and schists (Myers, In preparation). Mineral assemblages commonly found in the amphibolites are plagioclase-hornblende $\pm$ cummingtonite $\pm$ garnet $\pm$ quartz.

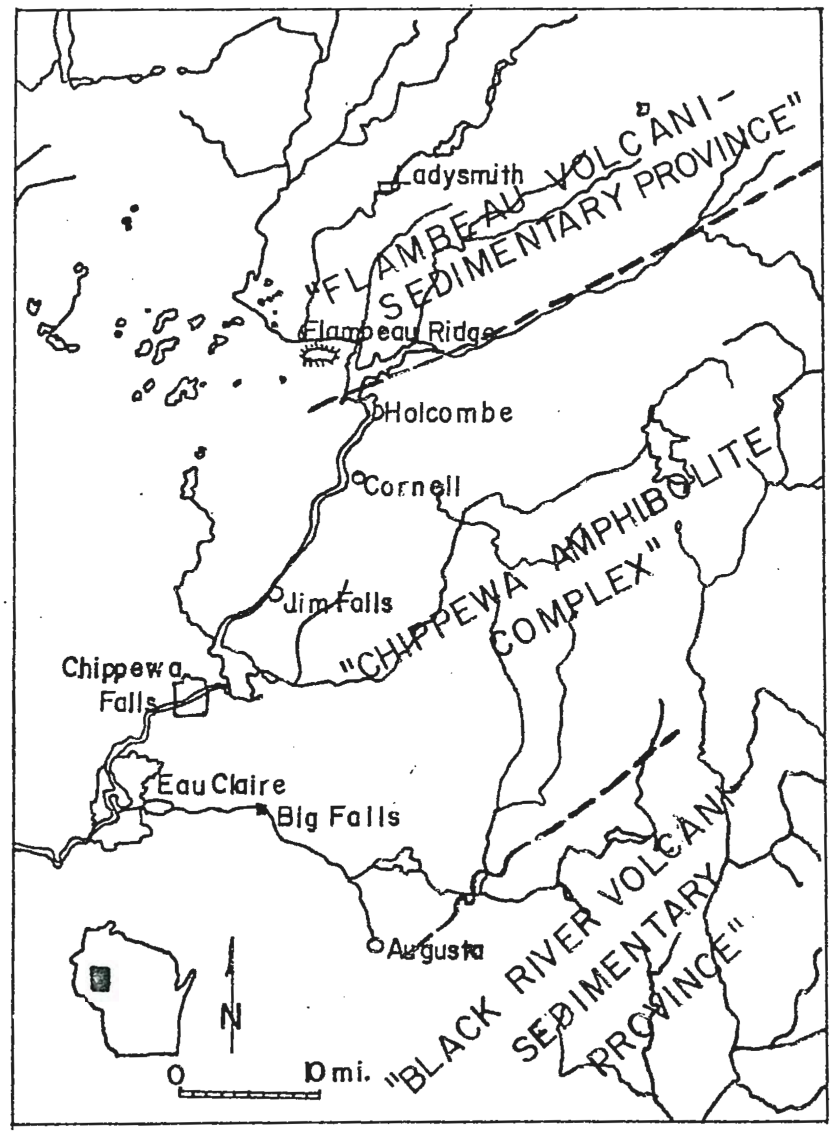

Figure 1: Generalized Geologic Map of Eau Claire and Chippewa Counties.

Well developed compositional layering, schistosity and lineations are locally common. Evidence of shearing, flow-folding and boudinage is typical. Several outcrops have been found with amphibolite rafts in a gabbroic, presumably intrusive, phase, but these rocks have not been studied and present complications in regional interpretation, as well as raise questions as to their significance in relation to Big Falls, as these agmatitic rocks are known to crop out one mile to the east.

Granites of several ages intrude the amphibolites. The granitic intrusives are compositionally variable, and each intrusive event has associated with it, its own set of pegmatitic dikes. Fabric of the granitic rocks ranges from foliated and strongly gneissic to more typical igneous textures, xenoliths of amphibolite are commonly present.

In the south east corner of Eau Claire County and extending into Clark County are tuffaceous metasiltstones, metaconglomerates, schistose greenstones and metatuffs. The relation between the amphibolites and granites and these less intensely deformed rocks is unclear at present. It has been suggested (Myers, oral communication) that the metasediments unconformably overlie the amphibolite terrain and have been infolded into the amphibolites.

The youngest-known Precambrian rocks are mafic plutons and dikes. One of these late unmetamorphosed dikes cuts the exposures at Big Falls County Park.

Structural trends, defined by compositional layering, foliations and lineations, in the amphibolite-granite terrain are northwesterly with variability suggestive of massive flexures.

Precambrian rocks are in sharp angular unconformity with overlying Cambrian sandstones. The contact is marked by the development of a greenish clay representing a paleosol developed before the Cambrian. The green clay is easily spotted in river banks and serves as a good field indicator of the proximity of the Precambrian-Cambrian unconformity. The present topographic surface of eastern Eau Claire County is nearly at the elevation of the unconformity and the green clay horizon is common.

Cambrian Sandstones

By Late Cambrian time the seas had advanced into the Eau Claire-Chippewa County area and deposition of clastic sediments was widespread. The Mount Simon Formation, the basal Upper Cambrian, is essentially unfossiliferous, crossbedded sandstone with a quartz pebble conglomerate at its base. The upper part of the Mount Simon Formation becomes richer in clay and grades conformably into the Eau Claire Formation. The Eau Claire Formation is an argillaceous sandstone that is often fossiliferous. Fossil forms include the inarticulate brachiopods *Lingula* and *Obolella*, the trilobite genera *Cedaria* and *Crepicephalus*, as well as hyolithes, worm burrows and trails.

Quaternary Geology

During the Wisconsin Stage of the Pleistocene Epoch the Chippewa Lobe formed a large moraine and stagnant ice complex near the village of Cornell in Chippewa County. Large outwash plains and valley train spread south into the Eau Claire area forming deposits of sands and gravels that are often well bedded and crossbedded. Rivers throughout the area have cut through the outwash to expose the underlying Precambrian and Cambrian bed-rock.

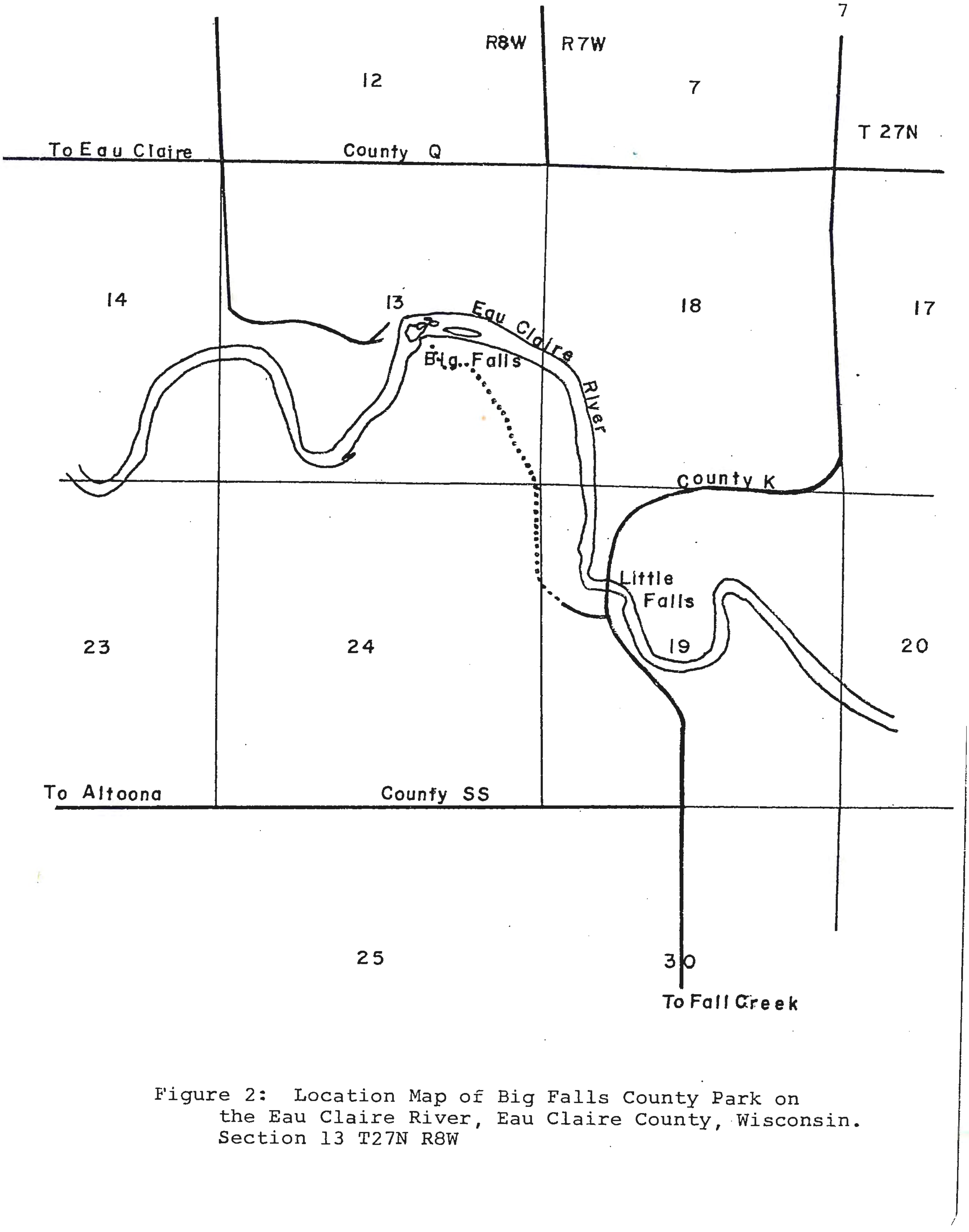

Figure 2: Location Map of Big Falls County Park on the Eau Claire River, Eau Claire County, Wisconsin. Section 13 T27N R8W

Geology of Big Falls County Park

Approximately eight weeks were spent mapping the Precambrian outcrop area during the summer of 1973. Mapping was carried out on scales of 1:30 and 1:60 by use of grid systems set on 5 and 10 feet squares respectively. The sides of the grid squares were oriented north-south and east-west by Brunton compass. The mapped area was tied together by use of low altitude air photographs from which figure 3 was drawn.

Figure 3 is a general geologic map of Big Falls with the location of the various definable geologic units and especially the Precambrian lithologies.

Cambrian Mount Simon Formation crops out along the west bank of the Eau Claire River. The basal Mount Simon is conglomeratic and cross bedded and is separated from the Precambrian by a green clay horizon. The green clays have acted as a slip surface allowing the formation of a large slump area along the west bank. A series of springs have formed along the Precambrian-Cambrian surface. Outwash sands form the east bank and have mixed with recent alluvial materials to form low bars and islands in the river channel.

The Precambrian gneisses and schists are exposed in the river channel and banks with a few scattered

Explanation

Q_{al} Quaternary alluvium

Unconformity

C_{ms} Cambrian Mount Simon Formation

Unconformity

	di	diabase dike
	fg	feldspathic gneiss
PC	tg	transition gneiss
	a	amphibilite schist
	bag	banded amphibolite gneiss

shear zones

contact inferred

fault with apparent sense of displacement

fault inferred

edge of slumped areas

direction of river flow

W1C, W2C, location of whole rock chemical analyses from the banded gneiss.

W-21, W-22, W-31, location of calculated whole rock chemical analyses from the amphibolite schist.

Fig, 22, 23, 24, 25, location of folds shown in these figures.

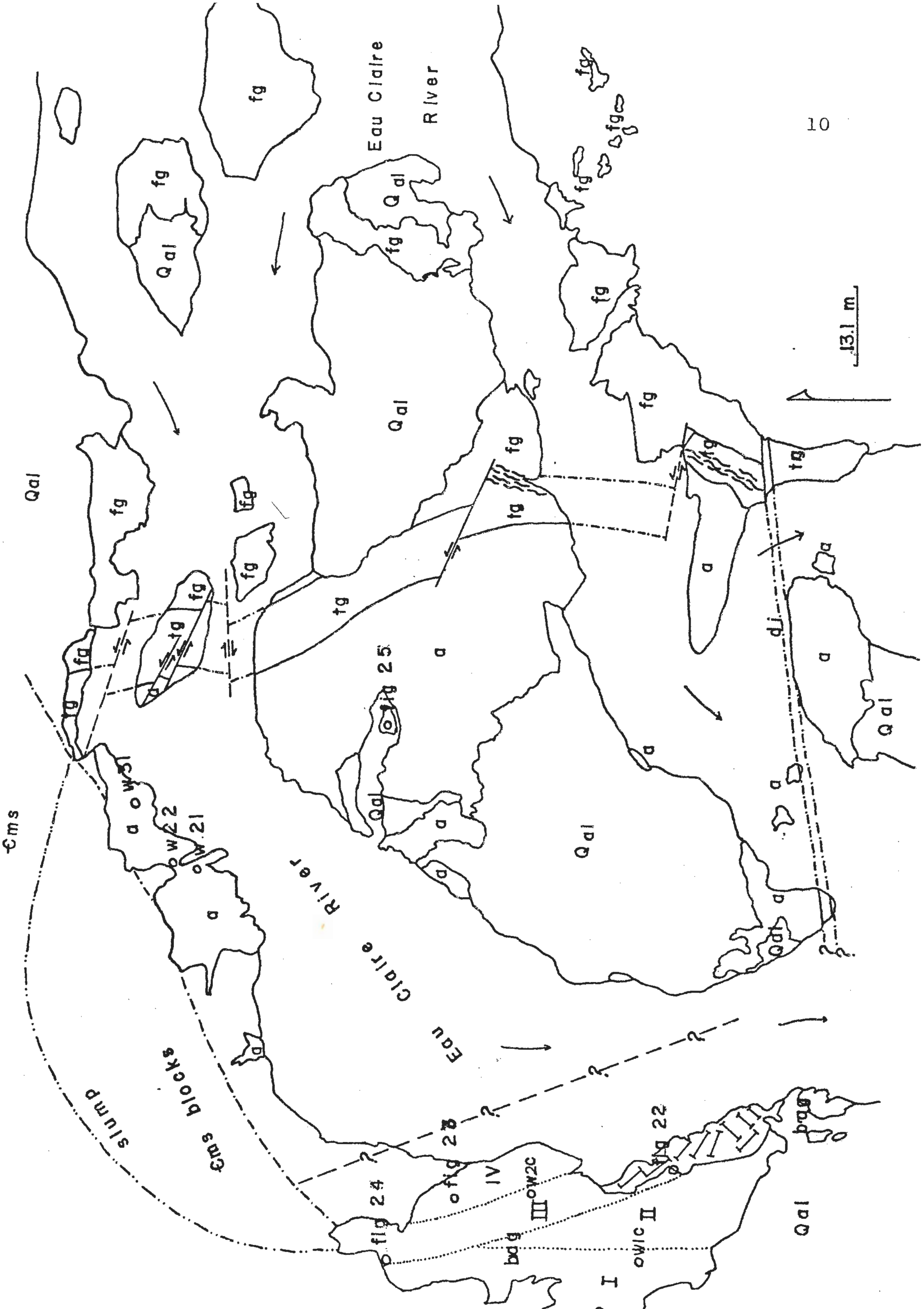

Figure 3: Outcrop geologic map of Big Falls

outcrops to the west. An olivine basalt dike crosses along the southern margin of the area and is lost from view on the west bank of the river. The Precambrian gneisses have been divided into four lithologic units on the basis of field characteristics. The four units are: (1) banded amphibolite gneiss, (2) amphibolite schist, (3) transition gneisses between the amphibolite schist and the feldspathic gneiss, and (4) the feldspathic gneiss.

(1) Banded Amphibolite Gneiss

The banded amphibolite gneiss crops out on the west bank and as scattered outcrops to the west, disappearing under outwash. The main outcrop can be subdivided on the basis of two criteria, 1) the prominence of compositional banding, and 2) the presence or absence of coarse garnet porphyroblasts. On the basis of these criteria four zones are defined as shown on figure 3.

Zone I: moderately well developed compositional banding with disseminated amphiboles, garnet porphyroblasts present. (See figure 5)

Zone II: well defined compositional banding with garnet porphyroblasts. (See figure 4)

Zone III: well defined compositional banding with garnet porphyroblasts absent.

Zone IV: poorly defined compositional banding with a low percentage of amphibole, garnet porphyroblasts absent.

Although the unifying feature of the outcrop is the banded nature of the rock, no single compositional band can be traced the length of the outcrop. Compositional banding may be folded, faulted or irregular in outline with hornblende-rich bands alternating with plagioclase-rich bands containing disseminated hornblende (figure 4). The width of individual hornblende-rich bands ranged from 0.6 cm. to nearly 20 cm. Minor plagioclase is common in hornblende-rich bands. The plagioclase-rich bands with scattered hornblende range from 0.6 cm. to 30 cm. or more. Units I and IV represent the extremes in compositional banding.

Two different sizes of garnet have been observed, 1) large anhedral garnet porphyroblasts and 2) fine euhedral garnets. Large porphyroblastic garnets range from 1.3 cm. to 13 cm. in diameter and are typically elongate parallel to compositional banding with banding foliation wrapped around the porphyroblast (figure 5). Coarse hornblende crystals are intergrown with the fractured garnets. The large garnet porphyroblasts are restricted to Units I and II.

Figure 4: Compositional banding typical of the banded amphibolite gneiss. Note garnet porphyroblasts. Photo taken in Unit II.

Figure 5: Coarse garnet porphyroblast with typical hornblende sheath and wrapped compositional banding. Banded amphibolite gneiss Unit I.

The fine grained euhedral garnets are rare and seem to be associated with narrow shear zones. The crystals are less than 0.3 cm. in diameter (figure 6) and were found only in two samples, one from Unit III and one from Unit IV.

Figure 6: Euhedral garnet porphyroblasts near narrow shear zone - light colored band dipping to the right. Banded amphibolite gneiss Unit III.

Amphibolite Schist

The amphibolite schist forms a band of black rock found on the west bank, island and east bank (see figure 3). Lithological changes are common, especially due to variation in the amount of amphibole in the rock. Hornblende composes 50 to 70 per cent of the rock but may be as high as 95 per cent or nearly absent. The variation is exemplified by a section 42 meters thick of the amphibolite schist as measured and described on the island (Table 1). The percentage of amphibole was estimated in the field but is fairly consistent with results obtained from point counts. Garnet bearing bands usually contain cummingtonite and are distinguished by faint pink weathered surfaces. The garnets form lenticular clusters 0.6 cm. by 0.3 cm. and are wrapped by the compositional foliation, however garnet porphyroblasts 2.5 cm. to 5.0 cm. have been observed. A band, 30 cm. to 60 cm. wide and traceable for most of the outcrop area, is composed of thin plagioclase-rich and hornblende-rich contorted and folded folia with the surrounding rock showing evidence of flowage into areas of irregularity in the band (figure 7). Figure 8 is a map with the location of this band along with other mapable bands that have been correlated across the various river channels. Problems in correlation exist, possibly due to thinning and thickening of units, mesoscopic folding or faulting.

Figure 7: Contorted fine hornblende-rich and plagioclase-rich bands with evidence of flowage of the country rock into areas of irregularity. Strings are part of the grid system used in mapping. Amphibolite schist. Band is 0.3 to 0.6 meters wide.

Table 1: Measured representative section of amphibolite schist from island outcrops. Section measured from west to east.

3.6 meters: Homogeneous to finely banded with 60 percent hornblende, one rootless intrafolial fold.

3.8 meters: Variable lithologies, individual bands 6-20 cms. wide, 20-90 percent hornblende, hornblende-rich clots with coarse grained hornblende, compositional bands are irregular, discontinuous garnet-cummingtonite-hornblende bands.

2.4 meters: 2-5 cm. garnet porphyroblasts scattered in compositionally banded rock with 40-60 percent hornblende.

4.0 meters: Variable lithologies, similar to above, but bands are 16-50 cms. wide.

2.9 meters: Massive, not banded, plagioclase forms isolated spots in 60-70 percent hornblende, some thin feldspathic bands folded into high amplitude fold forms.

2.1 meters: Banded, hornblende 50-60 percent.

9.2 meters: Good compositional foliation with folding common, folds are low amplitude, and short-wave length, plunge to the south.

7.2 meters: Rootless intrafolial folds to high amplitude shear folds in a compositionally foliated rock, amphibole content 50-60 percent, higher in area of shear folds.

2.4 meters: 60 percent hornblende, homogeneous rock with little variation.

1.2 meters: 45-70 percent feldspar and quartz, boudins of high amphibole material.

0.6 meters: Contorted hornblende-rich and plagioclase-rich bands, complexly folded, width of band is irregular.

3.0 meters: Homogeneous with 60 percent hornblende, schistose.

Transition gneisses

Section is 42.4 meters in thickness and includes outcrop bounded by the river on the west and the transition gneisses on the east. The section is faulted and repeated in some areas.

Transition Gneisses

The transition gneisses are located between the amphibolite schist and the feldspathic gneiss (see figure 3). Two distinct rock types comprise the transition gneisses. The rock type immediately next to the amphibolite schist is a lenticular amphibolite gneiss between 2 m. and 2.3 m. wide and is composed of lenticular pods of hornblende and plagioclase (figure 9) associated with fine scale banding produced by tightly folded compositional layers. The second unit of the transition gneisses, a feldspathic amphibolite, is characterized by a higher percentage of plagioclase, 0.2 cm. or less compositional bands of hornblende and plagioclase and silvery gray chlorite.

Feldspathic Gneiss

The feldspathic gneiss is a fine grained gray rock, weathering to buff white, with poorly defined compositional banding. Compositional banding is due to variations in the percentages of hornblende and plagioclase. The grain size of hornblende is not uniform from band to band. The strike of compositional banding lacks consistency and can change markedly near faults. Zones of crushed rock are common and are concordant with the compositional banding and

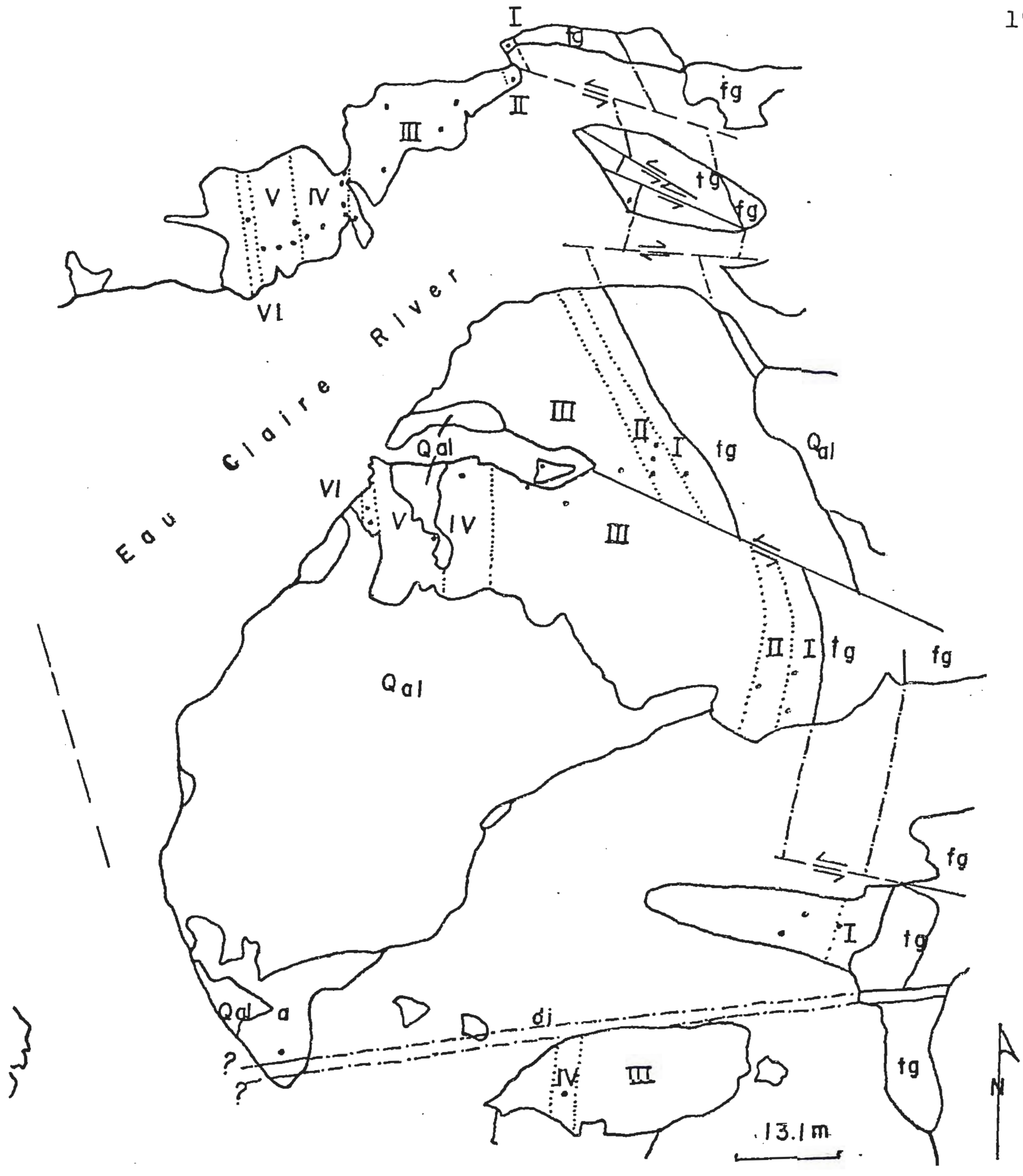

Figure 8: Correlation of zones in the amphibolite schist
Unit I: Homogeneous, 60-70 percent hornblende, schistose.
II: 20-25 percent hornblende, boudins (figure 15), contorted hornblende-rich and plagioclase-rich bands (figure 8)
III: 40-60 percent hornblende, with cummingtonite, folds common.
IV: hornblende-garnet-cummingtonite layers
V: variable lithologies, hornblende from 20 to 90 percent, hornblende-rich clots
VI: coarse garnet porphyroblasts, 60 percent hornblende.

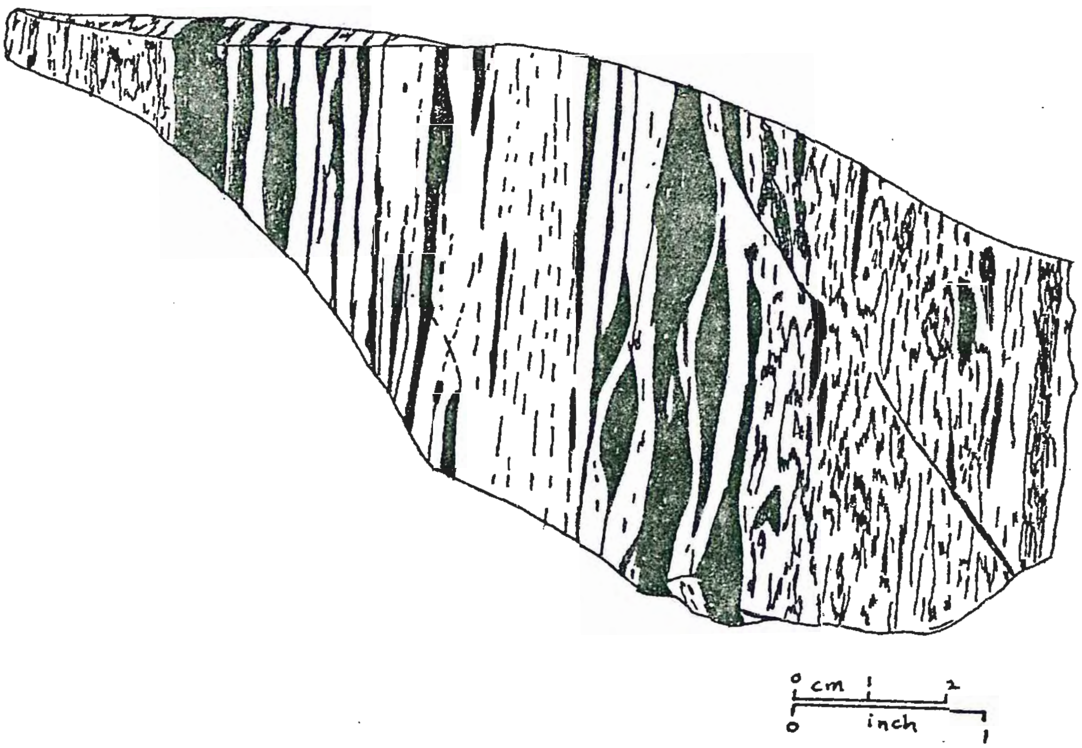

Figure 9: Typical appearance of the lenticular amphibolite gneiss amphibolite schist. Fine compositional banding and lenticular masses of hornblende and plagioclase are common textural features.

are also displaced by faults. Fine shear zones are a common feature along with alteration to epidote and chlorite along fractures. Mapping of the unit was difficult because of the discontinuous and contorted nature of the compositional banding. Correlation from the east bank to the island and the west bank is not possible.

Mesoscopic Structures in Precambrian Units

The structural elements at Big Falls indicate a complicated evolution with several deformational episodes. Structural domains are often small in areal extent or may be as large as the entire area of outcrop. Each of the major structural elements observed in the area will be described for all four lithologic units and then will be considered in terms of their evolutionary sequence.

Continuous Structures: Foliation and Schistosity

Foliation planes in the banded amphibolite gneiss are defined by the hornblende-rich compositional bands which in many cases are folded. The attitude of the foliation surface was measured only where folding had not occurred. The foliation planes are steeply dipping to vertical with an average strike of N 12° W (figure 10).

Schistosity in the amphibolite schist is often well developed and present in most areas of outcrop. Hornblende grains defining the schistosity are oriented in a plane but are not aligned within the plane. Strike of schistosity is between N 8° W and N 24° W with dip of the plane from 75° E to vertical (figure 11). Lineations are often developed when the dip of the schistosity is 75° to 76° E, whereas lineations are absent when the schistosity is vertical. Schistosity cuts compositional foliation where the foliation has been folded.

In the transition gneisses the foliation is defined by compositional banding. The foliation plane is vertical with strike from N 6° W to N 24° W depending on the location of the site of observation with reference to late flexures associated with faulting. The lenticular amphibolite gneiss displays a pattern of lenticular mineral segregations that may represent a recrystallized example of a braided foliation (Weiss, 1972) (see figure 9).

Foliation in the feldspathic sneiss is also defined by compositional banding and is typically vertical with variable strike.

Schistosity is poorly developed in the transition and feldspathic gneisses.

Foliation and schistosity data from the different units indicates considerable agreement, foliation planes dip steeply to vertical and strikes range from N 6° W to N 24° W except in areas disrupted by faulting.

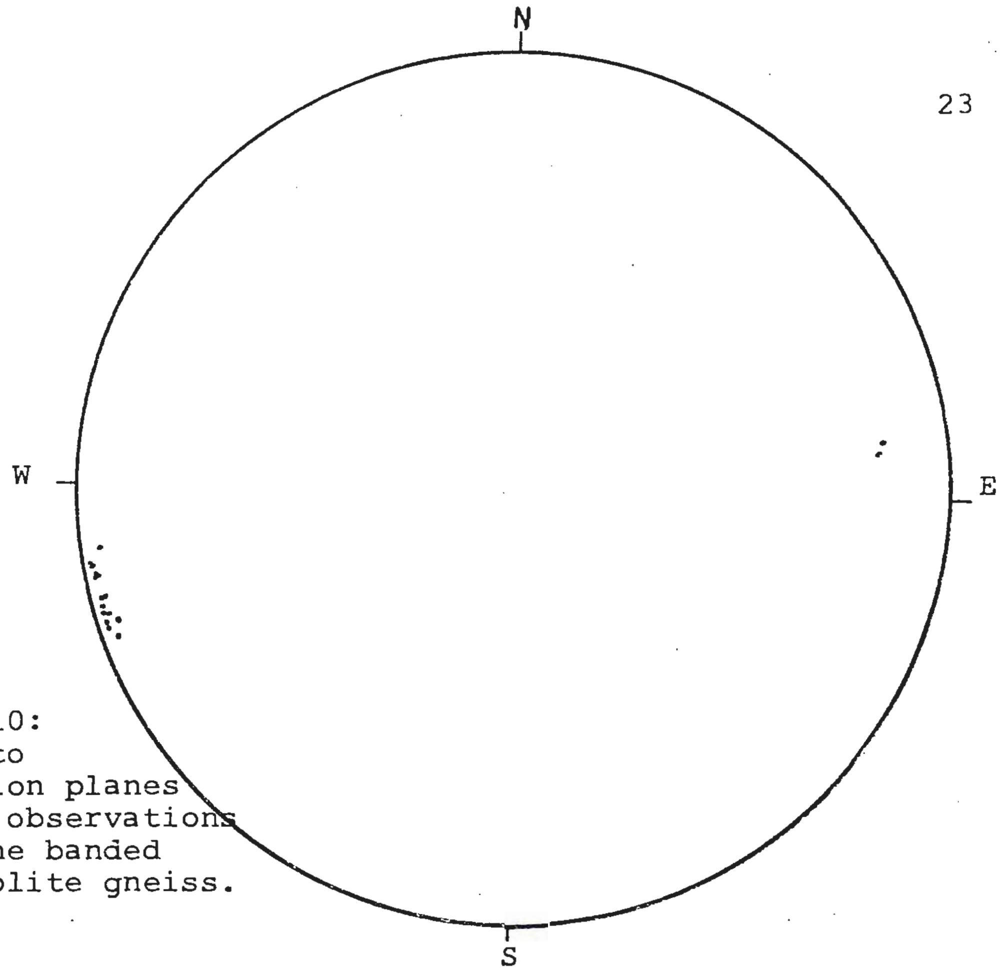

Figure 10:
Poles to
foliation planes
for 17 observations
from the banded
amphibolite gneiss.

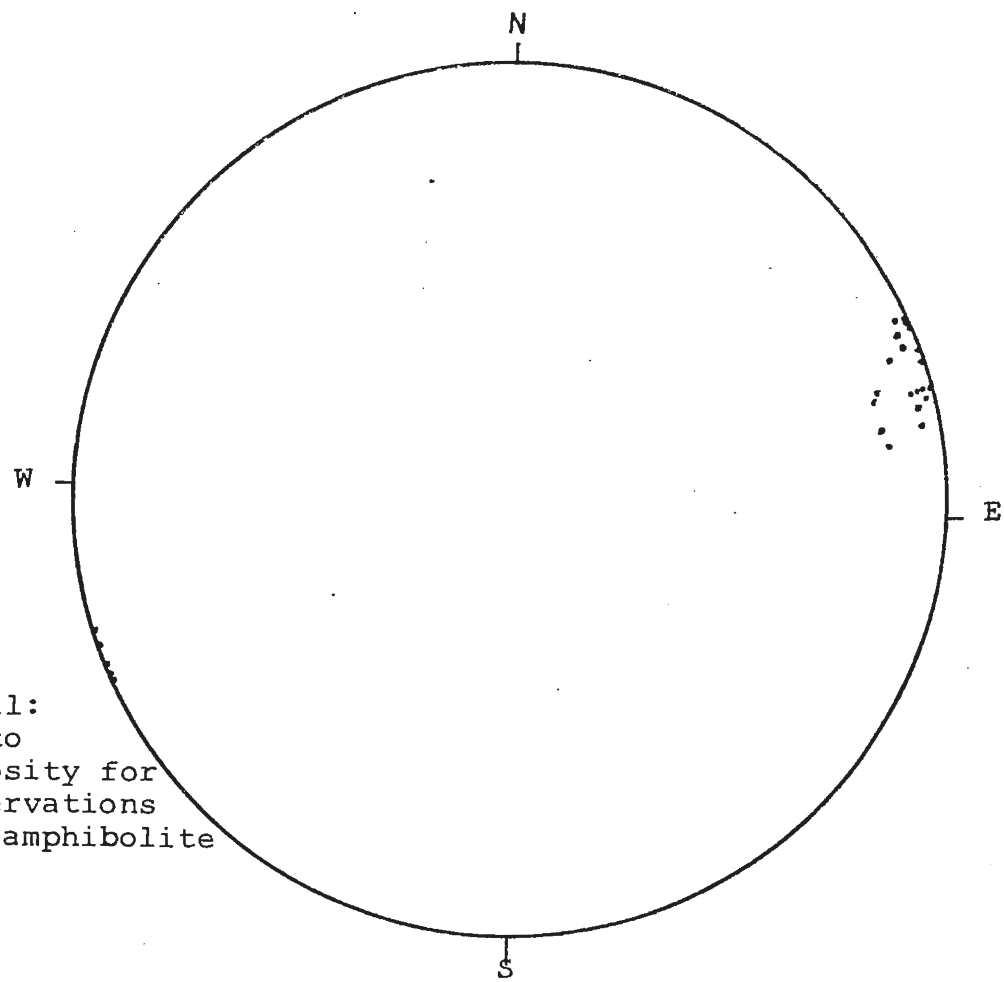

Figure 11:
Poles to
schistosity for
20 observations
in the amphibolite
schist.

In many areas of outcrop a second, less well-developed schistosity may be defined. In outcrop, this schistosity is most easily observed in the feldspathic gneiss and the banded amphibolite gneiss, but is only observable in thin sections of the amphibolite schist. The dip of this schistosity is not known because of difficulty in observing the third dimension in outcrop; the strike of the foliation plane ranges from N 45° W to N 60° W.

Lineations

Lineations were measured in the banded amphibolite gneiss and the amphibolite schist. Lineations are difficult to interpret because of lack of uniformity of development and orientation and uncertainty with regard to the sequence of formation in relation to other structural elements. A girdle is defined by combining lineation data from the two units but its significance is questionable.

Three types of lineations occur in the banded amphibolite gneiss, 1) lineation of coarse hornblende crystals, 2) lineation of fine hornblende crystals, 3) crenulations of the foliation plane and mineral streaking on the foliation plane. All lineations observed in the field lie in the foliation plane. The lineation of coarse hornblende crystals occurs locally and does not represent a pervasive structure. These 1 cm. hornblende grains form a well defined lineation plunging 32° to 48° to the south with one observation dipping south at 85° (figure 12). Lineation of fine-grained hornblende crystals is hard to define in the field and values of plunge are recorded as estimated average plunges. This lineation is the result of a crude orientation of hornblende crystals in the 1-2 mm. size range. The lineation was measured on vertical hornblende-rich compositional bands because the paucity of hornblende grains in plagioclase-rich bands made estimation of plunge impossible. Plunge of the lineation is north at 33° to 55° (figure 12). The third group of lineations occurs as fine crenulations of the foliation surface or as mineral streaking on the foliation plane. Both types plunge north at 16° to 48° and are limited in extent.

Age relations of the three lineations are difficult to determine. Type 1 lineations can be found overprinting type 2 lineations in which case the type 2 lineation may be faint or absent but the grain size is characteristic of type 2. Type 3 lineations warp the foliation plane which contains type 2 size crystals. The relation between type 1 and 3 is not known since they have not been found on the same foliation surface. It would seem that type 2 lineations are oldest with 1 and 3 following in unknown sequence.

Lineations in the amphibolite schist often occur in cummingtonite-bearing rocks and are absent or poorly developed in rocks lacking cummingtonite. Lineations plunge steeply (62° - 77°) to the north (figure 13). The plunge of lineations in the amphibolite schist falls on the girdle defined by lineations in the banded amphibolite gneiss (figure 12), however, as mentioned earlier the lineations observed are probably not of the same age and so the significance of the girdle is questionable.

Boundinage structures are present in the amphibolite schist but with only two dimensional exposure available their exact orientation is not known. The boudins (figure 14) are elongate in the plane of the schistosity with well developed pull-apart structures with flow of the surrounding matrix.

Flinn (1965) pointed out that lineations and schistosity are not independent structures but are one and the same structure. Restriction of freedom of orientation gives rise to schistosity; when the freedom of orientation is equally restricted in all planes normal to the schistosity there is no lineation, only a schistosity. The relation between

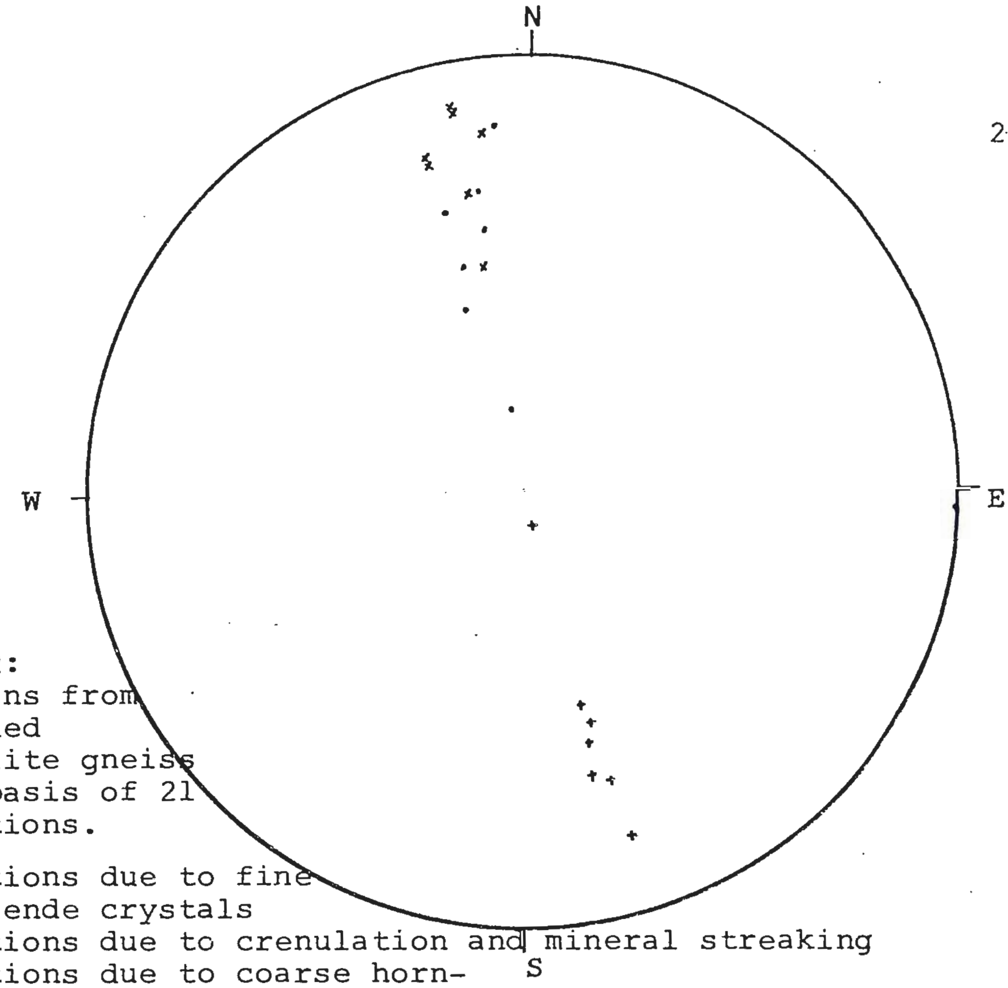

Figure 12:
Lineations from the banded amphibolite gneiss on the basis of 21 observations.

. Lineations due to fine hornblende crystals
x Lineations due to crenulation and mineral streaking
+ Lineations due to coarse horn-blende crystals

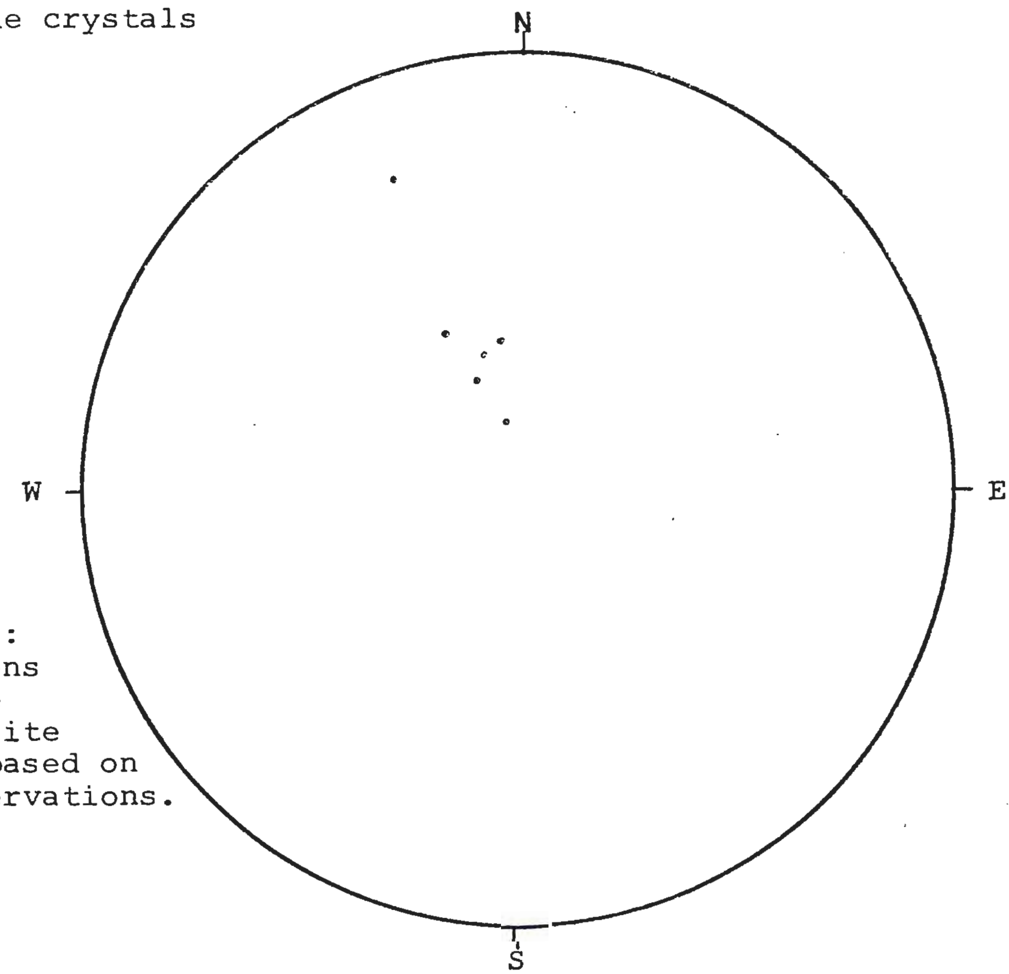

Figure 13:
Lineations from the amphibolite schist based on six observations.

Figure 14: Boudinage in the amphibolite schist.

rocks containing only schistosity and rocks only with lineations is gradational. Flinn stated that the schistosity and lineation may be correlated to two possible orientations of the deformation ellipsoid. Lineation may be oriented parallel to Z of the deformation ellipsoid and the schistosity parallel to YZ, or lineation may be parallel to X and schistosity parallel to XY. In the first case, which is the more commonly accepted view, the tectonite with lineation corresponds to the prolate ellipsoid of deformation.

Folds

Folding of compositional banding is commonly observed in the banded amphibolite gneiss. Eleven folds were exposed so that the axial surface as well as the plunge of the fold axis could be measured with some degree of confidence. Axial plane cleavage or schistosity were not observed in any folds so the axial surface has been arbitrarily selected as the surface bisecting the arc produced by the crest of the folded layer and connecting crests of the various layers in the fold form. Axial surfaces are steeply dipping to vertical with the strike of the axial trace between N 1° W and N 20° W. The plunges of the fold axes are north at 40° to 57°, with one fold plunging 10° north. (figure 15).

Folds characteristically occur in layers bounded by major nonfolded hornblende-rich bands, and are sinistral with the west side of the fold to the south. This typical occurance suggests that the major hornblende-rich bands were deformed by slip parallel to the band while the interlayered plagioclase-rich bands were deformed by folding. The sinistral nature of the folds suggests a left-hand couple across the plagioclase-rich layers.

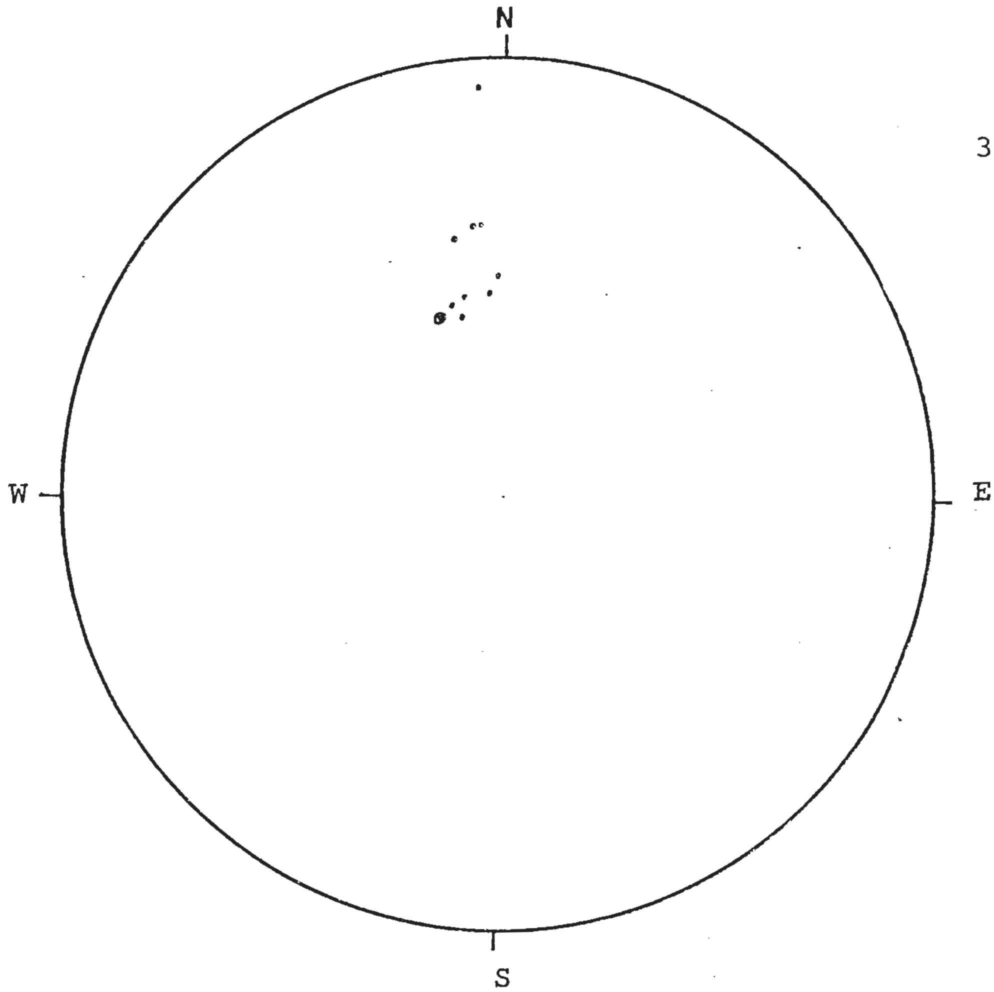

Figure 15: Plunge of fold axes from the banded amphibolite gneiss based on 11 observations.

Folds in the amphibolite schist include, 1) rootless intrafolial folds, 2) folds with sheared axial surfaces, 3) folds without sheared axial surfaces.

Rootless intrafolial folds are common throughout the amphibolite schist. Internal foliation of the folds bears no apparent relation to the external foliation leaving a rootless or "floating" fold surrounded by non-folded rock (figure 16). The folds are elongate in the plane of the schistosity and are cut by the schistosity. Some folds are nearly a meter long and six centimeters wide. Rootless intrafolial folds are tectonic in origin and are one of the criteria presented by Turner and Weiss (1963, p. 117) for recongnizing transposition of an original s-surface.

Figure 16: Rootless intrafolial fold cut by schistosity. Amphibolite schist.

Folds with sheared axial surfaces (figure 17) are not common but some excellent examples have been found. The folded layers are truncated in the hinge region of the fold by a surface of discontinuity. Reesor (1965) in a study of the Valhalla Gneiss complex in British Colombia, described such truncated relationships as occurring by slip planes developing parallel to the axial surface of the fold. As the fold evolves slip is concentrated in certain layers. Movement on such slip planes catches up passive elements of earlier folds or boudins as remnants or "tectonic inclusions" in or between the slip planes.

Folds without sheared axial planes seem to be most strongly developed when the percentage of plagioclase reaches 35 to 40 percent of the rock. Such folds plunge south at 20° to 38° (figure 18) with axial surfaces which strike N 9° W to N 18° W dipping 72° E to 86° W (figure 19). Two folds were found on the west bank with aberrant axial plunges to the north at 12° and 20° with the strike of the axial surface N 21° W (figure 18). The style of folding is similar to the style observed in the banded amphibolite gneiss, with movement along specific zones resulting in isoclinal folding. The strike of axial surfaces in the amphibolite schist and the banded amphibolite schist are quite similar, but the plunge of the fold axes are in opposite directions.

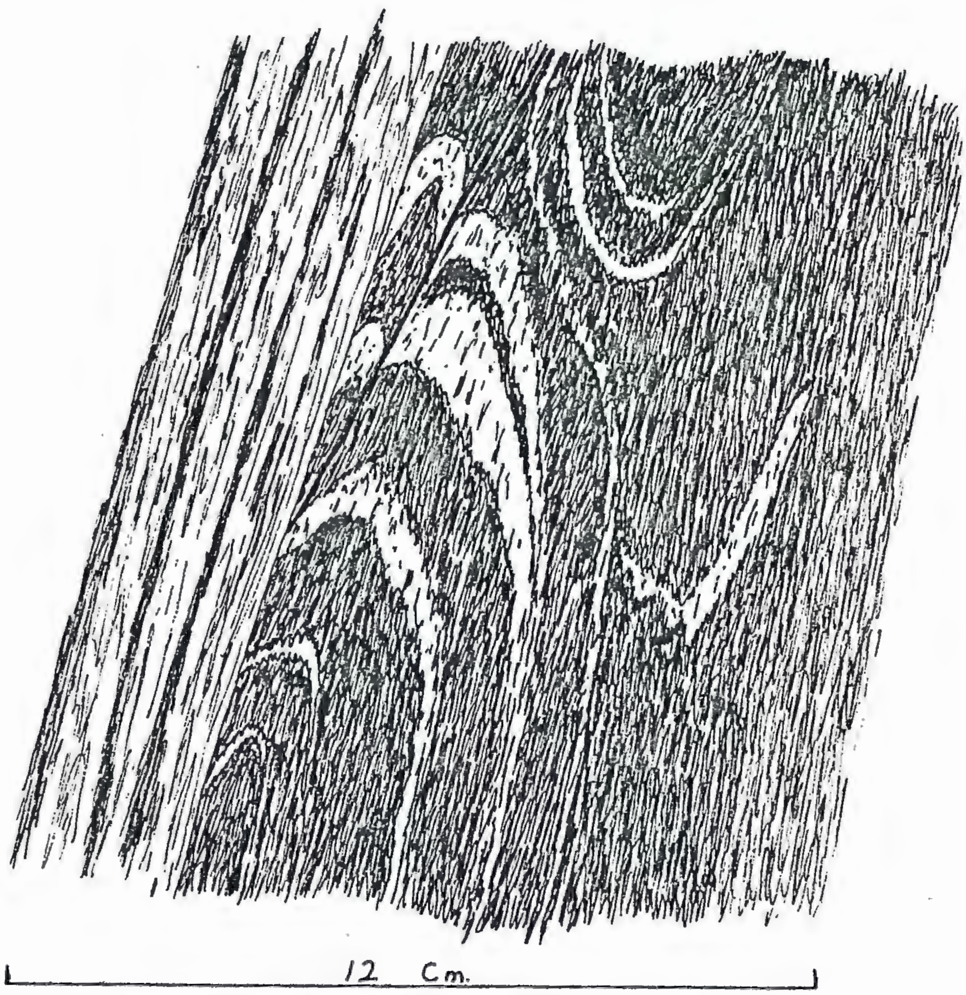

Figure 17: Fold with sheared axial surface. Amphibolite schist.

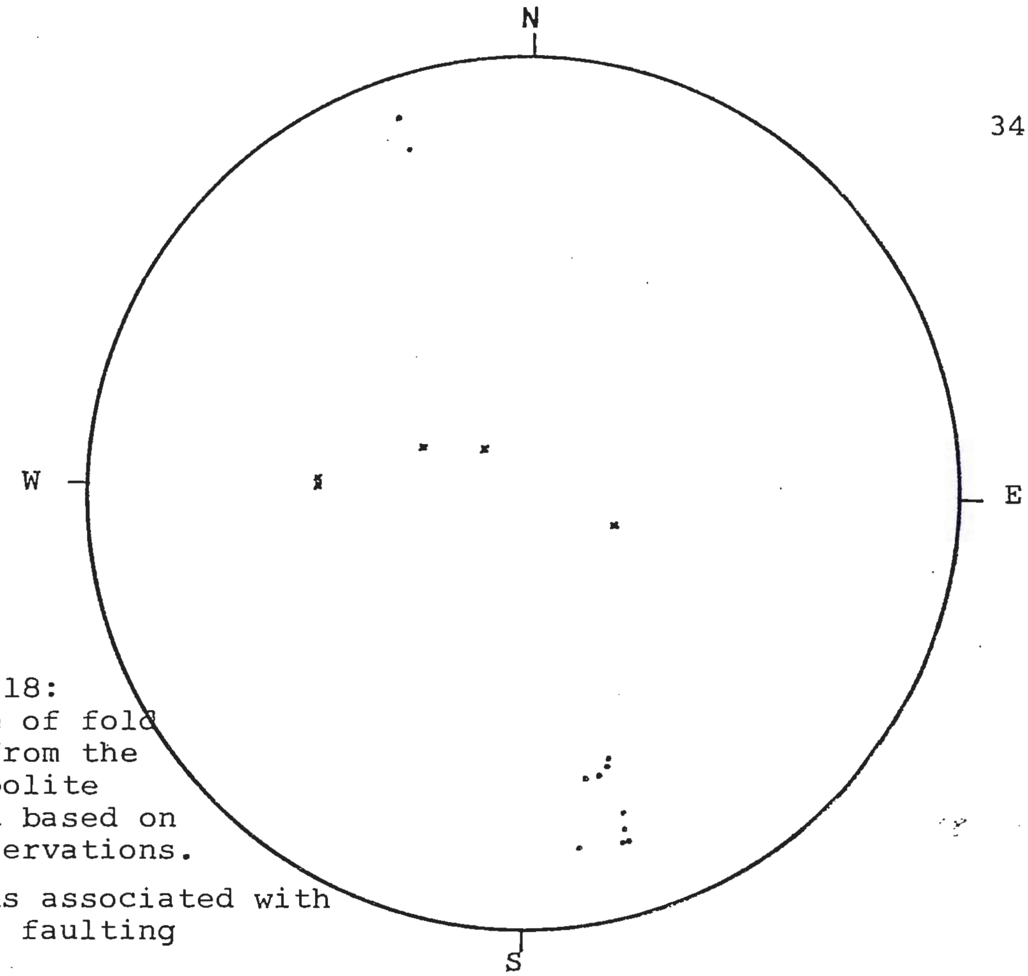

Figure 18:
Plunge of fold axes from the amphibolite schist based on 16 observations.

x folds associated with late faulting

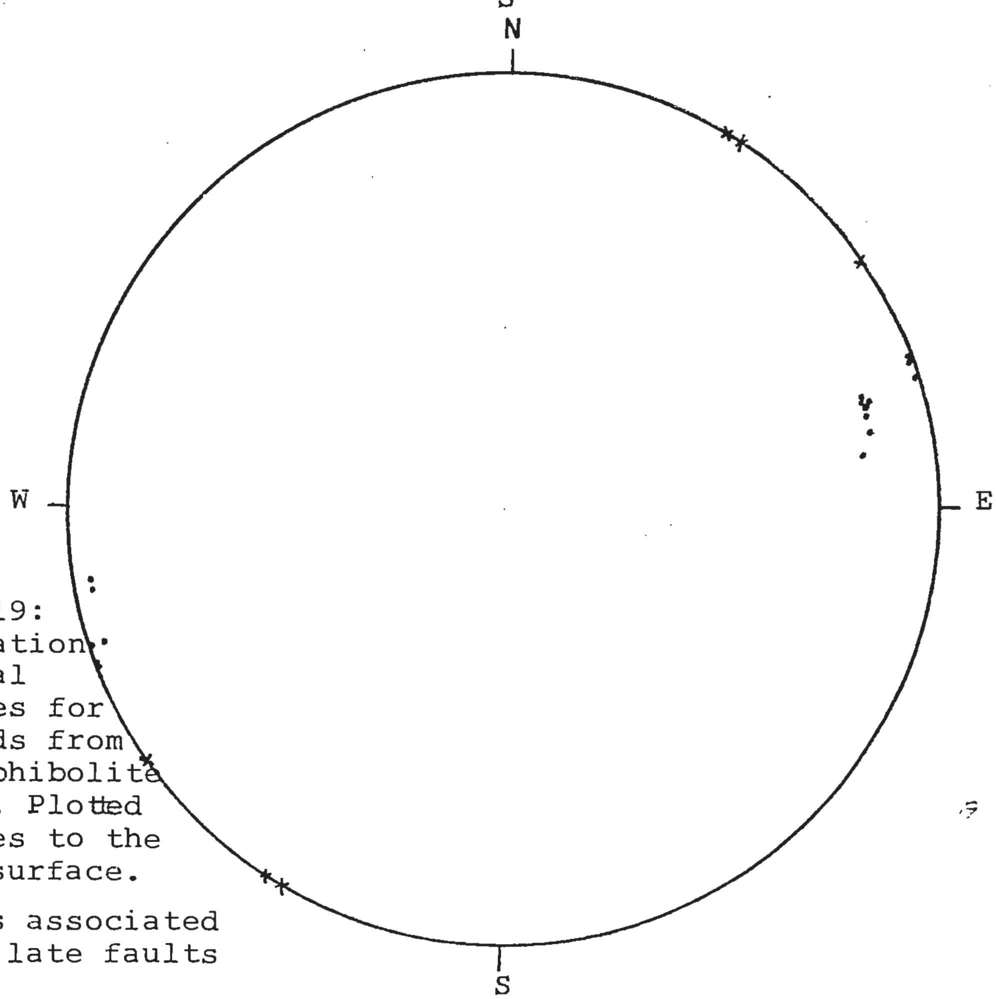

Figure 19:
Orientation of axial surfaces for 16 folds from the amphibolite schist. Plotted as poles to the axial surface.

x folds associated with late faults

The morphology of folds is variable and often the trace of the axial surface is the only observation that can be made. Because of the limited availability of data, an attempt to describe the folds and classify them by the use of dip isogons and analysis of the layer geometry has been performed on various fold forms from the amphibolite schist and the banded amphibolite gneiss.

Ramsay (1967) proposed a method of fold classification that could be applied to folds where the profile of the fold is observed. Hudleston (1973), working with the basic parameters proposed by Ramsey, modified the method of description of layer geometry so that folds that were not observable in profile could be classified. The thickness of a folded layer is measured between tangents drawn to the bounding surfaces of the fold layer at apparent dip α. The thickness of the layer can be measured in two ways, 1) normal to the tangent, the orthogonal thickness t_α, or 2) parallel to the axial surface of the fold T_α. The two thicknesses are related by the expression;

$$T_\alpha \cos\alpha = t_\alpha$$

At the fold hinge $\alpha = 0$ and $T_o = t_o$ which is the thickness at the hinge. Defining $t'_\alpha = t_\alpha/t_o$ and $T'_\alpha = T_\alpha/T_o$, t'_α or T'_α can be plotted against the value of α, as in figure 20, to determine the class of the fold under consideration.

Another parameter, θ_α , for a folded layer, is defined as the angle between the normal to the tangents drawn to either fold surface at the angle of apparent dip, α , and the isogon. θ_α can be plotted against α (figure 21) producing areas on the graph characteristic of the various classes of folds.

Plots of t'_α / α and θ_α/α have different advantages depending on the folds being measured. The advantages of the θ_α/α plot are: 1) the plot is independent of the datum line established in measuring the fold, while the correct location of the datum is essential for t'_α / α plots. 2) the measurement of θ_α is direct, while t'_α is a ratio of t_α / t_o. 3) θ_α against α is more sensitive to changes in the geometry of the fold layer than t'_α against α . The advantages of t'_α / α plots are: 1) t_α is easier to measure than θ_α which requires careful positioning of tangent points to the fold surface. 2) errors in θ_α are larger than errors in t'_α. 3) at high limb dips θ_α becomes most inaccurate because of the low curvature of the folded surface while t'_α / α becomes most useful when working with high limb dips. t'_α is best used if fold boundaries cannot be accurately defined by a smooth curve and θ_α is most accurate for folded layers

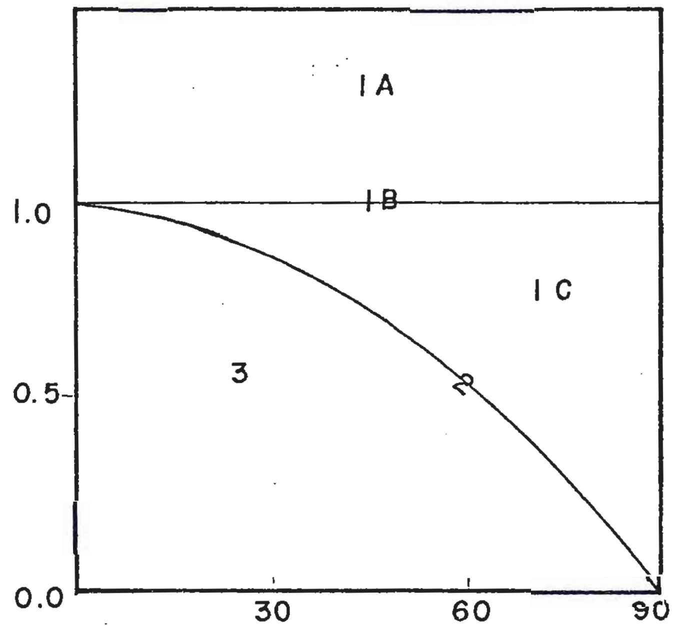

Figure 20: t'_α vrs. α showing different fold classes defined by the two parameters. (Hudleston, 1973)

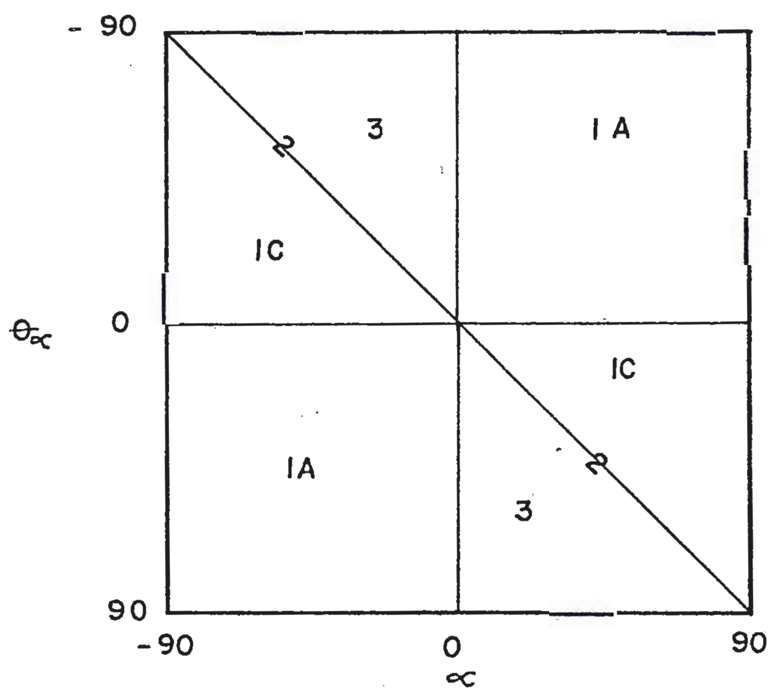

Figure 21: θ_α vrs. α with various fold classes indicated (Hudleston, 1973)

with clearly defined boundaries of high curvature and folds with obscure hinges (Hudleston, 1973).

Three folds in the banded amphibolite gneiss and one fold in the amphibolite schist were analyzed using the various thickness parameters and isogon patterns to classify them in one of the five fold classes proposed by Ramsay (1967). Figures 23, 24, and 25 show that folds in the banded amphibolite gneiss are open folds with thickened axial portions. Folds in the amphibolite schist (figure 26) also show axial thickening but are tighter than in the banded amphibolite gneiss.

Figures 22 a, b, c, are a fold in the banded amphibolite gneiss with open folds of shallow amplitude and long wave-length changing to greater amplitude and shorter wave-length through the fold form. The isogon pattern (figure 22b) indicate a class 3 fold (Ramsay 1967). The plot of t'_α and α is in agreement with the isogon pattern. The various fold limbs plot close to the line defining similar folds, or class 2 folds.

Figures 23 a, b, c, are from the banded amphibolite gneiss. Isogon patterns indicate class 3 folds, and while the t'_α vrs. α plot is in agreement, one limb falls in the class IC field and all limbs plot near class 2, similar folds.

Figures 24 a, b, c, from the banded amphibolite gneiss, show crossing isogons in one hornblende-rich layer and illustrates a poorly defined fold form.

Figure 22 a: Fold form from the banded amphibolite gneiss. For location see figure 3.

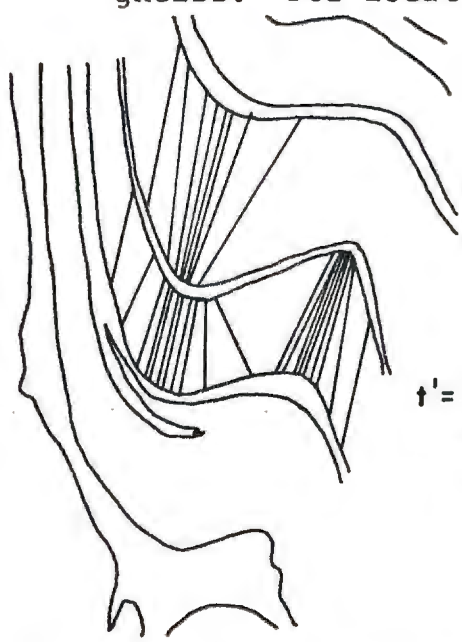

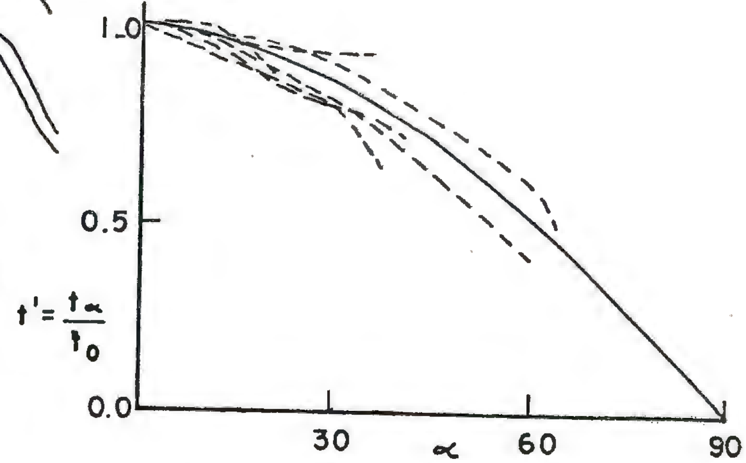

Figure 22 b: Isogon pattern

Figure C: $t'\alpha$ vrs-α plot.

Figure 23a: Fold from the banded amphibolite gneiss. For location see figure 3.

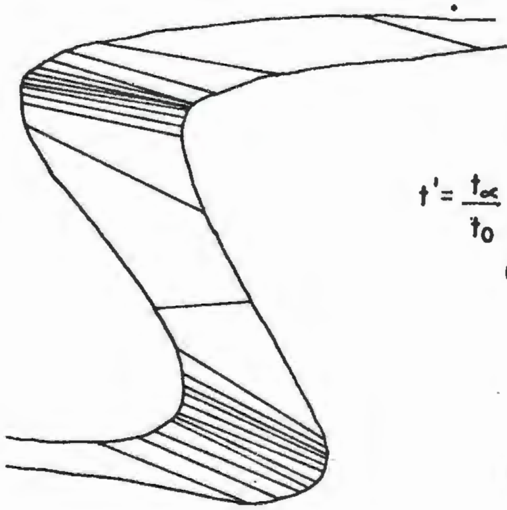

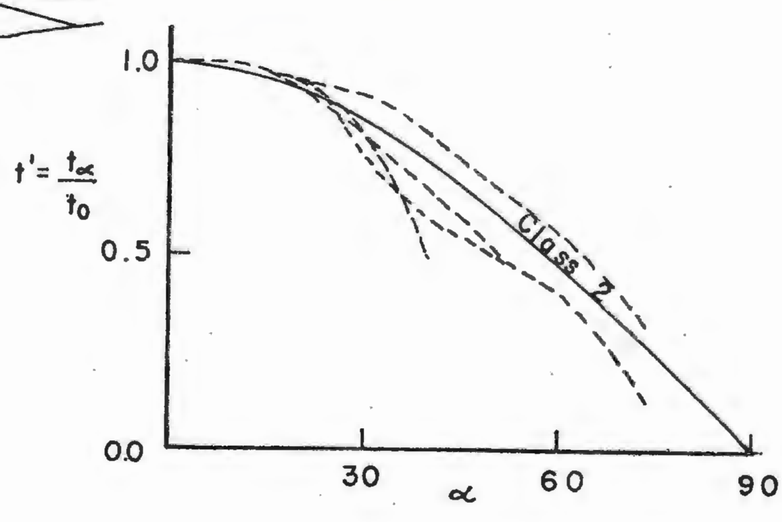

Figure 23b: Isogon pattern

Figure 23c: t'_α vrs- α plot

Figure 24a: Folds from the Amphibolite schist. For location see figure 3.

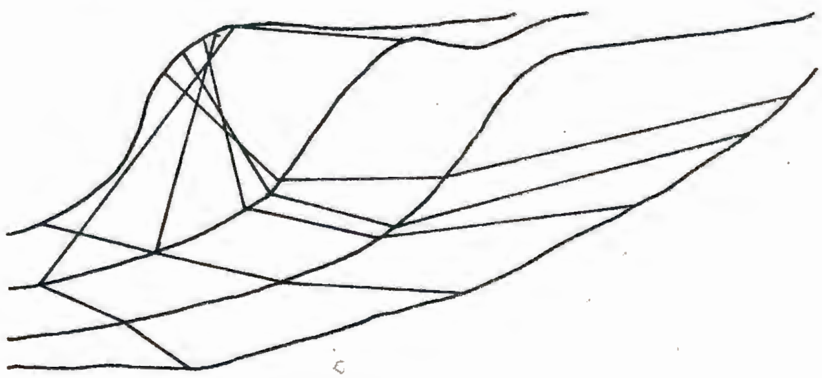

Figure 24b: Isogon pattern

Figure 25a: Folds from the banded amphibolite gneiss. For location see figure 3.

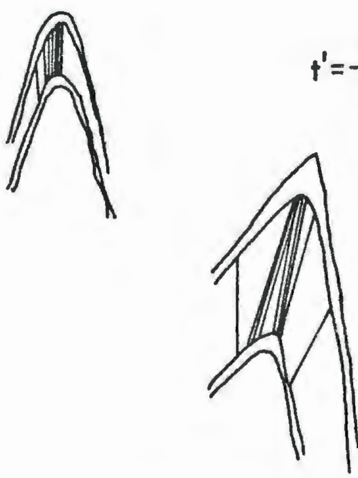

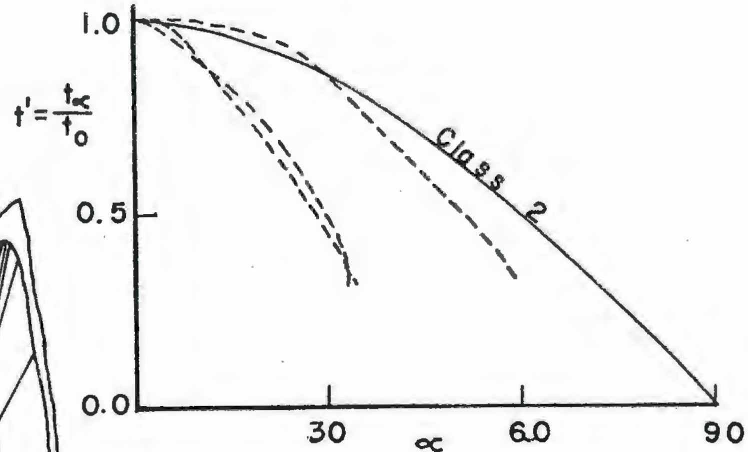

Figure 25b: Isogon pattern Figure 24c: t'_α vrs-α plot

Figures 25 a, b, c, are two folds from the amphibolite schist, the two folds are small and are definitely class 3 folds, as shown by the isogon pattern and the t'_α vrs. α plot for the limbs.

Folds from the amphibolite schist are clearly class 3 folds with thickened crest and narrow limbs, while folds in the banded amphibolite gneiss are close to similar folds with limbs plotting in class 3 and class IC fields.

Various genetic mechanisms have been proposed for the fold classes (Ramsay, 1967). It is believed that class IC folds may be flattened flexural slip folds. The fold may be an initial parallel fold that has been flattened so it looks like a similar fold. The fold results from homogeneous strain. Class 2 folds are produced by inhomogeneous simple shear, by slip, shear or flow across layers. Class 3 folds form under conditions of inhomogeneous strain.

Folds in the amphibolite schist, formed by a mechanism involving inhomogeneous compressive strain while in the banded amphibolite gneiss the patterns are not as conclusive. The folds may have formed as class IC folds and later deformed to give class 3 folds.

The differences in fold styles can be due to many factors including rheologic properties of various compositional bands, state of stress, temperature and pressures during deformation.

Discontinuous Structures: Shear Zones

Major shear zones, 4 to 5 meters wide, trend subparallel to compositional banding. Two of three shear zones are developed between the transition gneisses and the feldspathic gneiss, while the third shear zone is developed in the feldspathic gneiss. Figure 26 is a map of a shear zone involving the amphibolite schist, transition gneisses and the feldspathic gneiss units. This zone has been studied most closely and will be used as an example, with exceptions noted in the other zones where applicable.

The maximum width of the zone is approximately 6.5 meters with variability along strike. The zone is composed of three essential components: 1) the matrix, 2) the included blocks, and 3) the wall rock. The matrix is the result of intense granulation producing a fine-grained, black rock with thin, white bands. Where hornblende-rich rocks were sheared, the matrix is best developed, and where the original rock contained more feldspar, the matrix is less uniform and is transitional into the surrounding rocks. Within the matrix are blocks of the wall rock ranging from amphibolite to feldspathic gneiss. The blocks show varying stages of disintegration and rotation within the matrix. The wall rock is essentially unaffected if

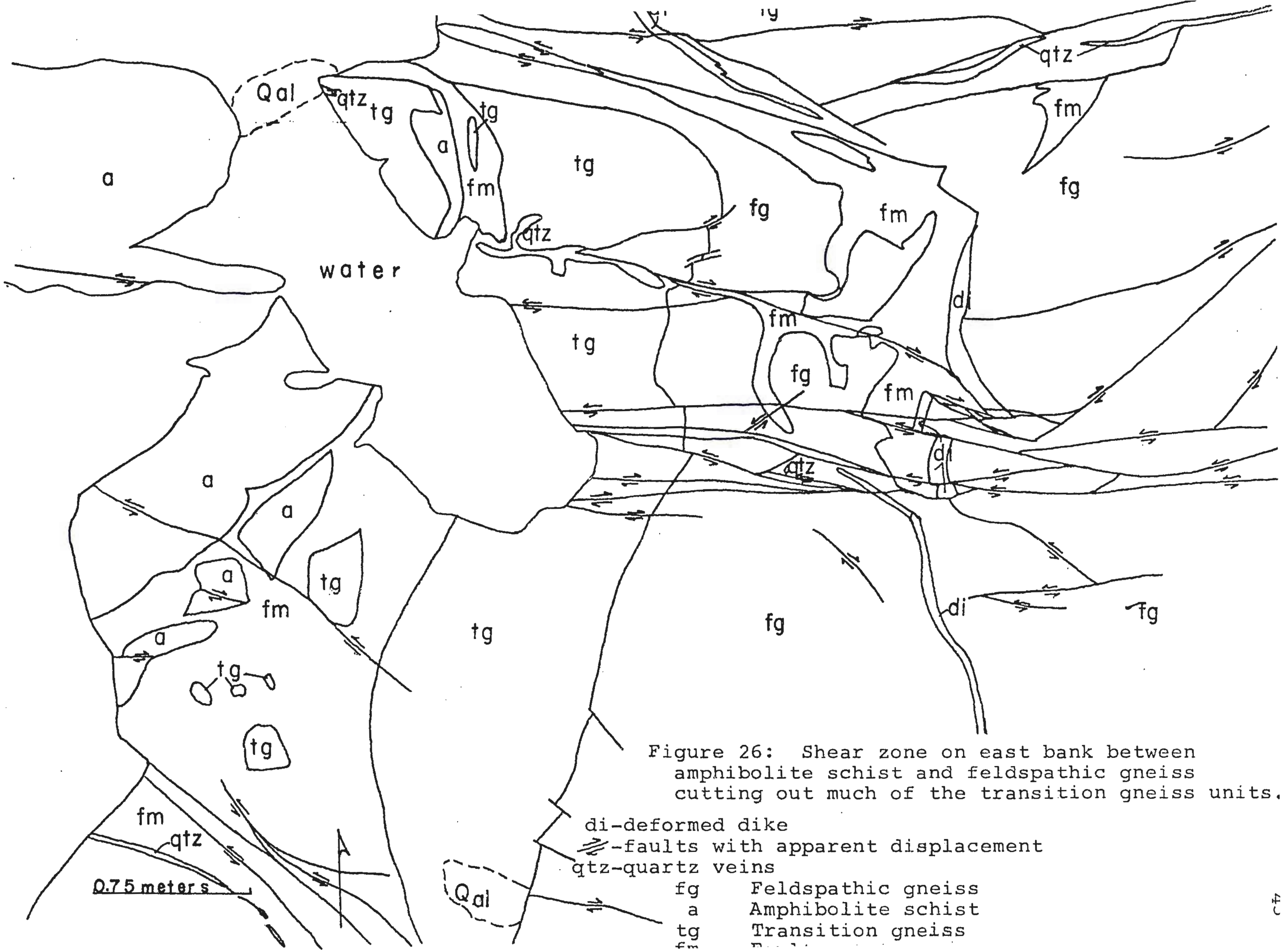

Figure 26: Shear zone on east bank between amphibolite schist and feldspathic gneiss cutting out much of the transition gneiss units.

di-deformed dike
-faults with apparent displacement
qtz-quartz veins
fg   Feldspathic gneiss
a   Amphibolite schist
tg   Transition gneiss

high in amphibole while the feldspathic gneiss is strongly deformed. The shear zone in figure 26 is truncated on the north by a left-lateral fault and on the south is lost under alluvium.

A second shear zone is located on the east side of the island in a similar lithologic setting as described above (see figure 3). Neither the north nor south end of the zone are exposed but available evidence indicates fault displacement.

The third zone is narrow, rich in chlorite, and located totally within the feldspathic gneiss and is exposed only on the west bank. Structural disruption associated with the shear zone is extensive.

One to two centimeter shear bands are very common in the more feldspathic units. The relation of the fine bands to the major zones is not clear, however, they seem to be related to the episode of deformation that produced the main zones.

Faults

Several episodes of faulting have been determined from cross-cutting relations. The faults are characterized by simple fault surfaces of finite width. Four main sets include: 1) Recrystallized fault planes, 2) faults bounding lenses, 3) right-lateral faults, 4) left-lateral faults.

Faults with recrystallized fault planes are present in the banded amphibolite gneiss and may be present in the amphibolite schist. In the banded amphibolite gneiss the faults cut compositional banding at a low angle that is suggestive of cross bedding. The strike of the faults is North to N 7° W and the fault plane dips west at 84° where observed. The cross bedding origin for these features is not valid since distinct compositional bands can be traced across the fault plane. The sense of displacement is left-lateral. Small drag folds are also found along some of the faults (figure 27). Coarse hornblende and plagioclase crystals occur in some of the faults (figure 28). The faults cannot be traced the length of the outcrop because of later faulting.

Faults bounding lenses are well developed in the banded amphibolite gneiss and to a lesser extent in the amphibolite schist. The faults bound lenticular masses of rock which are essentially undeformed except for a border 5 to 6 centimeters wide along the edges of the lenses. The border of a typical lens is a set of discrete fractures and seldom shows evidence of significant mylonitization. Rotation of lenses, determined from compositional banding, and local displacement have not been sufficient to determine a coherent sense of displacement along the bounding slip

Figure 27: Surface of discontinuity representing early faults in the banded amphibolite gneiss.

Figure 28: Early fault in the banded amphibolite gneiss with coarse hornblende and plagioclase grains along the fault plane.

planes. Lenses vary in size from microscopic to over 6 meters in length with the long axis (in two dimensions) north to northwest essentially parallel to compositional banding. The border of a lens may follow a hornblende-rich band, but in the majority of cases the lens boundaries are clearly discordant to compositional banding. Careful mapping of the lenses suggest that the outcrop of the banded amphibolite gneiss can be represented as the intersection of four large lenses (figure 29) with small lenses formed between the major lenses. The lenses are harder to define in other units but appear to be present in a subdued manner.

Right lateral faults are northeast to east trending with most falling between N 85° E and East (figure 30). The right-lateral fault set is usually associated with alteration. The amount of displacement is typically a matter of 5 to 10 centimeters but larger displacements up to several meters may be found.

Left-lateral faults are present in the entire area and may have associated displacements up to 6 meters. Construction of rose diagrams indicate a strong maximum between N 70° W and N 75° W (figure 31).

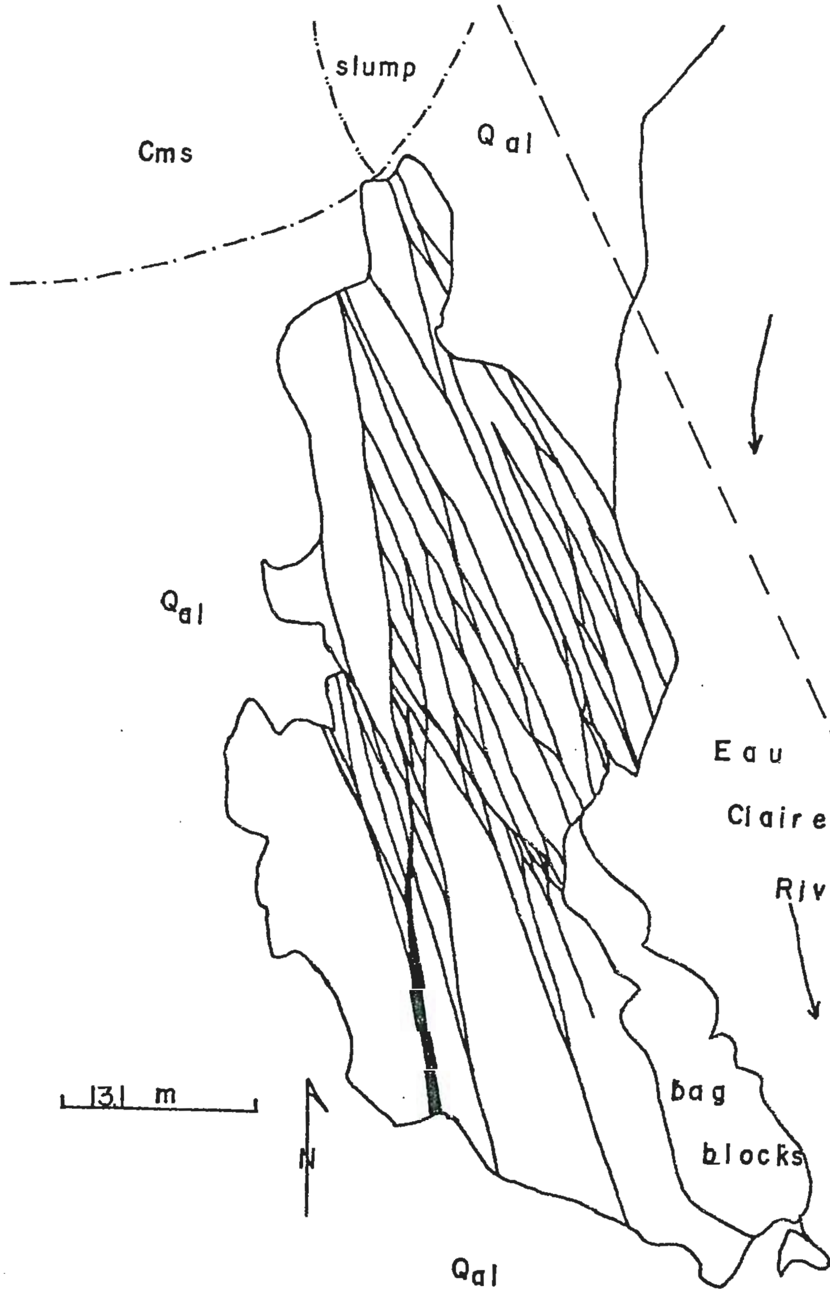

Figure 29: Schematic map of lens forms in the banded amphibolite gneiss.

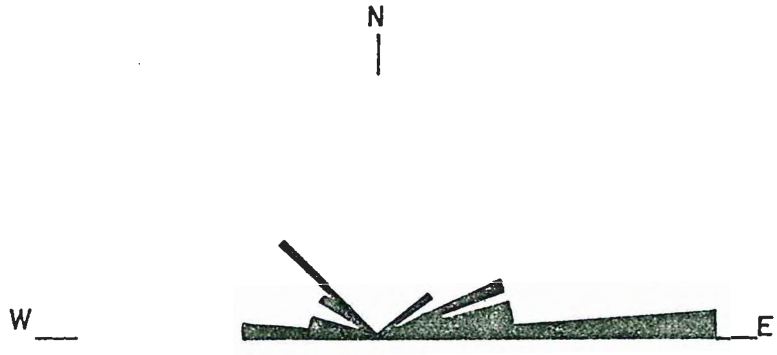

Figure 30: Azimuths of right-lateral faults.

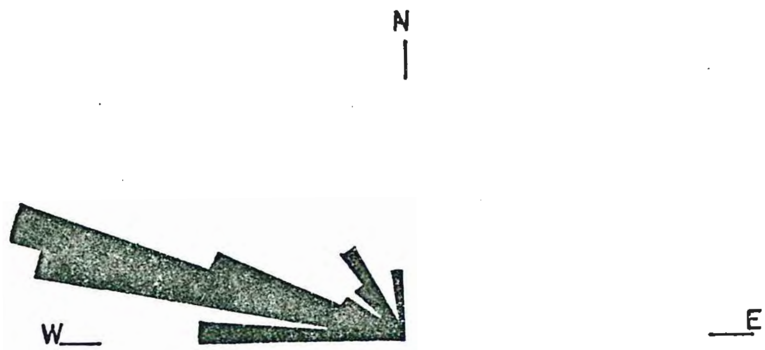

Figure 31: Azimuths of left-lateral faults.

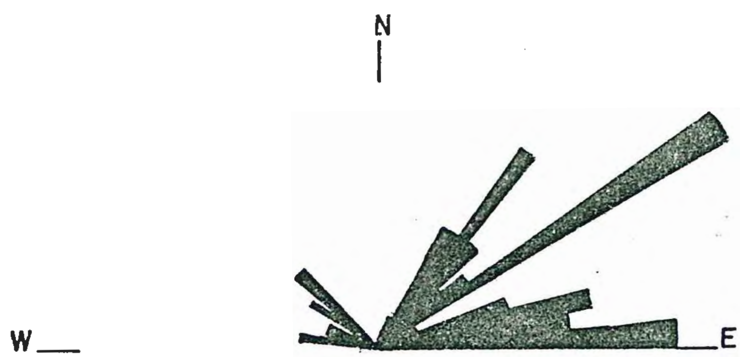

Figure 32: Azimuths of joints.

The sequence of faulting is often difficult to determine since the right-lateral and left-lateral set have not been found together. Faults with recrystallized fault planes are clearly the oldest in the area. The faults bounding lenses are considerably younger with no evidence of recrystallization observed. The left and right lateral fault sets displace the lens boundaries. Alteration associated with the right-lateral fault set also has effected the rock along some of the major lens boundaries which in turn were displaced by the left-lateral fault set. The sequence of faulting is first, lensing, followed by right-lateral faulting and lastly by left-lateral faulting.

A major fault is proposed between the banded amphibolite gneiss and the amphibolite schist, evidence will be discussed later.

Jointing

Three joint sets have been defined (figure 32). One set strikes N 35° E to N 40° E and dips 50° to the south. Another set strikes N 55° E to N 60° E but the dip on this set is rarely observed and is believed to be steep. The third set ranges from N 70° E to east with the majority between N 85° E and east. This set is roughly coincident with the right-lateral fault set described above. The common occurrance of an alteration zone along the joints suggests contemporaneous devélopment of the two structures.

Quartz Veins and Tension Fractures

On the west bank in the amphibolite schist are a number of en-echelon quartz filled fractures trending N 45° W suggesting a possible tensional orientation to major stress direction during a late phase of deformation. Another set of quartz filled fractures trend N 6° W but have been strongly deformed. Other randomly oriented, undeformed quartz veins occur in the amphibolite schist.

Petrofabrics

Petrofabric analysis was undertaken to determine any marked preferred orientation in the quartz fabric and to determine the relative time of recrystallization in reference to the main folding in the area. A preferred orientation was not observed indicating recrystallization after the deformation that produced the folding. (For more detail see Appendix I)

Interpretation of Structural Data

The main purpose of the structural analysis has been to analyze the different possible deformations that have affected the rocks at Big Falls. In an attempt to relate the different structural elements to specific deformational phases, the author suggests that three deformational phases can be supported by the structural evidence.

The three phases represent significant readjustments in the rock accompanied by metamorphism. However, it must be realized that all three proposed phases may represent response to one major deformational-metamorphic event under a varying regime of temperature and fluid pressure. The author feels that three phases are discernible based on structural and petrologic data to be presented later. The three main deformations are: 1) the earliest deformational phase is associated with the development of garnet porphyroblasts and the rock contained in the rootless intrafolial folds, 2) the second phase involved folding and faulting, and 3) the third phase resulted in major north-south shear zones and a cross-cutting schistosity. Brittle deformation, involving development of faults and joints is considered to have occurred after a significant time interval from the three main phases of deformation.

Phase I: Two lines of evidence suggest the first phase of deformation: 1) the coarse garnet porphyroblasts with foliation wrapped around the crystals, and 2) rootless intrafolial folds.

The coarse garnet porphyroblasts in the banded amphibolite gneiss and the amphibolite schist are consistantly enclosed in the surrounding foliation (see figure 5). Also the garnet porphroblasts are cracked and slightly elongate in the plane of the foliation; therefore, the textural evidence is in agreement with a later foliation taking on a curved form around a pre-existing crystal (Spry, 1969, p. 150). This line of reasoning places the formation of the garnet prior to the formation of the foliations which wrap the garnets.

The second line of evidence for an early deformational phase is the rootless intrafolial folds in the amphibolite schist. The internal foliation within the folds predates the external foliation of the enclosing rock. Based on the presence of internal foliation, the protolith of the folds appears to have been compositionally banded, either as a gneiss or a primary layered sedimentary or igneous rock.

Phase II: The fact that an early phase of deformation can be recognized suggests that a metamorphic rock was the protolith at the onset of the second deformational phase. The second phase of deformation produced the major structural elements (folding and compositional segregation) in the Big Falls area.

The features that have been assigned to the second phase suggest deformation under different conditions of temperature and pressure than that of phase one.

Most folding occurred during the second phase, however the plunge of folds in the amphibolite schist are south while in the banded gneiss the plunge is north. As note above, layer geometry of the folds from the two units also indicate differences in fold forms and thus, distinctive strain histories. The evidence cited suggests possible fault juxtaposition after fold formation, the timing of faulting will be considered after discussion of petrologic evidence.

Although the orientation of axial planes in both units are essentially the same, when lineations are considered along with plunge of folds, the picture is more confused. As note above, although lineations from the amphibolite schist and the banded amphibolite gneiss plot on a great circle, they are apparently not of the same age. Lineations in the banded amphibolite gneiss are roughly coincident with the plunge of fold axes in the gneiss, however, as the lineation is poorly developed this suggests either weak crystallization after fold development or partial blotting out of the earlier lineation by recrystallization.

Lineations in the amphibolite schist are poorly developed, but, where present are discordant to fold axial plunges. Lineations plunge steeply to the north while fold axes plunge gently to the south, which along with petrographic data suggests that the lineations in the amphibolite schist may have resulted from recrystallization during the third phase deformation.

Schistosity in the amphibolite schist and compositional foliation in the banded amphibolite gneiss are similar in attitude and in both cases roughly parallel the attitude of axial planes of the folds in these rock units. However schistosity and lineations cut the fold forms observed in the field, the deformation ellipsoid responsible for the schistosity and lineations in the amphibolite schist is not related to the deformation ellipsoid responsible for folding.

The deformation of garnets and development of boudinage are the result of the second phase of deformation and indicate that the Z axis of the deformation ellipsoid was steeply dipping with the YZ plane oriented parallel to present compositional banding and schistosity. Orientation of the deformation ellipsoid may be gained by measuring direction of elongation of fragments of shattered garnet porphyroblasts in planes cut in horizontal and vertical sections perpendicular to lineation. In this case, maximum elongation is measured in the vertical section. Orientation of the deformation ellipse may also be measured from boudin structures, however, the elongation direction is not observable at Big Falls, although the direction of stretching is parallel to the plane of schistosity.

Early faults found in the banded amphibolite gneiss formed late during the second phase of deformation, cutting compositional banding that was associated with folding. The fault planes are healed by crystals formed during recrystallization associated with the second deformational phase. Tension fractures that have been deformed in the amphibolite schist are possibly of the same period.

Phase III: The third phase of deformation was not as extensive as the second. Features associated with the third phase are the north-south trending shear zones and a cross-cutting schistosity. South-plunging lineations in the banded amphibolite gneiss may also have developed during this phase. The degree of structural readjustment in the amphibolite schist during this phase is not clear due to extensive recrystallization, however a cross-cutting foliation is easily observed in thin section. This schistosity (Strike N 55° W) cuts both schistosity and compositional foliations associated with the second phase.

Three separate faulting events followed the third deformational phase: 1) lens development, 2) right-lateral faulting, and 3) left-lateral faulting. The development of lens structures, especially in the banded amphibolite gneiss, suggests brittle failure since the bounding slip planes of the lenses are usually very discrete fractures with disruption of the edges of the lens restricted to a few centimeters at most. The orientation of the lenses in two dimensions suggest a compressive stress in an east-west direction and the extensional stress in the north-south direction, however the third-dimension shapes of the lenses are not known and any estimate of stress directions is subject to question.

Right-lateral faulting and associated jointing occurred when significant quantities of mobile components were present, indicated by alteration associated with the faults and joints. The left-lateral faulting was not associated with such fluids and is the last significant structural development.

Petrography

Petrographic relations between major phases are complex and a wide range of textures are present in the Big Falls gneisses and schists. Each of the major rock types will be described separately with mineral properties, textures, mineral assemblages and point count data.

Banded Amphibolite Gneiss

In the banded amphibolite gneiss, hornblende, plagioclase and epidote are the most common phases, with garnet abundant in some samples. Quartz, sphene and ilmenite are accessory phases. Alteration minerals developed along late fractures include chlorite, epidote, sericite and quartz.

Hornblende is subhedral to anhedral and occurs in bands, clots or as single isolated grains. Pleochroism is not strong with colors typical of blue-green hornblendes, α -straw yellow, β - green and γ - blue green. Crystals are optically (-) with 2V approximately 70 degrees. Extinction angles range from 14-16° for $\gamma \angle c$. A bimodal distribution of grain sizes is characteristic, with 0.75 to 1 mm. grains typical in most of the rock (figure 33) and 1.5 to 4 mm. grains common in many hornblende-rich bands (figure 34), intergrown with garnet porphyroblasts

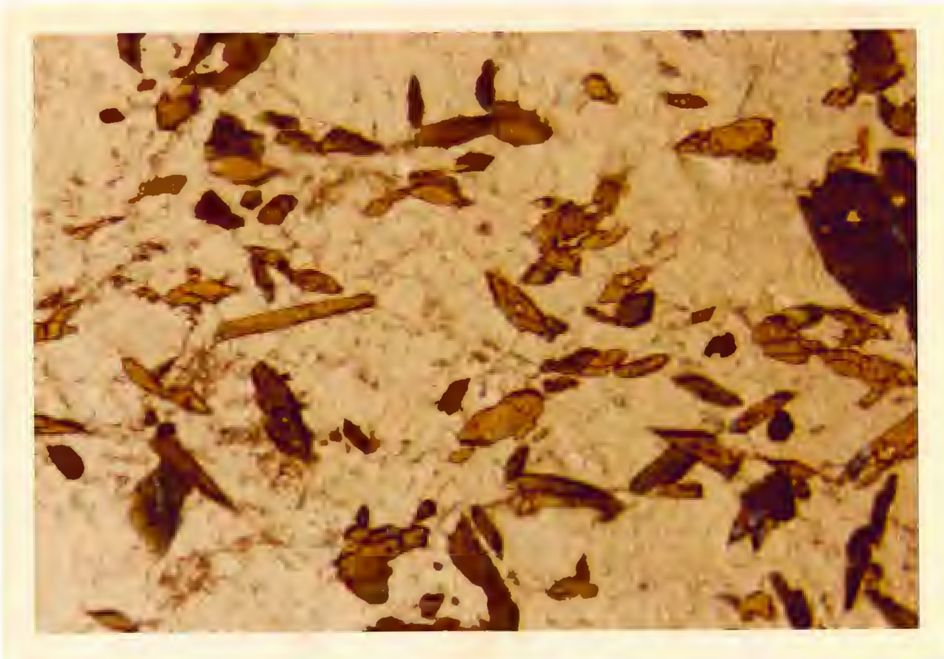

Figure 33: 0.75 to 1 mm. prismatic hornblende, background is plagioclase. 20 power polars crossed Sample wp-7

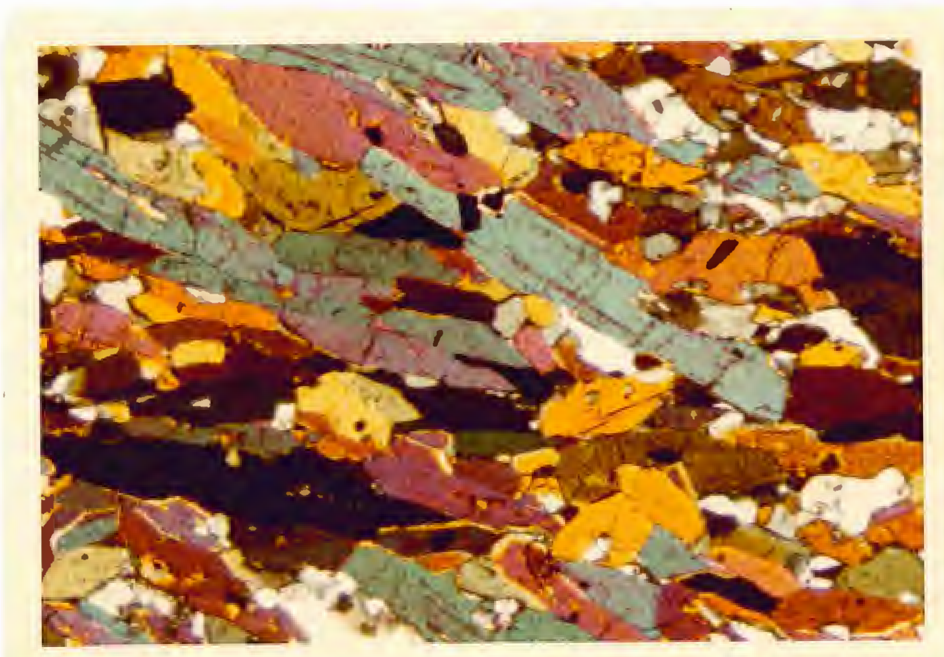

Figure 34: 1.5 to 4.0 mm. prismatic hornblende in a hornblende-rich compositional band. X 20 polars crossed Sample wp-7

and is isolated 1 to 2 cm. clots. The finer grain size is usually present as isolated grains but may occur in groups of three or four crystals. The fine-grained hornblende also defines compositional banding but the bands are faint and may be discontinuous. Chlorite and quartz are present as partial replacement products in the alteration of hornblende. Alteration is confined to narrow zones along fractures where solutions have moved. In some cases severe alteration has resulted in the development of sericite pseudomorphs after prismatic hornblende (figure 35).

Plagioclase feldspar is typically the dominant mineral in the banded amphibolite gneiss. Because of the complex textures of the plagioclase, common techniques based on albite twinning could not be used in determination of composition, however microprobe analysis indicated An 50-60. The optic sign is (+) with a large 2V. Textural variation allows definition of three main textural types. 1) relict coarse grained plagioclase (figure 36). 2) granoblastic fine grained plagioclase (figure 43). 3) granoblastic plagioclase of intermediate grain size as compared to type 1 and 2 (figure 42).

Relict plagioclase grains are compositionally zoned with an irregular and patchy pattern (figure 36).

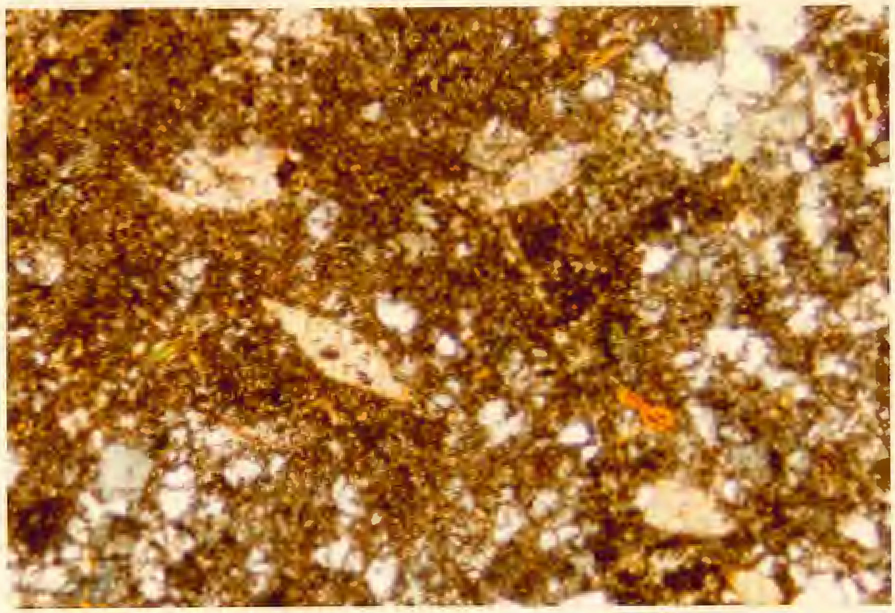

Figure 35: Sericite pseudomorphs after hornblende in strongly altered banded amphibolite gneiss. X 20 crossed polars. Sample 7-29-72-9

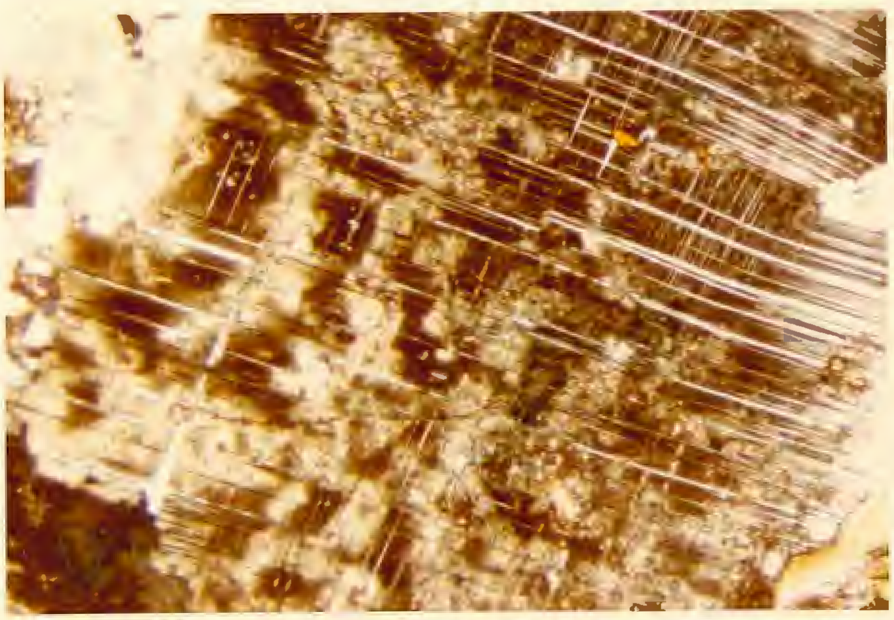

Figure 36: Patchy compositional zoning in plagioclase feldspar grain with bent cleavage. X 20 crossed polars

The original plagioclase grains are 1.5 to 2.5 mm. in diameter. The zoning is the step after bending of twin lamellae and cleavage planes which supplies strain energy that is expended in the disintegration of the grain. The development of compositional zoning is accompanied by grain boundary migration forming sutured and lobate grain boundaries. The lobes developed at this stage can still be identified with the parent grain (figure 37). With continued migration the lobe becomes separated from the parent grain and forms grains about 0.1 mm. in diameter. Internally sets of lamellae develop at an acute angle to the normal albite twin lamellae (figure 38). The edges of the lamellae are irregular as in the albite twin planes which are destroyed early in the disintegration process. The identity of twin individuals is maintained by local polygonization of the twin lamallae with slightly different optic orientation within each twin individual (figure 39). The form of the parent is often maintained even when the grain is completely polygonized as illustrated in figures 40 and 41. Figures 40 and 41 are photomicrographs of the same parent grain but the stage has been rotated between pictures. The development of the polygonal texture in relict plagioclase grains is not uniform in any given thin section.

Figure 37: Plagioclase - plagioclase grain boundary showing lobate advances caused by grain boundary migration. X 80 crossed polars Sample W-6

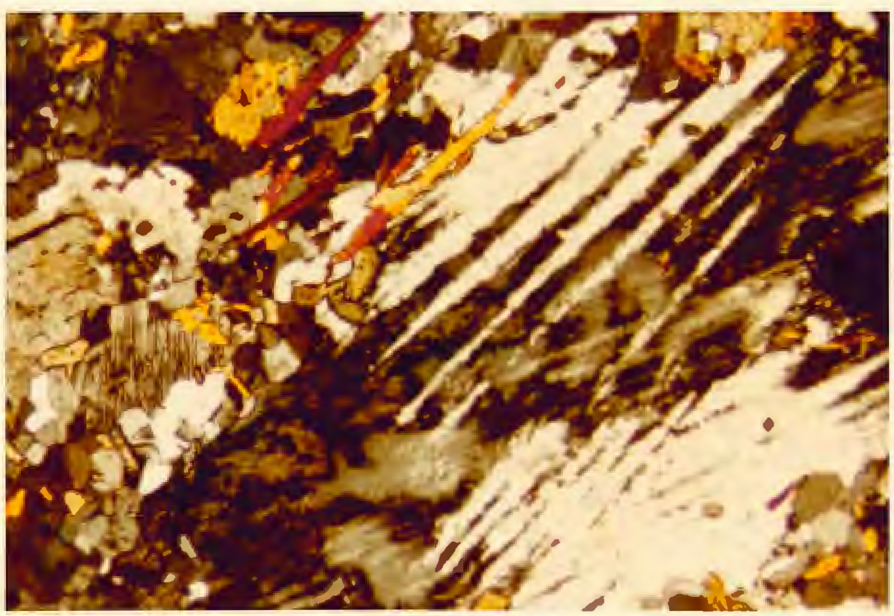

Figure 38: Plagioclase grain with development of deformation lamellae at an acute angle to albite twin lamellae. X 20 crossed polars Sample W-6

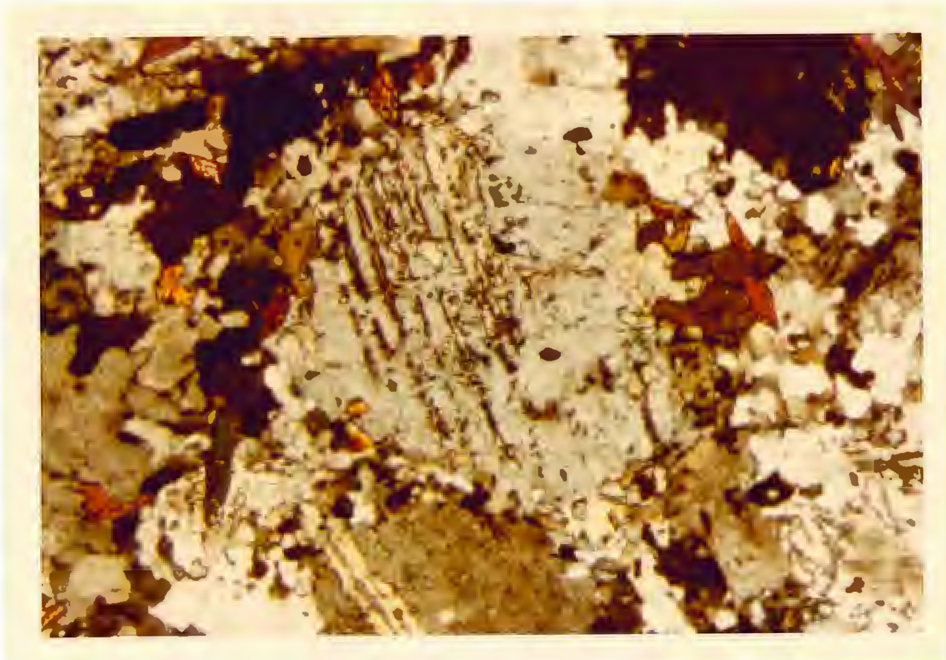

Figure 39: Plagioclase with relict albite twinning after a high degree of internal polygonization. X 20 crossed polars Sample WP-7

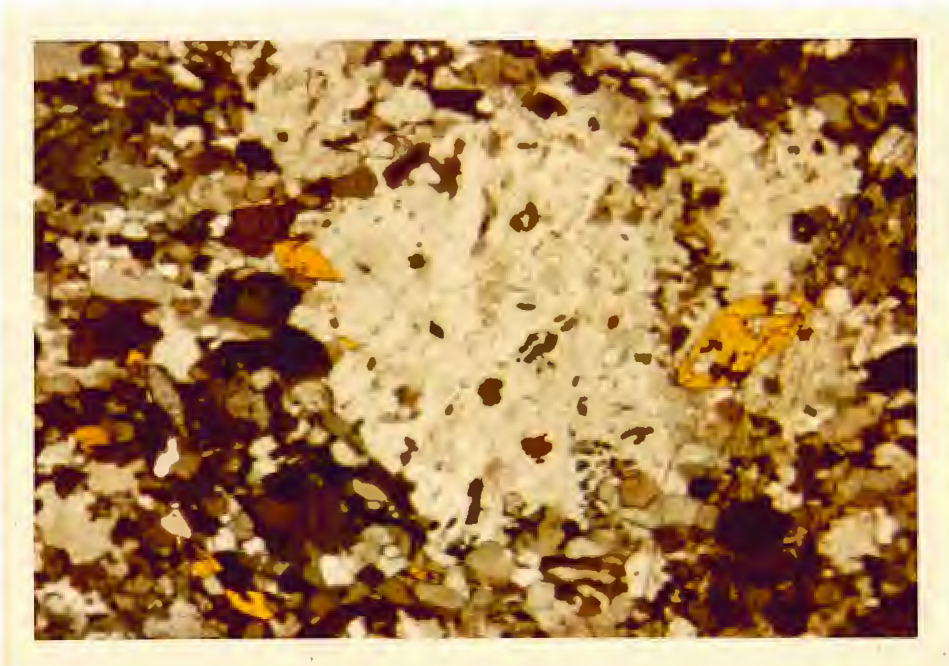

Figure 40: Relict plagioclase grain. X 20 crossed polars Sample WP-3

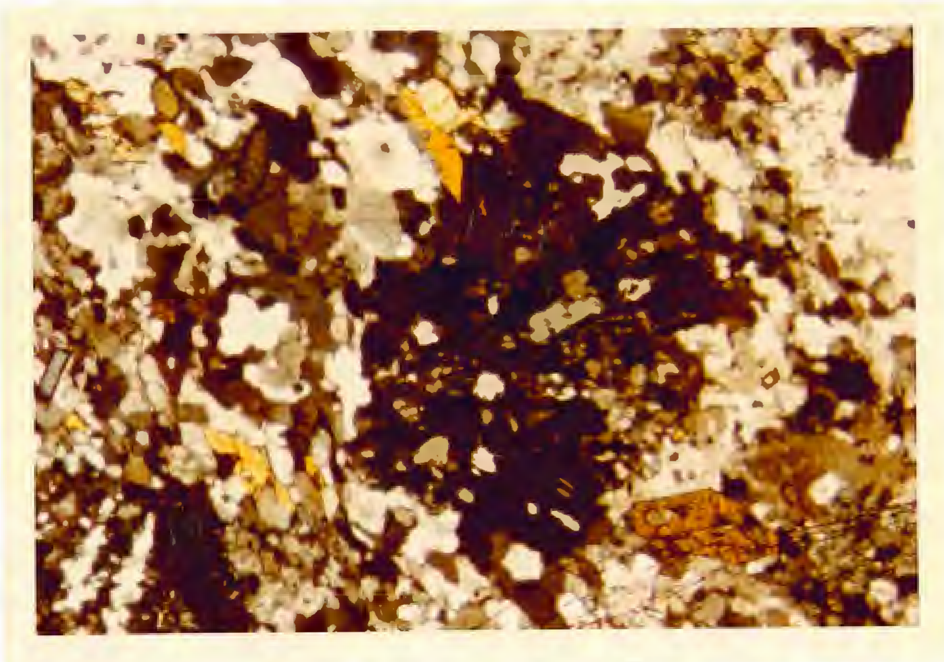

Figure 41: Relict plagioclase grain pictures in figure 40 after rotation of the grain. X 20 crossed polars. Sample WP-3

The variability suggests that the amount of disintegration of a grain probably reflects its physical orientation to the applied stress.

The second textural type of plagioclase is the end result of the disintegration process, yielding grains that are granoblastic and approximately 0.1 mm. in diameter (see figures 40 and 41). Twinning and compositional zoning are consistently absent. Granoblastic grains occur around relict plagioclase grains resulting from necking during grain boundary migration. Destruction of the parent grain by intragranular polygonization replaces the parent grain by fine-grained granoblastic aggregates of crystals. As intergranular and intragranular processes continue the original coarse grained assemblage is destroyed. Narrow bands of fine grained polygonal plagioclase can be traced as a continuous feature across thin sections, and within these bands all coarse plagioclase grains have been destroyed. Complete granulation of the original texture is rare, generally relict grains can be defined.

The third plagioclase textural type, granoblastic medium-grained, is twinned on the albite law and displays only slight compositional zoning. The texture is the result of recrystallization of the fine grained granoblastic plagioclase into an aggregate of 1 to 1.5 mm. grains (figure 42). Intersection of grains is often at triple-points, some with equal angles between grain boundaries, and an approach to straight boundaries suggests an approach to equilibrium. The recrystallized texture is not common, occurring locally.

Epidote is present as euhedral to subhedral prismatic crystals. Grain size ranges from less than 0.1 mm. to 1 mm. or more. The distribution of epidote is not uniform varying from zero to several

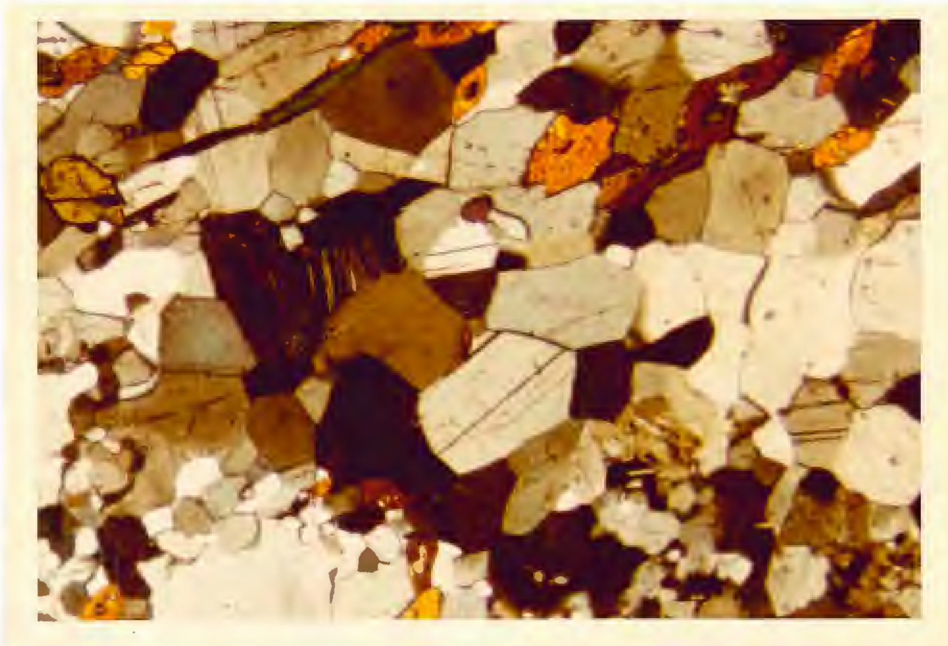

Figure 42: Textural type 3 plagioclase-recrystallized granoblastic. 20 X crossed polars Sample 7-29-72-2B

percent. Epidote is common in rocks with high percentage of fine granoblastic plagioclase (figure 43). Epidote crystals often cross-cut banding and tend to show little control by any surrounding phases, suggesting late crystallization. In some cases, however, epidote is preferentially aligned indicating crystallization while some stresses were still active.

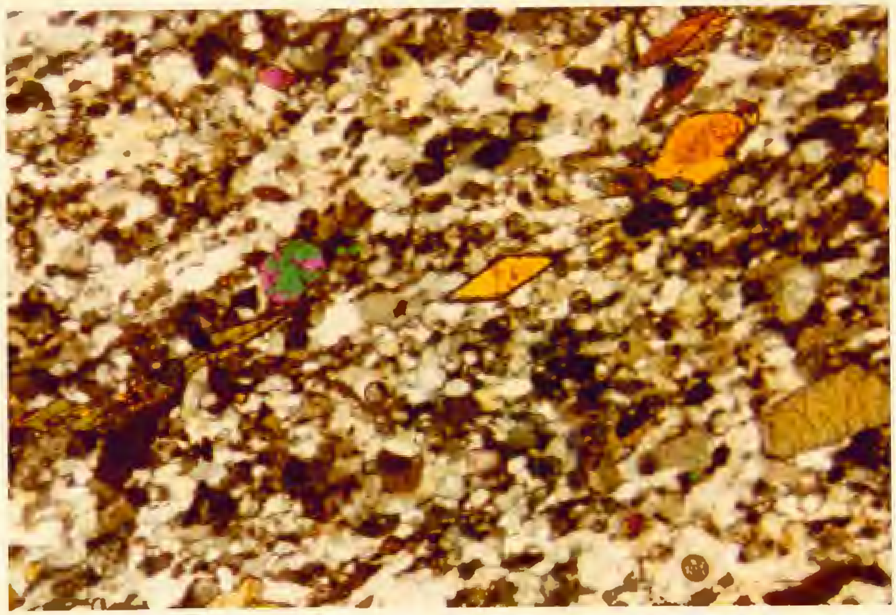

Figure 43: Epidote in fine grained type 2 plagioclase.
X 20 crossed polars Sample WP-5

The distribution of garnet is irregular and two distinct grain sizes and occurances are definable. Grain sizes are either several centimeters up to about 10 cm. in diameter or 0.5 mm. in diameter. The coarse garnets are invariably anhedral while the fine garnets are euhedral.

The coarse anhedral garnets are fractured and intergrown as well as surrounded by coarse hornblende prisms up to 1 cm. in length. (figure 44).

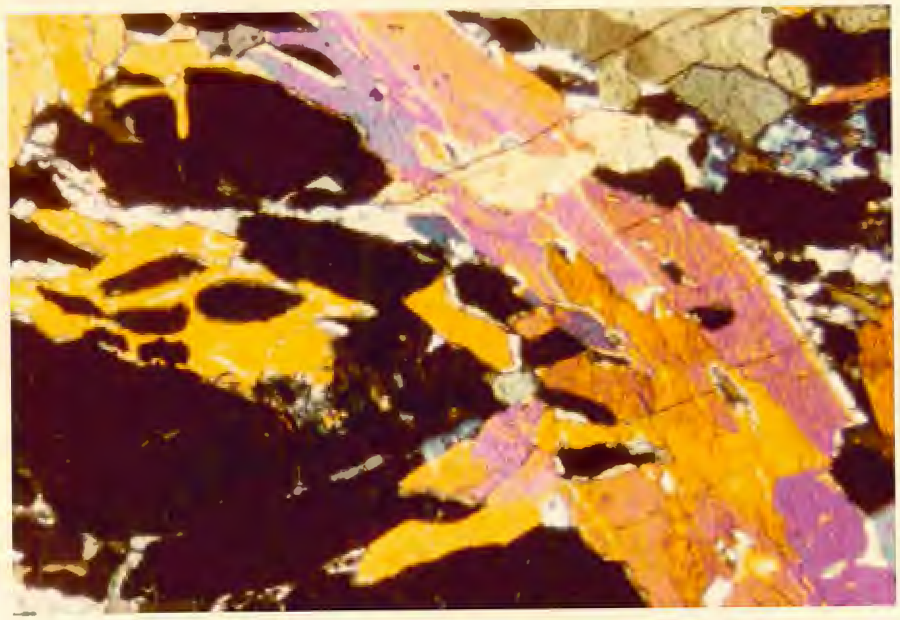

Figure 44: Hornblende intergrown with large garnet porphyroblast. Note the garnet inclusion in hornblende. Epidote and quartz are also present. 20 X crossed polars Sample 7-29-72-8

Compositional banding bends around the garnet porphyroblast and its sheath. The hornblende envelope conforms to the surrounding banding while the internal hornblende is randomly oriented. Epidote, quartz, chlorite and sericite may be found in the large garnet grains. Textural relations suggest replacement of garnet by hornblende and in some cases the replacement is complete.

0.5 mm. garnets are euhedral (figure 45) and are found in the banded amphibolite gneiss in Unites III and IV (see figure 3). The garnets have

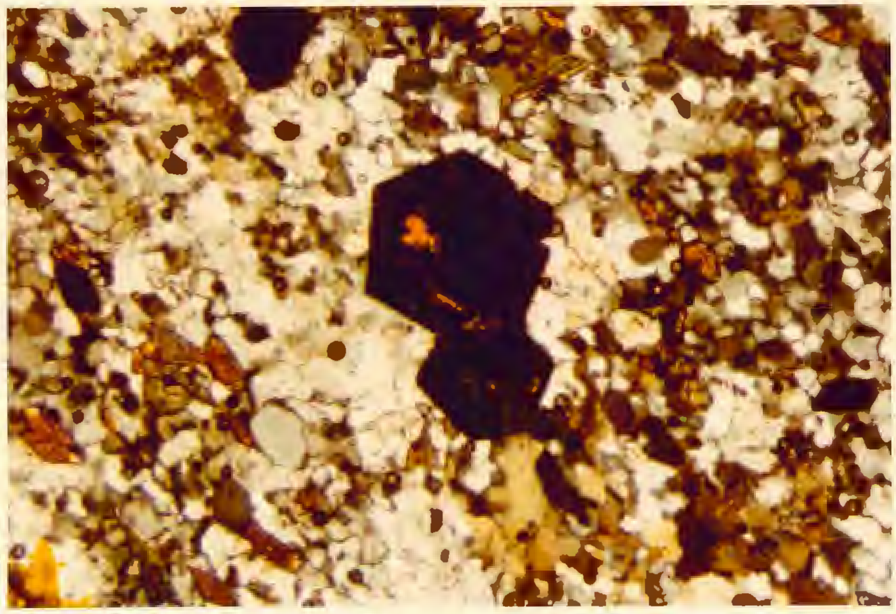

Figure 45: Garnet crystals 0.5 mm. in diameter.
X 20 crossed polars Sample W-8

been found next to narrow shear bands which tend to be deficient in hornblende compared to the rest of the rock, but contain euhedral epidote and fine grained granoblastic plagioclase. Braided fractures occupy the shear zones and cut all phases including garnet.

Sphene is an accessory mineral forming anhedral grains closely associated with hornblende, especially in hornblende-rich compositional bands. The concentration of sphene is significant in some hornblende-rich bands. Ilmenite grains may be rimmed by sphene. Quartz rarely occurs as an accessary mineral.

Secondary minerals include chlorite, quartz, sericite, epidote and pyrite. Alteration is generally confined to fractures trending N 85° E. Pyrite occurs along fractures and is rimmed with epidote and chlorite. Hornblende alters to chlorite and quartz. Epidote, when occurring as a secondary mineral, is anhedral. Plagioclase alters to sericite along fractures, however alteration is very minor in most plagioclase grains. Two generations of chlorite occur in association with garnet porphyroblasts. The first generation is Fe-Mg rich (positive sign of elongation (Albee, 1962)) while the second generation in the garnets and along fractures is Mg rich (negative sign of elongation). Both generations of chlorite have first order gray interference colors.

Mineral assemblages in the banded amphibolite gneiss are: hornblende-plagioclase $\pm$ sphene, hornblende-plagioclase-epidote $\pm$ sphene, and hornblende-plagioclase-garnet-epidote, $\pm$ sphene. Ilmenite and quartz may be present in trace amounts.

Point count data from selected thin sections based on 1000 points are presented in table II. The volume percentages must be viewed with caution and should not be considered as truely representative of the bulk composition of the banded amphibolite gneiss. The data are presented as an indication of the compositional variation within the rock unit.

Table II

Point Count Data from Banded Amphibolite Gneiss

Sample	Hbe.	Plag	Epidote	Sphene	Ilmentite	Qtz	Garnet
WP-3	6.4	91.1	1.9	0.2	0.1	0.8	
WP-7	40.2	57.3	0.7	1.6	0.2	-	
W-6	35.4	61.3	1.8	1.0	0.4	0.1	
JT-1	22.9	74.6	1.6	1.0	0.1	-	
PRM-2	14.7	81.3	1.2	2.5	-	0.2	
W-8	7.8	88.5	2.4	0.7	0.1		0.4

Amphibolite Schist

Minerals in the amphibolite schist include hornblende, cummingtonite, garnet, plagioclase, quartz, apatite, epidote, biotite, sphene and ilmenite. Secondary minerals include dolomite, chlorite, sericite, and epidote.

Hornblende is the major component in most samples but may range from a trace to more than 95 per cent. Three major textural types are defined: 1) prismatic hornblende, 2) poikiloblastic hornblende, and 3) hornblende containing fine opaque inclusions. Minor textural varieties can be found in some samples; these textures will be described later.

Prismatic hornblende is the most common textural type. This hornblende is subhedral, often inclusion free and typically lies in the plane of schistosity, seldom showing a distinct lineation. Pleochroism is marked, with α - straw yellow, β - deep green and γ - dark blue-green. Pleochroism is more distinct in hornblende from the amphibolite schist than from hornblendes in either the banded amphibolite gneiss or the feldspathic gneiss. Extinction angles range from 15° to 17° $\gamma \angle c$ with negative optic sign and 2V approximately 70° to 75°. Grain size is from 0.5 mm. to 1 mm. with 1 mm. the most common. Some samples contain very fine hornblende and cummingtonite

(0.1 mm.) with the amphiboles finer grained than the associated plagioclase and quartz.

Poikiloblastic hornblende occurs in certain bands and is essentially restricted to those bands. Figure 46 is a photomicrograph showing poikiloblastic hornblende associated with prismatic hornblende and hornblende with fine opaque inclusions. Inclusions are quartz and plagioclase that are distinctly finer grained than the same phases in the surrounding material. Inclusions may show the imposed shape of the hornblende lattice by being elongate parallel to cleavage, but this is not always the case.

Anhedral hornblendes with fine opaque inclusions (figure 47) occur in compositional bands alternating with bands of prismatic hornblende, and may comprise up to 60 per cent of the total hornblende in some samples. Grain size ranges from 1 mm. to 5 mm. The opaque dust is ilmenite when viewed under reflecting light. Inclusions are concentrated near the center and along fractures in the grains. The rims of grains are nearly free of the ilmenite inclusions. Grain shape is more equant than prismatic hornblende and grain boundaries are irregular and irrational.

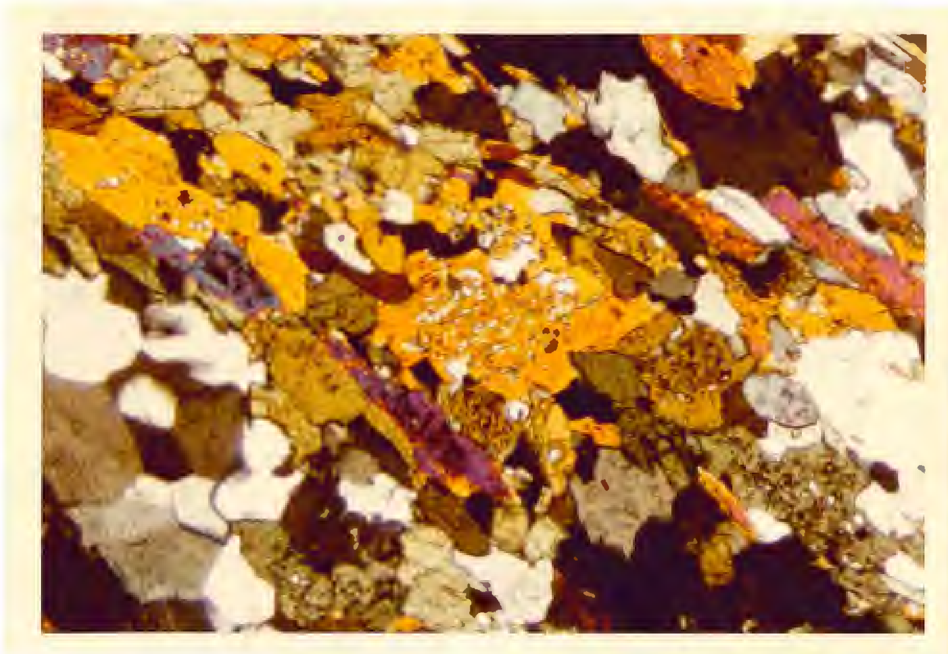

Figure 46: Poikiloblastic hornblende with prismatic hornblende and hornblende with opaque inclusions. Other phases include plagioclase, quartz and apatite. 20 X crossed polars Sample W-31

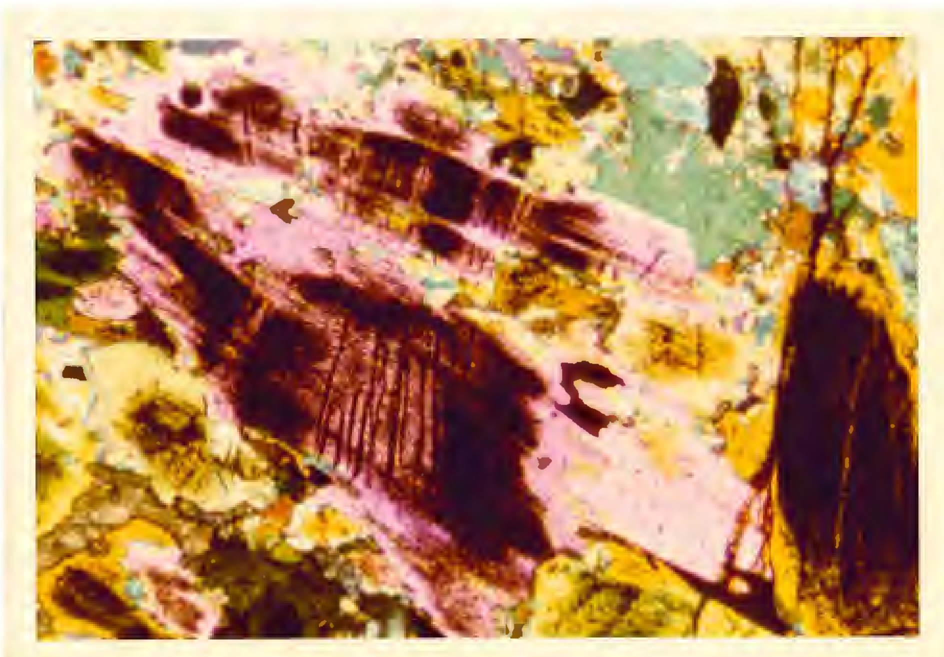

Figure 47: Coarse hornblende with ilmenite inclusions. Other phases include sphene and prismatic hornblende. X 20 crossed polars Sample W-20

Two distinctive textures involving hornblende are illustrated in figures 48 and 49, each was found in only one sample. Figure 58 shows a skeletal growth of hornblende and plagioclase with some quartz. Skeletal hornblende and some plagioclase are optically continuous suggesting a complex intergrowth of the two phases. The roughly spherical intergrowth is surrounded by prismatic hornblende grains with their long axes tangential to the surface of the sphere. Other phases present in the intergrowth are isolated anheral grains of garnet, and secondary epidote. The textural pattern suggests at least two possible origins. The texture may represent a microenvironment where nucleation of hornblende was difficult while growth was relatively easy. The hornblende crystallized from a few scattered nuclei and formed symplectic intergrowths with plagioclase, enclosing quartz and garnet grains that got in the way. An alternative possibility is a replacement texture. The enveloping pattern of prismatic hornblende is similar to the pattern around large garnet porphyroblasts in the banded amphibolite gneiss. The presence of a few isolated garnet crystals may be remnants of the original coarse grained garnet porphyroblast.

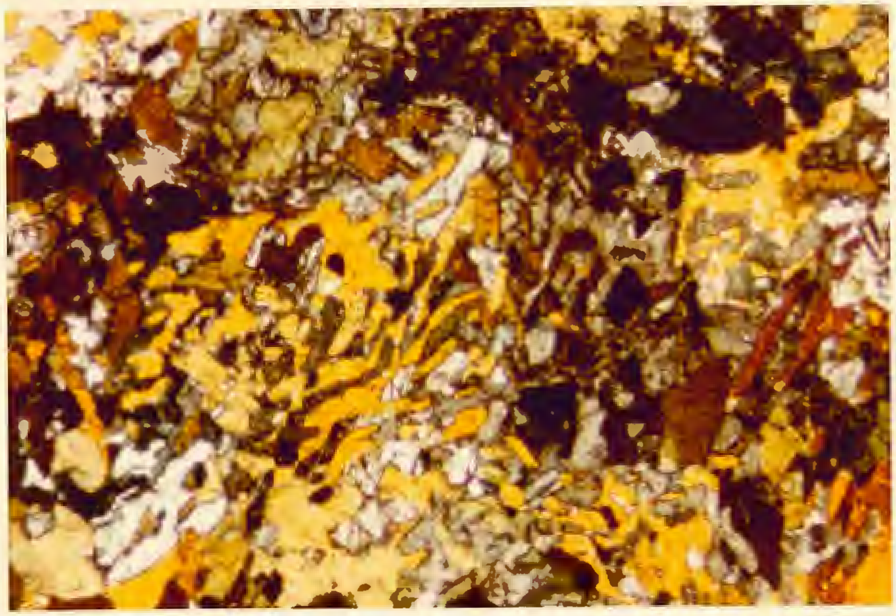

Figure 48: Intergrowth of skeletal hornblende with plagioclase and quartz. X 20 polars crossed Sample W-23

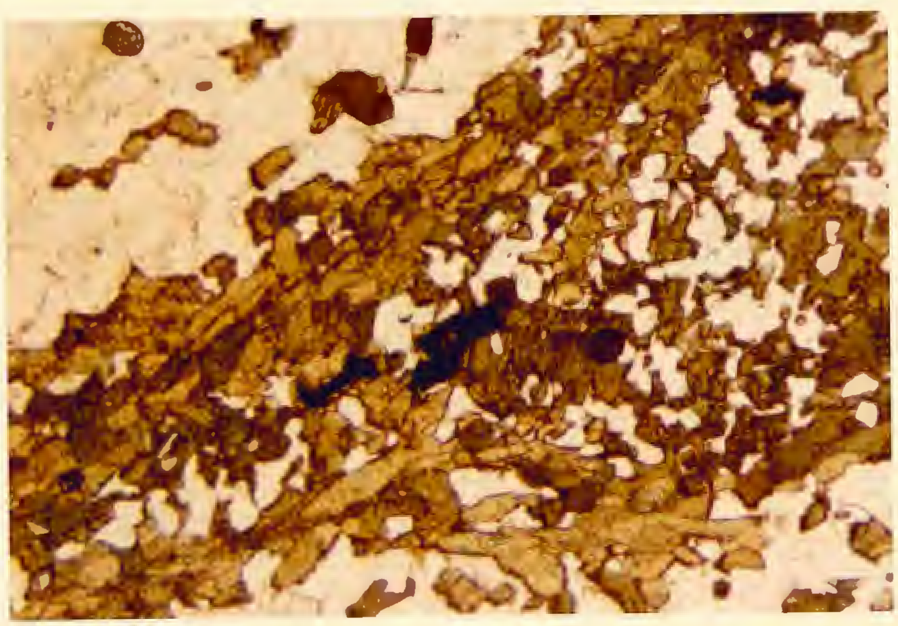

Figure 49: Lens of hornblende, quartz and magnetite surrounded by prismatic hornblende and plagioclase. X 20 uncrossed polars Sample 201Y

The other texture shown on figure 49, is a lens shaped intergrowth of hornblende and quartz with scattered ilmenite. The lens is elongate parallel to compositional banding. The lens is outlined by prismatic hornblende crystals which define a clear boundary between the interior of the lens and the surrounding rock consisting of hornblende and plagioclase. The lens is 0.7 cm. long and 0.1 cm. wide.

Hornblende and cummingtonite form irregular intergrowths that are not crystallographically oriented. Hornblende is present in all samples studied and forms individual grains as well as intergrowths in cummingtonite hosts. Cummingtonite when present in small amounts occurs only as intergrowths in hornblende.

Cummingtonite is colorless in this section, biaxial positive, with extinction angles of 20° $\gamma \angle c$ and dispersion r>v. The dispersion and high extinction angles are commonly associated with magnesium-rich cummingtonite. Prismatic habit is common (figure 50) and grains are subhedral to anhedral. Cummingtonite may be rimmed by hornblende or in some cases by biotite. Where biotite forms on the rim of cummingtonite grains the cummingtonite grain is very irregular in outline and is replaced by biotite.

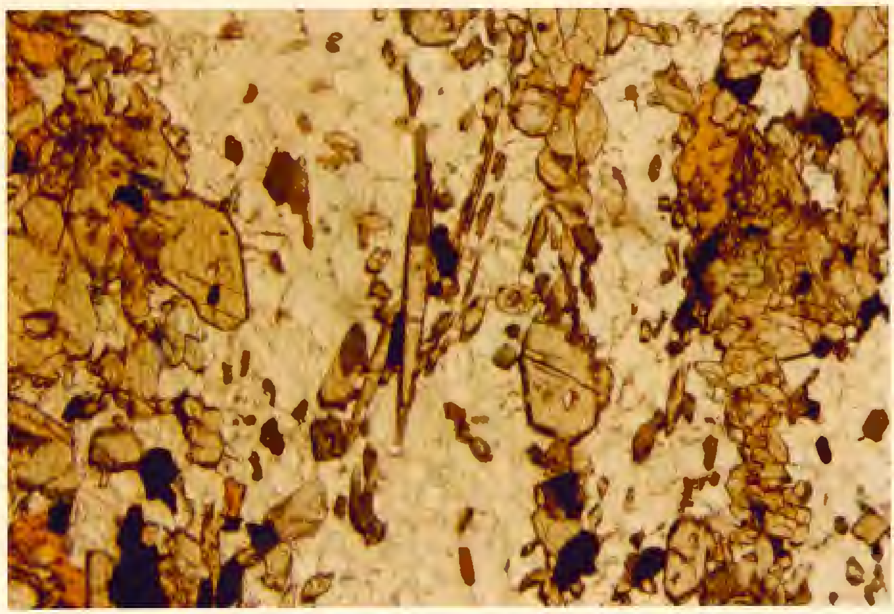

Figure 50: Prismatic cummingtonite intergrown with hornblende. Other phases include biotite, ilmenite and plagioclase. X 20 uncrossed polars. Sample W-21

Garnets are found in narrow zones associated with cummingtonite. They occur as clusters of anhedral, fractured grains with one large grain surrounded by small grains (figure 51), the clusters being up to 3 cm. in diameter. The group of grains forms a small lens in the plane of the schistosity with the schistosity wrapping around the garnet cluster. The clusters of small garnet crystals suggests that all the grains were formed by break-up of one original large grain.

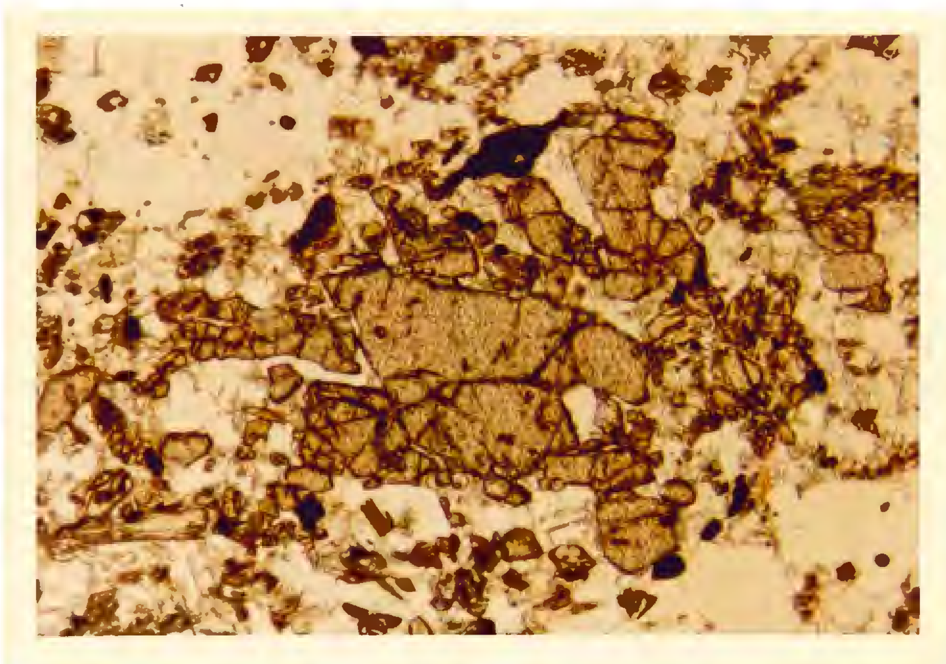

Figure 51: Garnet crystals that are fractured and fragmented. Other phases include quartz, plagioclase, cummingtonite, hornblende and ilmenite. X 20 uncrossed polars Sample 26IY

Plagioclase can be divided into three textural types similar to textures observed in the banded amphibolite gneiss. The main difference is in relative proportions of the various textural types.

Granoblastic plagioclase of grain sizes near 0.5 mm. is the most common textural type. The texture is interpreted to represent recrystallized finer grained plagioclase as proposed for type 3 plagioclase from the banded amphibolite gneiss. Albite twinning is common. Compositional zoning is developed on a regular pattern with a distinct break between the core and rim of the grain (figure 52). Optic sign is negative with high 2V. Composition, as determined by the Michel-Levy method and on grains oriented perpendicular to X, ranges from An_{45} to An_{58}. See table III. Grain boundaries approach straight lines and plagioclase-plagioclase grain intersections often approach equiangular triple points suggesting some degree of equilibration during recrystallization.

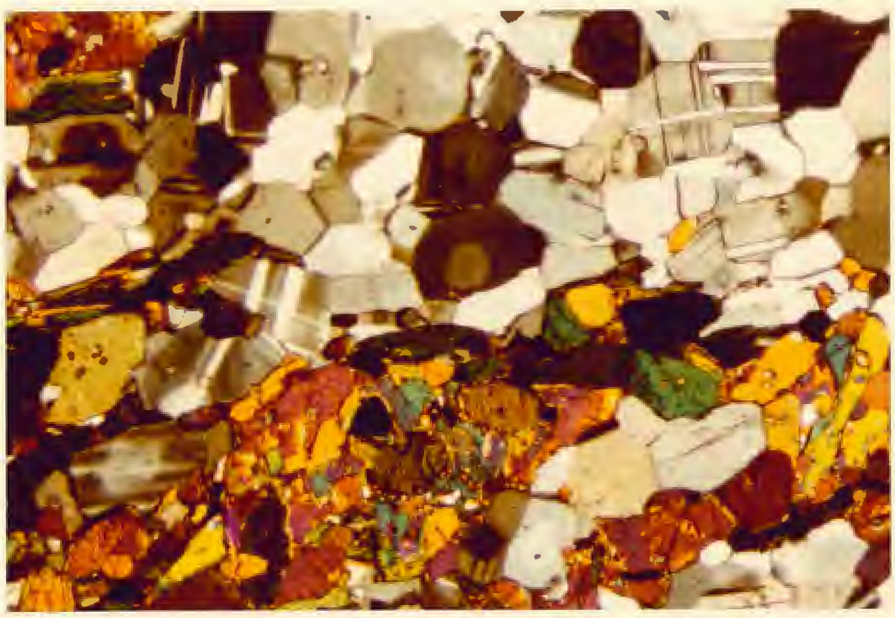

Figure 52: Recrystallized granoblastic plagioclase with albite twinning, compositional zoning and approach to triple-point grain intersections. X 20 crossed polars Sample W-29

Table III

Point Count Data (1000 Points) and Plagioclase Compositions for Samples of Amphibolite Schist

Sample Number	Hbe	Cum	Plag	Qtz	Gar	Bio	Il	Sph	Ap	An Content of Plag
W-20	78.8		19.8	0.4			0.2	0.9		
W-21	7.2	39.2	47.9	0.5	0.5	1.2	3.5			
W-22	58.5	2.8	29.7	7.1			1.2		0.6	
W-24	66.5	4.6	24.4	0.5			3.2		0.8	An_{47}
W-27	7.2	41.5	48.5	0.2	0.2		2.3		0.2	
W-30										An_{58}
W-31	62.3		33.7	2.7			1.0		0.3	
W-40	64.7		11.2	3.9			0.3	4.6	0.2	*
W-43	74.8		21.9	1.1		0.4	1.7		0.1	
10IG	59.1		25.6	12.3			2.5		0.8	
26IW	7.6	4.3	68.9	14.9		3.7	0.5		0.1	An_{47}
16IY										An_{54}
28IY	30.6		54.6	13.9			0.7		0.1	
18Iα-3										An_{47}
20Iα										An_{46}
18IB	58.3		27.0	11.9			2.8			
50E										An_{44}
51E	62.4		17.3	7.7			11.7		0.9	
52E										An_{44}

*Sample contains 14.9 percent euhedral epidote

The other two textural types-granoblastic grains about 0.1 mm. in diameter and coarse relict plagioclase grains, occur together. The two textural varieties are not common and are similar to textures described in the banded amphibolite gneiss.

An interesting textural variation occurs between plagioclase and quartz. Plagioclase and quartz occur as equigranular $\pm$ 0.1 mm. grains with some poikiloblastic plagioclase enclosing quartz. The included quartz grains are crystallographically controlled by plagioclase. Quartz inclusions in poikiloblastic hornblende and plagioclase are similar in grain size but are smaller than quartz in the rest of the rock.

In the main body of the rock quartz ranges from a trace to 15 percent. Unit extinction and granoblastic habit are typical. Quartz may occur in 6 to 10 grain trains parallel to compositional banding and may represent either elongation of original coarse grained quartz or segmentation of early veins. Quartz occurs in veins and as an accessory mineral. Quartz veins range from 5 mm. to 10 cm. wide with most veins 1 cm. wide. Vein quartz is coarsely crystalline with undulatory extinction. Vein boundaries are smooth with all bounding phases in the country rock rounded against the vein. Alteration of the surrounding rock has not been observed.

Epidote is typically an alteration mineral, but in one case is found as euhedral to subhedral prismatic grains with hornblende, plagioclase and quartz. Textural relations indicate crystallization of the hornblende and epidote to have been coeval.

Secondary alteration is limited to a set of N 80° E to fractures. Dolomite, chlorite, epidote and sericite are typical alteration phases. X-ray analysis of a 1 cm. quartz-dolomite vein with an 8 cm. alteration band indicated quartz, dolomite, and magnesian chamosite, an oxidized chlorite mineral, as the main phases in the alteration band. Thin section analysis indicates that primary compositional banding is preserved by the replacement minerals. The vein is of constant thickness for 120 feet and the alteration band varies in width.

Primary mineral assemblages in the amphibolite schist are: hornblende-cummingtonite-plagioclase, hornblende-plagioclase, hornblende-plagioclase-epidote, hornblende-cummingtonite-garnet-plagioclase, and hornblende-garnet-plagioclase, all assemblages may contain accessory quartz, sphene, biotite and apatite. The hornblende-plagioclase assemblage is the most common with the other assemblages local in extent but traceable in some cases across the entire area.

Plagioclase compositions and point count data for thin sections in the amphibolite schist are presented in table III. Total amphiboles range from 12 to 95 percent but generally from 45 to 70 percent with an average of 52 percent. Average percentage of plagioclase is 35 percent with a range from 20 to 69 percent. Quartz clusters at 1 percent and at 12 percent while ilmentite content is 1 to 2 percent with a high value of 11.7 percent.

Transition Gneisses

Primary minerals in the transition gneisses are hornblende, plagioclase, and quartz with secondary carbonate, epidote, pyrite and chlorite. The petrography of the two transition gneisses are similar and will be treated together. Petrography of major shear zones in the transition gneisses are described immediately after that.

Hornblende is not as strongly pleochroic as in the amphibolite schist or the banded amphibolite gneiss, but with the same pleochroism scheme, α - straw yellow, β - pale green, γ - pale blue green. Extinction angles are $\gamma \angle c = 18^{\circ}$, crystals are biaxial negative with 2V approximately 75°. The hornblende is poikiloblastic in the lenticular amphibolite gneiss next to the amphibolite schist, otherwise hornblende is prismatic, subhedral to anhedral. Some coarse hornblende grains have been polygonized to form smaller grains of slightly differing optical orientations (figure 53). The texture is developed near major shear bands in the thinly banded transition gneiss unit.

Cummingtonite was found in two samples, in one, intergrown with hornblende, while in the other cummingtonite occurred as individual prismatic crystals. Both samples were from finely banded feldspathic amphibolite unit.

Plagioclase compositions in the transition gneisses range from An_{45} to An_{48} with minor compositional zoning. Albite twinning is common but twin lamellae are bent (figure 54). Grain boundaries are well defined but are not straight and triple-point intersections are not equiangular. Patchy compositional zoning is found near fractures with alteration. Grain size is 1 to 1.5 mm. which is coarser than recrystallized plagioclase in either the amphibolite schist or banded amphibolite gneiss. Grain size is more similar to the relict plagioclase grains in the other two units.

Quartz rarely occurs as a primary phase, but commonly occurs with chlorite as an alteration product.

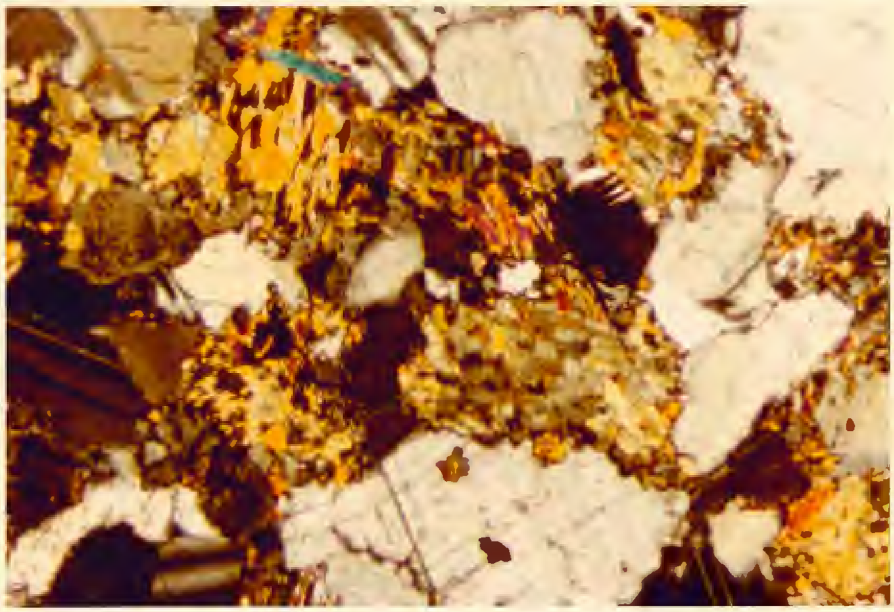

Figure 53: Polygonized hornblende crystals in transition gneisses. X 20 crossed polars Sample 54-E

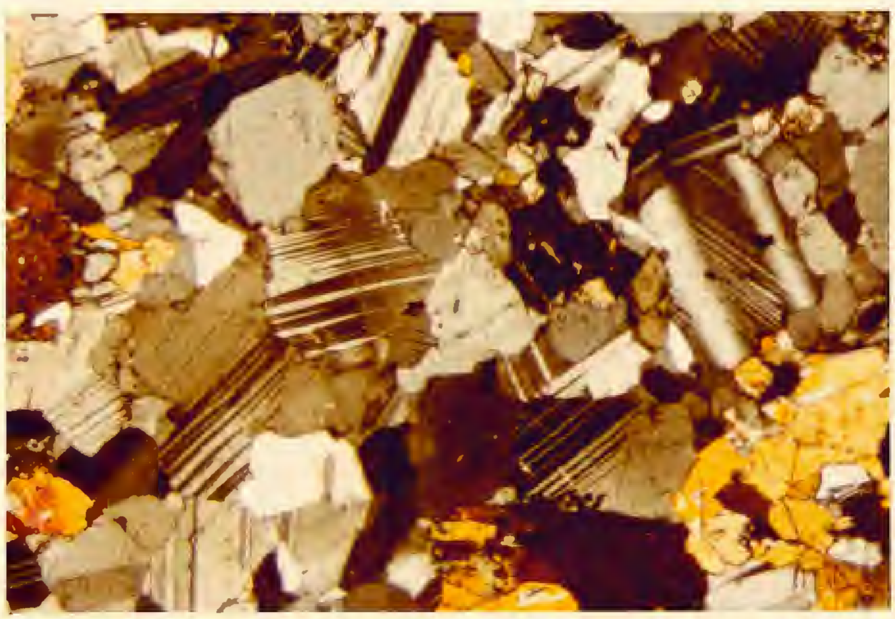

Figure 54: Bent plagioclase crystals from the transition gneisses. X 20 crossed polars Sample 54-E

Epidote, chlorite, carbonate and pyrite are secondary minerals associated with fractures. Pyrite is rimmed by epidote and chlorite in a concentric pattern. Chlorite also occurs as masses of platy crystals that cut earlier compositional banding and earlier textures. The chlorite has low first-order gray interference colors with faint green to colorless pleochroism. Chlorite is Mg- rich (negative sign of elongation) but some Fe-Mg chlorite (positive elongation, abnormal blue or violet interference colors) is intergrown with the Mg-rich chlorites (Albee, 1962).

Typical mineral assemblages of the transition gneisses are hornblende-plagioclase, and hornblende-cummingtonite-plagioclase which is not common. Table IV contains point count data and composition of plagioclase from the two transition gneisses.

Petrography of Major Shear Zones

The major north-south shear zones on the island and east bank have been described under the structure section (for map see figure 26). The black matrix of the shear zones is composed of hornblende, plagioclase quartz, apatite, epidote and sphene. Hornblende is the main mineral forming anhedral to subhedral grains that are neither bent nor sheared.

Table IV

Point Count Data (1000 Points) and Plagioclase Composition
for Transition Gneisses and Shear Zones

Sample Number	Hbe	Plag	Qtz	Opaque	Ap	Ep	Chl	Plagioclase An Content	
3E	64.6	33.6		0.3	0.4	0.1			*
0I0-1	30.7	66.3	0.7	0.2		1.6	0.4	An_{54}	
14Iδ	34.3	63.1	1.0			0.1	1.0	An_{48}	#
16Iρ	40.3	56.2	0.2				1.9	An_{63}	+
s-16	33.0	64.4	0.1	0.1		0.7	1.3	An_{45}	
1E	60.6	39.0	0.1	0.3				An_{48}	

* Contains 1.0 percent sphene

0.3 percent carbonate

+ contains 1.3 percent cummingtonite

Some hornblende grains, confined to narrow bands, contain fine ilmentite inclusions as described in the amphibolite schist. One-crystal-wide bands of ovoid apatite grains form compositionally distinct lines in the predominantly hornblende matrix. Sphene forms anhedral masses of crystals that are also segregated into compositional bands. Epidote is subhedral with prismatic habit and like plagioclase is more typical of the lighter colored rocks of the shear zone than in the black matrix. Significant features of the shear zone rocks are: 1) similarity of textures between matrix and isolated tectonic inclusions, 2) lack of alteration within the matrix, and 3) the recrystallized textures in the matrix and included blocks. These features indicate that recrystallization occurred after the main deformation. This fact sets the shear zones apart from brecciated and crushed zones associated with later faults.

Feldspathic Gneiss

The feldspathic gneiss is rich in plagioclase with hornblende occurring as a minor phase; cummingtonite sphene and apatite have been found locally. Muscovite, carbonate, epidote, chlorite, quartz and pyrite are alteration phases.

Textural features of plagroclase are similar to those observed in the banded amphibolite gneiss. Hornblende is of two grain sizes also typical of the banded gneiss but hornblende is present in lesser amounts in the feldspathic gneiss.

Alteration is associated with faults and fracture systems of a general N 80° E trend. Alteration extends into the surrounding rock from the central fracture by as much as 15 centimeters. Two compositions of chlorite are also present, the main chlorite is a Mg-rich chlorite but small amounts of Fe-Mg chlorite can be found.

Table V contains point count data from thin sections of the feldspathic gneiss. The modal values compare with the values obtained in the banded amphibolite gneiss except for the much higher percentage of plagioclase typical of the feldspathic gneiss. The mineral assemblage hornblende-plagioclase is the most important with the hornblende-cummingtonite-plagioclase insignificant by comparison.

Table V

Point Count Data (1000 Points) for the Feldspathic Gneiss

Sample Number	Plag	Hbe	Ap	Ep	Chl	Carb	Sph	Musc	Ilmen	
15M	83.9	15.7	0.2						0.2	
11K-1	51.8	40.2			1.6				0.5	An_{53}*
6E	76.3	22.7		0.3	0.3				0.3	
11E2	89.1	10.4		0.6						
5J	86.5	8.8		3.2	0.9	0.3		0.1	0.2	
15J	60.6	31.6		4.9	1.1			1.3		#
2KM	84.1	15.0		0.4	0.5					

* Contains 1.1 percent quartz and 4.8 percent cummingtonite

Contains 0.4 percent quartz

Summary of Petrographic Data

Several conclusions about the metamorphic history of Big Falls can be drawn from textual evidence.

1) Interpretation of plagioclase textures

Textual relationships, especially in plagioclase, indicate disequilibrium conditions during recrystallization. Several lines of evidence support this conclusion: a) Relict plagioclase grains, common in the banded amphibolite gneiss and the feldspathic gneiss, and to a lesser extent in the amphibolite schist, with strong irregular compositional zoning and development of a wide range of grain sizes are typical of disequilibrium textures. Plagioclase crystals range in size from 0.1 mm. to 2 mm. in diameter. The development of strong compositional zoning is an early step in the disintegration of a plagioclase grain until the original grain is composed of granoblastic fine-grained plagioclase. Ca and Al are released from the plagioclase under conditions of lower temperature, accompanied by stress, and the zoning pattern is the result of differential stress on the crystal. b) Strongly sutured grain boundaries between plagioclase grains indicate a lack of equilibration during recrystallization. Gently curved grain boundaries in the amphibolite schist and locally in the banded amphibolite gneiss indicate a local approach to equilibrium. c) In the banded amphibolite gneiss and the feldspathic gneiss equiangular triple-points are commonly lacking. Most plagioclase grains do not meet at triple-points and where triple-points are present they are not equiangular. Again triple-points and triple-points approaching equiangularity can be found in the amphibolite schist and locally in the banded amphibolite gneiss. d) Granoblastic plagioclase in the amphibolite schist are compositionally zoned with a distinct compositional break between the core and rim of the grain. Where straight grain boundaries and triple-points are present the rims of grains approached equilibrium with the surrounding rock. However, the core of the grain cannot be assumed to be in equilibrium with the surrounding rock.

2) Interpretation of hornblende-garnet relations

Textural relations between coarse garnet porphyroblasts and hornblende suggest a replacement of garnet by hornblende. Three aspects of the garnet porphyroblasts in the banded amphibolite gneiss indicate a replacement. a) The garnet porphyroblasts are older than the surrounding and intergrown hornblende. Garnet inclusions are common in the coarse intergrown hornblende grains.

b) Hornblende crystals occur as sheaths around the coarse garnets, totally separating the garnet from the surrounding rock. Since the garnets are not in direct physical contact with the enclosing rock a major incompatability may exist, with hornblende developing between the two incompatible systems. c) Clots of coarse hornblende form pseudomorphs after garnet. The hornblende clots show typical textures associated with the garnet porphyroblasts except that there is no garnet. Textures in the amphibolite schist are less convincing. Garnets are fractured and separated into lenticular groups of grains that are wrapped by compositional banding. The garnets are earlier than the surrounding compositional layering. Skeletal intergrowths of hornblende with plagioclase and quartz with isolated garnet grains may represent replaced garnet porphyroblasts. The presence of a sheath of hornblende grains around the intergrowth is similar to replacement textures in the banded amphibolite gneiss.

The replacement reaction of hornblende after garnet, in most cases, did not go to completion.

Hornblende recrystallized under two different sets of metamorphic conditions as evidenced by differences in grain size and texture. a) Two distinct sizes of crystals are present in the banded amphibolite gneiss. 1 mm. long hornblende grains are typical in the main body of the rock unit, in some cases the prismatic habit of the grains has been affected by separation along cleavage. 2 to 4 mm. hornblendes are associated with isolated clots, hornblende-rich compositional bands, and around garnet porphyroblasts. Coarse hornblende is restricted to preferred sites. b) Two distinct grain sizes are also found in the feldspathic gneiss. c) The two different grain sizes in the amphibolite schist are texturally dissimilar. The coarse hornblende grains are anhedral, nearly equant and contain fine opaque dust. The grains characteristically show evidence of fracturing. Fine grained hornblende is prismatic, subhedral and lacks the fine inclusions. The coarse hornblende grains are older than the prismatic grains. d) Orientation of coarse hornblende in the banded amphibolite gneiss is often at an angle to the crude orientation of the fine hornblende. Two directions of orientation of hornblende and compositional banding are common in the amphibolite schist. Tectonic clasts in the feldspathic gneiss have internal foliations that are different from external foliations, in both cases the foliation is defined by hornblende grains. The occurance of different orientations of hornblende grains in the three units indicates recrystallization of hornblende under two different stress conditions.

Epidote is typically subhedral to euhedral and crystallized late. Euhedral grains cross-cut earlier structures in the banded amphibolite gneiss.

3) Paragenetic synthesis

Three separate recrystallizations are represented in the textural suite. The minerals and textures associated with each recrystallization include:
a) The only surviving evidence of the first recrystallization is the coarse garnet porphyroblasts in the banded amphibolite gneiss and the fractured garnets in the amphibolite schist. The garnets predate the deformation of the compositional banding that is wrapped around them. The alteration and replacement evidence indicates that the garnets recrystallized under conditions that were different from conditions that the rest of the minerals formed under. b) The second recrystallization is represented by relict plagioclase grains and fine hornblende in the banded amphibolite gneiss. In the amphibolite schist coarse hornblendes with opaque inclusions may be the relics of the second recrystallization as well as local patches of relict plagioclase. c) The third recrystallization is associated with polygonization of plagioclase produced under the second recrystallization and the recrystalization of

hornblende to produce the coarse hornblende in the hornblende-rich compositional bands of the banded amphibolite gneiss. The main new phase to appear is epidote and possibly sphene is a late arrival. Recrystallization was extensive in the amphibolite schist with formation of hornblende, cummingtonite, plagioclase and quartz. Epidote crystallized only in restricted bands. The third recrystallization was not extensive in the transition gneisses but was extensive in the feldspathic gneiss. Figure 55 shows the times of recrystallization of the various phases with reference to the three recrystallizations determined by textural relations.

Major north-south trending shear zones in the transition gneisses were developed before the third recrystallization. Textures in the fault zones indicate extensive recrystallization since deformation and the fault zones cut textures and structures produced during the second recrystallization placing the event somewhere between the second and third recrystallizations.

Alteration of earlier phases occurs predominantly along northeast trending fractures and faults of general azimuth N 85^{o} E.

Figure 55: Inferred Times of Recrystallization of Various Phases*

	Recrystallization			
	First	Second	Third	Alteration
Hornblende	?	1 mm. subprismatic anhedral with opaque inclusions	+1.5 mm. prismatic subprismatic	
Cummingtonite		?	subprismatic prismatic	
Plagioclase	?	1.5-2.0 mm. grains	polygonized 0.1 mm. recrystallized 0.5+	
Garnet	Coarse anhedral	fine euhedral		
Quartz			anhedral grains	veins and fractures
Epidote			prismatic	along fractures
Sphene		?	anhedral associated with hornblende	
Chlorite			?	along fractures

*Based on textures observed in thin section

Chemistry

Chemical data for major phases and bulk rock compositions of the banded amphibolite gneiss and the amphibolite schist were determined to study variations within and between the different rock units.

Banded Amphibolite Gneiss

Microprobe analyses of coexisting major phases was completed for two thin sections from the banded amphibolite gneiss. The compositions of hornblende, garnet, plagioclase and epidote were determined from different associations of the minerals.

Three hornblende grains were analyzed from thin sections WP-7 and 7-29-72 (Table VI). Hornblende WP-7 P1-1 is from a hornblende-rich compositional band, hornblende WP-7 P2-1 is from a plagioclase-rich band, and hornblende from 7-29-72 is intergrown with garnet.

The analyzed hornblende grains in sample WP-7 are very similar in composition. Both hornblende grains contain small amounts of the cummingtonite molecule. Titanium is significant at weight per cents of 1.12 for WP-7 P1-1 and 1.18 for P2-1 WP-7. Hornblendes from the highest temperatures in the amphibolite facies rarely exceed 2.0 weight per cent TiO_2 (Leake, 1972).

Table VI

Hornblende Compositions from the Banded Amphibolite Gneiss

Oxide	WP-7 P1-1	WP-7 P2-1	7-29-72
SiO_2	41.97	43.43	42.59
Al_2O_3	13.65	14.07	18.76
TiO_2	1.12	1.18	0.27
FeO*	17.79	18.64	15.44
MgO	7.99	7.59	6.87
MnO	0.42	0.35	0.48
CaO	11.21	11.18	10.92
Na_2O	0.43	0.58	0.59
K_2O	0.34	0.34	1.13
Total	94.92	97.36	97.79

*All Fe as FeO

For recalculation of data see Appendix II.

Elemental Ratios for Hornblende from the Banded Amphibolite Gneiss

Ratio	WP-7 P1-1	WP-7 P2-1	7-29-72
$\frac{100\ Mg}{Mg + Fe}$	44	42	45
$\frac{100\ Mg}{Mg + Fe + Mn}$	42	42	44

Hornblende 7-29-72, adjacent to garnet, is comparatively low in titanium, iron and magnesium but high in aluminum. This pattern results from the tschermakite molecule being more abundant in 7-29-72 than in either hornblendes in WP-7 (see Appendix II).

Aluminum in six fold coordination greater than 1.00 ion per formula unit (based on 23 Oxygen) has been proposed by Leake (1968) as a prerequisite for fixing the prefix alumino to the amphibole name. Hornblende 7-29-72 easily qualifies to be an alumino-hornblende while the other two hornblendes (WP-7) do not contain enough aluminum. (see Appendix II).

In the above discussion iron has been assumed to be ferrous iron. The presence of ferric iron is not differentiated by microprobe analytical techniques and all iron is reported as FeO. Without independent determination of the Fe^{+3} component the amphibole end members cannot be calculated exactly and only an approximation of the ferric component can be made. It is possible for nearly half the total iron to occur as Fe^{+3} in the calcic amphiboles produced under metamorphic conditions (Deer, et al., 1963). Different methods of estimation have been based on stoichiometric and chemical considerations. Phillips and Layton (1964) proposed that an estimate can be derived from the valence balance in the structural formula.

In the basic atomic formula, derived by converting all Al, Fe^{+3} and Ti^{+4} substitution in the Y sites to equivalent aluminum (Al^{Y}) and all Na^{+} and K^{+} substitution in the A and X sites to sodium (Na^{A} and Na^{X}), the valency balance relationship:

$$Na^{A} + Al^{Y} = Na^{X} + Al^{Z}$$

must be satisfied. A difference in the two sides of the equation reflects the amount of ferric iron that can be present. The presence of Fe^{+3} would increase the value of Al^{Y}. From the three analyzed amphiboles the $Na^{A} + Al^{Y}$ is slightly lower than $Na^{X} + Al^{Z}$ either reflecting a small proportion of the iron is trivalent iron or error in the microprobe data which is suggested by low total weight percentages for the analyses.

Garnet 7-29-72 is a large garnet porphyroblast intergrown with hornblende of which hornblende 7-29-72 is a representative. Only one analysis was performed on the grain; compositional zoning was not investigated. In table VII all iron has been considered ferrous and all calcium has been assumed to be in grossular. The presence of Ti in the garnet suggests a small percentage of the andradite molecule but this has been ignored in the calculations. The ratio of magnesium to iron is typically lower in garnet than in coexisting ferromagnesian silicates as well as the bulk rock (Deer, et al., 1962, p. 88). For coexisting hornblende 7-29-72 and garnet 7-29-72 the ratio for garnet is less than half that for hornblende.

Table VII

Garnet 7-29-72, Elemental Ratios and Weight Percentages

Oxide	Weight Percent	Garnet End Members Molecular %
SiO_2	38.02	
Al_2O_3	20.34	Alm. 57.7
TiO_2	0.12	Gross. 24.2
FeO*	25.69	Pyr. 14.2
MgO	3.56	Spess. 3.8
MnO	1.66	
CaO	8.40	
Total	97.79	

*All iron as FeO

Elemental ratios based on ionic proportions

$$\frac{100\ Mg}{Mg + Fe} = 20 \qquad \frac{100\ Mg}{Mg + Fe + Mn} = 19$$

For recalculation of data see Appendix II

One grain of epidote, associated with hornblende WP-7 P2-1, plagioclase and sphene, was analyzed. No attempt was made to analyze for compositional zoning. Table VIII contains the analysis for epidote WP-7 P2-4, Column 1 assumes all iron is present in the ferrous state and Column 2 all iron is assumed in the ferric state. Recalculation of the results on the assumption that all iron is present in the ferric state is in close agreement with constraints imposed from the structural formula (Appendix II). One Fe^{+3} ion can substitute for aluminum in the formula unit, WP-7 P2-4 epidote contains 0.83 ions indicating oxidation during crystallization of epidote. The total weight percent for the probe analysis may be high since epidote may contain from 0.50 to 3.50 weight percent water.

Table VIII
Epidote WP-7 P2-4

Oxide	All Ferrous	All Ferric
SiO_2	39.92	38.26
Al_2O_3	25.31	24.26
TiO_2	0.28	0.27
Fe_2O_3		14.26
FeO	9.82	
CaO	23.75	22.77
MnO	0.19	0.18
Total	99.27	100.00

Determination of the anorthite content in plagioclase from sample WP-7 by microprobe was not extremely successful. Two analyses were made to determine the compositional range of zoning within a single grain. First estimates of composition were by graphical comparison of the weight percents Al_2O_3, SiO_2, CaO against anorthite content. The anorthite content for each oxide indicates agreement between SiO_2 and CaO while values for Al_2O_3 were low. SiO_2 determination in plagioclase has been reported to be lower than would be expected by stoichiometric considerations in several analyses (Deer, et al., 1962) therefore an average anorthite content based on CaO and SiO_2 was used to recalculate the weight percent of Al_2O_3 and Na_2O (table IX). No attempt was made to correct values for potassium. Recalculated results indicate a compositional difference of approximately ten percent anorthite in the grain.

Whole rock chemical analyses of two samples from banded amphibolite gneiss zones I and IV reflect the extremes in composition of the rock as qualitatively determined in the field (table X). Unusually high weight percentages of Al_2O_3 and CaO with low values for femic components reflect the high modal percentages of plagioclase in the unit.

Table IX
Recalculation of Plagioclase Compositions

Sample WP-7 P2-3

	Probe Values		Recalculated Values	
Oxide	Weight Percent	% An *	Recalculated Wt.	% Change
SiO_2	53.00	61.5	53.00	
Al_2O_3	26.77	42.6	29.75	+ 2.98
Fe_2O_3	0.20		0.20	
CaO	11.99	58.6	11.99	
Na_2O	2.63		4.44	+ 1.81
K_2O	0.05		0.05	
Total	94.52		99.43	

Average An % SiO_2 + CaO = 60.5%

Recalculated value $An_{59.7}$/ $Ab_{40.0}$ / $Or_{0.3}$

Sample WP-7 P2-2

	Probe Values		Recalculated Values	
Oxide	Weight Percent	% An *	Recalculated Wt.	% Change
SiO_2	55.22	52.5	55.22	
Al_2O_{33}	25.11	32.6	28.20	+3.09
Fe_2O_3	0.09		0.09	
CaO	9.97	49.4	9.97	
Na_2O	3.68		5.57	+1.88
K_2O	0.04		0.04	
Total	94.08		99.09	

Average An % SiO_2 + CaO = 50.8%

Recalculated value $An_{49.6}$ / $Ab_{50.2}$ / $Or_{0.2}$

*Determined graphically

Table X
Chemical Analyses for Whole Rock Samples from the Banded Amphibolite Gneiss

	Weight percent			Niggli Values	
Oxide	W1C	W2C		W1C	W2C
SiO_2	49.53	47.75	al	34.9	37.5
Al_2O_3	23.72	25.63	alk	8.0	6.0
TiO_2	0.28	0.33			
Fe_2O_3	1.23	1.28	mg	0.504	0.324
FeO	4.17	4.53	fm	22.6	17.7
MgO	3.05	1.55	si	135.7	127.9
MnO	0.08	0.08	c	34.5	38.8
CaO	12.89	14.61	k	0.064	0.082
Na_2O	3.09	2.29			
K_2O	0.32	0.31			
P_2O_5	0.11	0.11			
CO_2	0.22	0.26			
H_2O	1.32	0.95			
Total	99.83	99.68			

Chemical analyst
K. Ramlal
University of Manitoba

CIPW Norms

Mineral	W1C	W2C
Diopside	9.81	9.60
Olvine	0.57	
Hypersthene	8.31	5.88
Orthoclase	1.89	1.83
Albite	23.53	16.28
Anorthite	51.30	60.38
Quartz		1.40
Apatite	0.26	0.26
Magnetite	1.78	1.86
Ilmenite	0.53	0.63
Calcite	0.50	0.59

Sample WIC is from zone I which contains a higher percentage of hornblende and contains garnet porphyroblasts. Sample W2C is from zone IV where hornblende is less common and large garnet porphyroblasts are absent. W2C is east and north of sample WIC (see figure 3). Various ratios for the banded amphibolite gneiss point out several interesting relationships. The ratios of K_2O / Na_2O are extremely low, 0.103 and 0.135 respectively. The oxidation ratios, $2Fe_2O_3$/ ($2Fe_2O_3$ + FeO), for W1C is 0.371 and for W2C is 0.362. The ratio 100 Mg / (Mg + Fe) ranges from 52 to 34, values which bracket the same ratio values for hornblendes WP-7 and 7-29-72, but are higher than the same ratio for garnet 7-29-72. The femic components are lower in WIC than in W2C reflecting a decrease in hornblende, but it should be noted that the hornblende is probably more iron-rich in W2C as suggested by the ratio 100 Mg / (Mg + Fe) and the fact that magnesium is lower in W2C than in W1C while iron is higher. CIPW norms reflect fewer ferro-magnesian phases in W2C than in W1C. The presence of normative olivine in W1C and normative quartz in W2C indicate near saturation with respect to silica. The increase in normative anorthite accompanied by a decrease in normative albite reflects a higher weight percent of Na_2O in W1C than in W2C and suggests that anorthite content of plagioclase is greater in W2C.

Amphibolite Schist

Major phases in three thin sections from the amphibolite schist were subjected to microprobe analysis. Coexisting hornblende, cummingtonite and garnet were analyzed in section W-21, hornblende and plagioclase in section W-29 and hornblende in section W-24. The amphibole phases will be considered first, followed by garnet and plagioclase.

Hornblende from sample W-29 was analyzed as a representative grain of prismatic hornblende described under the section on petrography (p. 75). Cummingtonite is a major end member component accounting for nearly 25 mole percent of the hornblende (appendix II). Magnesium is greater than iron in the ionic formula and calcium is greater than 1.50 ions per formula unit indicating a calcic amphibole.

Hornblende W-24 is a typical grain of coarse hornblende with fine opaque inclusions described in the section on petrography (p. 76). Analysis of hornblende W-24 was from the inclusion free rim that surrounds this type of grain (table XI). Hornblende W-24 is calcic and has magnesium greater than iron in the ionic formula. The cummingtonite molecule forms about 25 mole percent of the hornblende.

Table XI
Hornblende W-29 and Inclusion in W-24

Oxide	W-29	W-24	Inclusion
SiO_2	40.32	41.78	31.74
Al_2O_3	14.02	13.12	8.03
TiO_2	0.75	0.90	11.19
FeO*	15.83	16.93	18.13
MgO	10.90	10.91	6.34
MnO	0.29	0.48	0.48
CaO	10.37	10.76	7.16
Na_2O	0.67	0.62	
K_2O	0.34	0.22	
Total	93.49	95.24	83.07

*All iron as FeO

The approximate composition of the included opaque phase is given in table XII, but because of the lack of appropriate standards and fine grained nature of the inclusions the results are of questionable value. The inclusions are high in titanium and iron.

Coexisting hornblende, cummingtonite and garnet were analyzed in section W-21. Hornblende W-21 is intergrown with a large cummingtonite grain, the typical relationship of the two phases in section W-21. The hornblende is strongly subcalcic, also reflected in low values of Al_2O_3 (table XII), and very high in the cummingtonite end member (appendix II).

Table XII
Cummingtonite, Hornblende and
Garnet from Section W-21

Oxide	Weight Percent Hornblende	Cummingtonite	Garnet
SiO_2	46.85	53.79	37.92
Al_2O_3	8.04	1.06	19.46
TiO_2	0.40	0.02	
FeO	21.29	23.24	29.11
MgO	14.68	16.96	2.65
MnO	0.36	0.52	2.80
CaO	5.20	0.52	3.59
Na_2O	0.77		
K_2O			
Total	97.59	96.11	95.23

Garnet End Members

Molecular Percent

Alm.	70.4
Spess	6.9
Pyr	11.5
Gross	11.1

The associated cummingtonite grains are richer in silica than coexisting hornblende and very low in calcium and aluminum. Both hornblende and cummingtonite W-21 have more magnesium than iron in the ionic formula. Magnesium greater than iron is evident in the elemental ration 100 Mg / (Mg + Fe) (table XIII).

Table XIII
Elemental Ratios for Hornblende, Cummingtonite and Garnet from the Amphibolite Schist

Ratio	Hbe W-29	Hbe W-24	Hbe W-21	Cum W-21	Gar W-21
$\frac{100\ Mg}{Mg + Fe}$	55	53	54	58	13
$\frac{100\ Mg}{Mg + Fe + Mn}$	55	52	54	58	12

The ratio 100 Mg / (Mg + Fe) for all analyzed amphiboles from the amphibolite schist are fairly constant with the ratio for cummingtonite higher in the hornblende associated with cummingtonite than in either hornblende W-29 or W-24. The weight percent of magnesium and iron in hornblende and cummingtonite W-21 is much greater than in other hornblendes in the rock.

Garnet W-21 is almandine rich, with 100 Mg / (Mg / (Mg.+ Fe) considerably lower than any hornblende or cummingtonite in the amphibolite schist.

Determination of plagioclase composition from the amphibolite schist required recalculation by the method described earlier. Core and rim of zoned plagioclase from W-29 and composition of a weakly zoned plagioclase from W-24 were analyzed (table XIV).

Table XIV
Plagioclase Recalculations for the
Amphibolite Schist

Sample W-24

Oxide	Probe data	Recalculated
SiO_2	57.59	59.35
Al_2O_3	25.60	25.76
Fe_2O_3	0.18	0.18
CaO	7.47	7.42
Na_2O	6.38	6.38
K_2O	0.06	0.06
MnO	0.18	0.18
Total	97.46	99.33

Sample W-29 core

Oxide	Probe data	Recalculated
SiO_2	59.10	62.12
Al_2O_3	23.84	23.83
Fe_2O_3	0.11	0.11
CaO	5.18	5.25
Na_2O	6.51	7.30
K_2O	0.05	0.05
Total	94.79	99.11

Sample W-29 rim

Oxide	Probe data	Recalculated
SiO_2	52.39	57.23
Al_2O_3	26.76	27.15
Fe_2O_3	0.24	0.24
CaO	9.40	9.05
Na_2O	3.77	5.80
K_2O	0.05	0.05
Total	92.61	99.52

The zoned plagioclase in W-29 has a calcium rich rim and a sodium rich core indicative of reversed compositional zoning. The overall composition of plagioclase from the amphibolite schist is in the andesine range. Minor amounts of iron were found in all samples.

Whole rock compositions for selected samples were calculated from modal analyses and the composition of the phases from microprobe data and published data for minor phases. Three calculated whole rock compositions are presented in Table XV. Sample W-31 is a typical hornblende amphibolite, sample W-21 is a cummingtonite-garnet amphibolite and W-22 is a cummingtonite amphibolite with cummingtonite the minor amphibole phase. For sample W-31 ilmenite is the opaque phase and plagioclase composition has been arbitrarily set at An_{39} in order to use plagioclase analysis W-24. For sample W-21 the An_{39} plagioclase composition is used and ilmenite is the opaque phase. The biotite composition is from the literature for a comparable assemblage. Sample W-22, cummingtonite from W-21 and hornblende from W-24 are used. The calculated results have been normalized in preparation of CIPW norms. 100 Mg / (Mg + Fe) ratios for the three samples range from 52 to 54 indicating cation percentages of magnesium greater than

Table XV
Calculated Whole Rock Compositions for the Amphibolite Schist

Oxide	W-21	W-22	W-31
SiO_2	54.00	49.83	47.82
Al_2O_3	13.67	15.88	17.41
TiO_2	1.90	1.07	1.00
FeO	12.68	10.50	10.36
MgO	7.88	6.38	6.80
MnO	0.24	0.16	0.18
CaO	4.15	8.63	9.13
Na_2O	3.12	2.28	2.57
K_2O	0.13	0.22	0.23
P_2O_5	-----	0.25	0.13
Total	97.77	95.70	95.63

CIPW Norms

Mineral	W-21	W-22	W-31
Diopside		7.6	7.6
Olivine			9.3
Hypersthene	40.0	31.8	18.8
Orthoclase	1.0	1.5	1.5
Albite	29.0	21.5	24.0
Anorthite	21.5	34.0	37.0
Corundum	0.8		
Quartz	5.0	1.5	
Apatite		0.5	0.3
Ilmenite	2.6	1.6	1.4

Modes

Mineral	W-21	W-22	W-31
Hornblende	7.2	58.5	62.3
Cummingtonite	39.2	2.8	
Garnet	0.5		
Plagioclase	47.9	29.7	33.7
Quartz	0.5	7.1	2.7
Apatite		0.6	0.3
Ilmenite-magneite	3.5	1.2	1.0
Biotite	1.2		

iron. Normative minerals indicate silica saturation in both W-21 and W-22, the cummingtonite bearing samples, while sample W-31 is silica under-saturated with normative olivine. Normative anorthite increases from sample W-21 to W-31. Albite is greater than anorthite in W-21 reflecting low contribution of calcium from modal subcalcic hornblende and cummingtonite. Normative hypersthene, diopside and olivine are based on the magnesium end member, 56 percent, and the iron end member, 44 percent.

Feldspathic Gneiss

The compositions of two samples (Table XVI) from the feldspathic gneiss were calculated using modal analyses and mineral compositions from the banded amphibolite gneiss. Minerals in the two units are optically similar and are assumed to be compositionally similar. Hornblende WP-7 Pl-1 (see Table VI) was used in the calculation, and plagioclase WP-7 (see Table IX) with $An_{50.8}$ was selected for agreement with an observed value of An_{53} in the feldspathic gneiss. The samples selected are representative of the majority of specimens collected in the feldspathic gneiss but do not reflect some of the minor zones high in percentage of amphibole.

Table XVI
Calculated Whole Rock Compositions from the Feldspathic Gneiss

Oxide	Sample 15M	11E2
SiO_2	52.92	53.79
Al_2O_3	25.80	26.69
TiO_2	0.18	0.12
Fe_2O_3	0.07	0.16
FeO	2.79	1.85
MgO	1.25	0.83
MnO	0.06	0.05
CaO	10.12	10.18
Na_2O	4.74	5.00
K_2O	0.08	0.07
Total	98.01	98.74

	Modes	
Plagioclase	83.9	89.1
Hornblende	15.7	10.4
Apatite	0.2	
Epidote		0.6

Summary of Chemical Data

Several chemical differences in the composition of single phases and the whole rock in the amphibolite schist, banded amphibolite gneiss and feldspathic gneiss are significant in interpreting the petrology and protolith of the units. Chemical variation in phases common to the amphibolite schist and banded amphibolite gneiss will be considered first followed by consideration of differences in whole rock chemistry among the three units.

In hornblendes from the two units, the most apparent difference arises from the importance of the cummingtonite and tschermakite molecules, reflected by the number of ions normally assigned to the Y sites during calculation of the ionic formulas. In the amphibolite schist the Y sites are occupied mainly by iron and magnesium reflecting low tschermakite molecular percentage. The placing of magnesium and iron into the X sites reflects high cummingtonite molecular percentages. In the banded amphibolite gneiss aluminum is important in the Y sites reflecting higher percentages of the tschermakite molecule. Low iron and magnesium in the X sites indicates minor cummingtonite molecule (see appendix II). Hornblende in the amphibolite schist is richer in magnesium than iron while the opposite is true in the banded amphibolite gneiss, as reflected in higher values for the ratio 100 Mg / (Mg + Fe) in the amphibolite schist (53-58) than in the banded amphibolite gneiss (42-45). TiO_2 is nearly the same between the two units with less reported in the amphibolite schist. The main TiO_2 difference in hornblende is from hornblende inter-grown with garnet (7-29-72) in the banded amphibolite gneiss where TiO_2 values are much lower than in other hornblendes.

Garnets are almandine rich in both units, but garnets in the amphibolite schist is 70 percent almandine while in the banded gneiss the garnet is 58 percent almandine. The grossular component is greater in the banded amphibolite gneiss (24 percent) than in the amphibolite schist (11 percent). 100 Mg / (Mg + Fe) illustrates iron greater than magnesium in the garnets, with garnets in the amphibolite schist more iron-rich (13.0) than garnets from the banded amphibolite gneiss (20.0).

The most significant difference in plagioclase compositions must be thought of in terms of compositional variation observed in zoning. The pattern of zoning in the amphibolite schist is predictable and regular with calcium-rich rims and sodium-rich cores, while zoning in the banded amphibolite gneiss is irregular with no definite pattern between calcium-rich and calcium-poor areas. The composition of the 0.1 mm. plagioclase is not known and might be of interest compared to the coarse parent plagioclase grains. Anorthite content in plagioclase from the banded amphibolite gneiss is higher than in the amphibolite schist.

Comparison of whcle rock chemistry shows a marked contrast in the weight percent of Al_2O_3 and CaO among the three units. The difference is tied to modal differences in the percentage of plagioclase and the composition of the coexisting amphibole. The various elemental ratios were not calculated for the feldspathic gneiss because no independent mineral composition determinations were made for the unit. Iron and magnesium are higher in the calculated composition of the amphibolite schist and contrasting 100 Mg / (Mg + Fe) ratios indicate magnesium greater than iron in the amphibolite schist and total iron greater than magnesium in the banded amphibolite gneiss. The change is one of the most significant changes between the two units. K_2O / Na_2O ratios in the amphibolite schist are low, as in the banded amphibolite gneiss, however, the ratios in the amphibolite schist may be artificially low due to error in analysis.

Protolith

Protolith for the schists and gneisses at Big Falls is based on arguments from the chemistry of the individual phases and the whole rock which suggest a basic igneous protolith and specifically imply a differentiated sequence.

Preliminary spectral analysis, by scanning electron microscope, of hornblendes from the amphibolite schist indicate trace amounts of vanadium, nickel and chromium, elements usually contained in the structures of olivine, pyroxene and spinels in gabbros or other mafic igneous rock types.

Table XVII contains analyses of rocks known to range from gabbros to anorthosites. Comparison of the whole rock composition of the banded amphibolite gneiss (see Table X) with the first four columns in Table XVII suggest an original anorthositic gabbro, possibly a labradorite cumulate as in column 2. Column 4 is an anorthosite from the Duluth Gabbro Complex which compares favorably with the calculated composition of the feldspathic gneiss (Table XVI). Columns 5 and 6 are an olivine gabbro and a gabbro respectively, with which the compositions calculated for the amphibolite schist (Table XV) compare favorably.

An alternative origin of amphibolites is by metamorphism of limestones containing siliceous and pelitic materials, however this mode of origin does not seem to be as reasonable as the suggested igneous origin of the Big Falls rocks.

The model for the origin of the Big Falls gneisses and schists must include differentiation resulting in production of gabbros, plagioclase cumulates and anorthosites. The transition gneisses between the amphibolite schist and the feldspathic gneiss appears to represent a transition zone between rocks of gabbroic and anorthositic compositions. The banded amphibolite possibly formed by metamorphism of a plagioclase cumulate with layers of mafic minerals.

Key to samples in Table XVII:

1) Sample 1960S from the Marcy Massif, Adirondack Mountains, De Waard, 1970, p. 2066
2) Sample 5109 from the Skaergaard Layered Series, labradorite cumulate, Wager and Brown, 1967, Table 5
3) Sample 23, Table 4, from the Duluth Gabbro Complex, gabbro, Ruotsala, A. P., Tufford, S. P., 1965, p. 31
4) Sample 11, Table 5, from the Duluth Gabbro Complex, anorthosite, Ruotsala, A. P., Tufford, S. P., 1965, p. 41
5) Sample 37, Table 4, from the Duluth Gabbro Complex, olivine gabbro, Ruotsala, A. P., Tufford, S. P., 1965, p. 37
6) Sample 1724 from the Skaergaard Layered Series, chilled marginal gabbro, Wager and Brown, 1967, Table 7

Table XVII
Composition of Selected Gabbroic Rocks from Various Igneous Complexes

Oxide	Sample 1	2	3	4	5	6
SiO_2	52.16	50.64	49.42	52.30	46.90	47.83
Al_2O_3	23.96	25.54	24.47	28.79	15.68	18.62
TiO_2	0.37	0.50	1.87	0.18	2.59	1.29
Fe_2O_3	1.93	1.11	3.13	0.49	1.23	1.16
FeO	2.13	4.07	6.13	0.72	10.58	8.87
MgO	2.69	1.90	1.00	1.06	8.61	7.92
MnO	0.05	0.09	0.11	0.02	0.16	0.09
CaO	10.12	11.74	8.45	11.93	10.11	10.59
Na_2O	4.16	3.54	4.98	3.99	2.32	2.54
K_2O	0.81	0.36	1.15	0.30	0.57	0.20
P_2O_5	0.10	0.16	0.04		0.10	0.06
H_2O		0.48	0.61	0.44	1.00	0.43
CO_2					0.03	
S			0.11			
Total	98.48	100.14	101.47	100.22	99.88	100.08

Iron-magnesium ratios suggest that the Big Falls area does not represent an early differentiated sequence but formed later in the crystallization of a mafic igneous complex.

Petrology

The interpretation of petrologic relationships is complicated by the presence of minerals that have crystallized under different conditions of metamorphism. Textural and structural information indicate three deformational-metamorphic phases, each accompanied by extensive recrystallization but not to the extent of obliterating earlier formed minerals and assemblages, thus disequilibrium textures are common in all rock units. Attempting to unravel the petrogenesis of the units has required the assumption that until late alteration phases were introduced along fractures, there was no influx of material from outside sources and the system was essentially closed.

The approach to petrologic relations in the various rock units will be consideration of information derived from individual phases, followed by consideration of phase assemblages and the significance of the phase assemblages. By this method hope to reconstruct some of the conditions and processes active during metamorphism.

Hornblende:

The complex chemical nature and the ionic "garbage can" behavior of hornblende in metamorphic rocks has resulted in little experimental work and only broadly defined trends in composition with changes in metamorphic conditions. However, defined trends have not always held in different regions resulting in confusion about the behavior of hornblende during metamorphism. Four general variations have been discussed. 1) Change in color of hornblende with grade of metamorphism, 2) Variation in aluminum with grade, 3) Variation of alkali content with grade, and 4) Variation of TiO_2 with grade.

Shido (1958), Shido and Miyashiro (1959) in mapping the Central Abukuma Plateau used the Z-axial color of amphiboles as an indicator to draw zone boundaries on the geologic map of the area. Four zones were defined. Zone A: pale green to practically colorless, Zone B: blue-green with the color deeper than in Zone A, Zone C: green, greenish brown or brown with the brown color representing the higher grade part of the zone, and Zone D: brown. The grade of metamorphism increases from Zone A to Zone D. The calcic amphibole in Zone A is actinolite while hornblende is the amphibole in the other zones. The blue-green color is usually characteristic of the epidote-amphibolite facies. The green color without bluish tint is higher temperature, usually the amphibolite facies, while the brown is highest temperature. The blue-green color is the result of higher water content and a higher Fe^{+3}/ Fe^{+2} ratio and the brown color to higher content of TiO_2 (Miyashiro, 1973, p. 254).

The second trend in metamorphic hornblendes is characterized by variation of aluminum with grade. The variation of aluminum depends not only on grade of metamorphism but bulk composition. The whole rock composition is the main control. Confusion that has resulted in considering the effect of metamorphic grade on Al^{IV} is probably the result of failure to distinguish between Al^{IV} introduced by the edenite substitution necessary for alkali increase and the tschermakite substitution. The amount of the tschermakite molecule should decrease with increasing grade of metamorphism. Tschermakite can be involved in several different reactions, as:

$$\underset{7\,Ca_2Mg_3Al_4Si_6O_{22}(OH)_2}{\text{7 Tschermakite}} + \underset{10\,SiO_2}{\text{10 quartz}} = \underset{3\,Mg_7Si_8O_{22}(OH)_2}{\text{3 Cummingtonite}}$$

$$+ \underset{14\,Ca\,Al_2Si_2O_8}{\text{14 Anorthite}} + H_2O$$

The reaction decreases both tetrahedral and octahedral aluminum (Miyashiro, 1973). According to Shido and Miyashiro (1959) the formation of tschermakite from cummingtonite and calcic plagioclase is promoted by higher solid pressure. However, under high solid pressure the tschermakite molecule tends to be transformed into garnet and the two effects should counteract each other.

Alkali content has also been reported to increase with increasing grade of metamorphism, however the bulk composition of the rock probably is more important than any increase due to change in grade.

The amount of TiO_2 in hornblende increases with grade of metamorphism and is probably responsible for brown colors in high grade hornblende. The maximum titanium content of hornblende is restricted by the temperature of crystallization. Within the amphibolite facies titania rarely exceeds two weight percent in hornblendes (Leake, 1965). In amphibolites, titanium occurs in ilmenite, sphene and hornblende.

Garnet:

The formation of garnet in amphibolites is dependent on many variables, including: 1) oxygen fugacity, 2) Niggli mg, 3) weight percent MnO, 4) various minor chemical components, and 5) temperature and pressure.

Oxygen fugacity is one of the more difficult variables to define because of the possibilities of internal or external control, and buffered or non-buffered systems. Due to the thermal dissociation of water the fugacity of oxygen is defined by the hydrogen fugacity, total pressure, and temperature (Eugster and Wones, 1962). The stability of a mineral containing elements of variable oxidation states will be affected as shown experimentally by Hsu (1968) in the case of the almandine end member of the garnet group. In amphibolites the oxidation state is highly variable since organic matter and graphite, which controls the oxygen fugacity in pelitic rocks, are absent. Variability in oxygen fugacity from point to point in an amphibolite terrain may be the controlling factor in garnet formation.

A low ratio of Mg / (Mg + Fe) or Niggli mg (Mol. MgO / (Mol. MgO + $2Fe_2O_3$ + FeO + MnO)) is common in garnetiferous amphibolites indicating that iron-rich minerals tend to occur in iron-rich bulk compositions.

MnO may play an important role in stabilizing almandine outside of its normal stability field, the relation between MnO in the parent rock and the presence of garnet is by no means clear (Muller and Schneider, 1971).

Minor chemical variations may influence the formation of garnet by removing certain elements essential to the formation of garnet. A low titanium content and low Ca + Na + K favors garnet. In these cases the availability of FeO is affected.

Even when temperature conditions are within the stability for crystallization of garnet the deciding factor may be pressure conditions. Garnet-hornblende-plagioclase assemblages are higher density than hornblende-plagioclase and are favored by higher pressure. The Dalradian amphibolite of Scotland have garnets occuring over a wide composition range and with the occurance of kyanite in pelitic assemblages are considered to be medium pressure. At Connemara, Ireland, garnet is rare, cordierite and andalusite are common in pelitic schists, indicating low pressure (Leake, 1972). In the central Abukuma Plateau of Japan, a low-pressure region, garnet is generally absent (Shido, 1958).

Cummingtonite:

The main chemical control determining the occurrence of cummingtonite is low Ca and Al, insufficient calcium and aluminum to meet the demands of hornblende and plagioclase. The excess femic constituents which normally combine with calcium to form hornblende, form cummingtonite instead.

The alternative is forming a Ca-poor hornblende which is prevented by a solvus between hornblende and cummingtonite (Leake, 1972, Klein, 1968). Cummingtonite occurs under medium to high temperatures and relatively low pressure metamorphic conditions and is absent from high pressure terrains. The cummingtonite molecule in common hornblende is expected to act the same as the mineral cummingtonite. The restriction of cummingtonite to medium to high-temperature conditions is limited by the lower temperature stability of talc and chlorite and by the lower temperature stability of talc and chlorite and by the increasing capture of more calcium by plagioclase as the albite component becomes unstable with temperature increase (Leake, 1972). The two amphibole assemblage of hornblende-cummingtonite is considered to represent an equilibrium assemblage in many areas. The associated plagioclase with such pairs has been shown to vary regularly with the atomic fractions Mg / (Mg + Fe) and Mg-Fe distribution coefficients for the associated amphiboles (Kisch and Warnaars, 1969). Unfortunately no hornblende-cummingtonite pairs were analyzed from Big Falls.

Garnet and cummingtonite occurring in the same rock can be explained by water content at the time of metamorphism, if water is sufficient, the stability fields of garnet and cummingtonite overlap producing garnet-cummingtonite amphibolites, otherwise cummingtonite is, in part, an alternate phase for garnet (Leake, 1972). Shido (1958) stated that he was unaware of any cummingtonite-garnet amphibolites, attesting to the rarity of such an occurrence.

Epidote:

Epidote stability is dependent on temperature, rock pressure, water pressure and oxygen fugacity. Dependence on the fugacity of oxygen is due to iron allowable in the epidote structure. Epidotes formed at low temperatures tend to have compositions near 33 mole percent Fe^{+3} end member. The composition range becomes larger with rising temperature, expanding both to lower and higher $Fe^{+3}/(Al + Fe^{+3})$ although expansion toward lower $Fe^{+3} / (Al + Fe^{+3})$ is more marked (Miyashiro and Seki, 1958). During retrograde metamorphism accompanying dislocation cataclasis calcium ions may be released from plagioclase and fixed in epidote and sphene (Deer, et al., 1961, p. 207). Epidote is often considered a stress mineral favored by shearing stress and low temperatures. The coexistence of medium plagioclase (An_{25} to An_{45}) with epidote occurs in rocks formed under high load pressure, sometimes augmented by shearing stress (Turner and Verhoogan, 1960).

Mineral Assemblages

Mineral assemblages in the rock units at Big Falls include minerals that are part of disequilibrium groupings of relict minerals and textures.

The earliest assemblage formed included coarse garnet porphyroblasts and probably hornblende and plagioclase. The relict garnets are found only in the banded amphibolite gneiss and the amphibolite schist. Stability relations of garnet suggest medium pressures, reducing conditions, and a general iron-rich bulk composition. Temperature and pressure conditions suggested by the garnet imply metamorphism in the amphibolite facies.

The second assemblage, formed during the second recrystallization, included hornblende, plagioclase, ilmenite, and locally garnet (fine euhedral grains in the banded amphibolite schist). Garnet suggests reducing conditions with temperatures and pressures common to the amphibolite facies. The coarse grained texture of relict grains from this assemblage in all rock units, suggest general equilibration was attained during the second recrystallizations.

The third assemblage, formed during the third recrystallization, includes hornblende, plagioclase, epidote, and sphene in the banded amphibolite gneiss, cummingtonite, hornblende, plagioclase and quartz in the amphibolite schist and hornblende, plagioclase, cummingtonite and occasionally epidote in transition and feldspathic gneisses.

In all rock units the Z-axial color in hornblende is blue-green suggesting recrystallization in the epidote-amphibolite facies. The common occurrence of sphene in hornblende-rich bands in the banded amphibolite gneiss and titanium rich inclusions in the hornblende from the amphibolite schist suggest expulsion of titanium from the hornblende lattice during the third recrystallization. If the observed hornblende is the result of recrystallization of hornblende formed in the amphibolite facies under conditions of the epidote-amphibolite facies such release of TiO_2 can be expected.

Hornblende associated with garnet porphyroblasts in the banded amphibolite gneiss are rich in the tschermakite molecule and texturally result from replacement of garnet. The production of tschermakite from garnet may be described by a reaction such as:

$$\underset{\substack{\text{2 Tschermakite} \\ (2 \times 260 \text{ cc})}}{2Ca_2Mg_3Al_4Si_5O_{22}(OH)_2} \quad \underset{\substack{\text{2 Pyrope} \\ (2 \times 113 \text{ cc})}}{2Mg_3Al_2Si_3O_{12}} + \underset{\substack{\text{Grossular} \\ (126 \text{ cc})}}{Ca_3Al_2Si_3O_{12}}$$

$$+ \underset{\substack{\text{Anorthite} \\ (101 \text{ cc})}}{CaAl_2Si_2O_8} + \underset{\substack{\text{Quartz} \\ (22.4 \text{ cc})}}{SiO_2} + 2H_2O$$

(Equation 9, Shido, 1958)

Total volumes of solid phases are 520 cc on the left-hand side and 475 cc on the right-hand side, therefore under higher rock pressures the reaction will go to the right, favoring the formation of garnet. Since the tschermakitic hornblende is found replacing garnet, lower rock pressures are indicated.

Euhedral epidote in the banded amphibolite gneiss, locally in the amphibolite schist and the transition and feldspathic gneisses, is consistent with the epidote-amphibolite conditions of metamorphism. The Ca and Al necessary for formation of epidote were derived by dislocation cataclasis of plagioclase producing the common 0.1 mm. plagioclase grains and irregular compositional zoning in all units. The occurrence of epidote with plagioclase in the composition range of An_{45} to An_{60} suggest considerable shear stress during crystallization, an inference supported by the major shear zones formed at the same time. The Fe^{+3} / $(Al + Fe^{+3})$ ratio for the analyzed epidote from the banded amphibolite gneiss is 0.83 which indicates relatively high temperatures during the crystallization of the epidote.

Cummingtonite in the amphibolite schists and locally in the transition and feldspathic gneisses, imply low load pressures but moderate to high temperatures. The cummingtonite-garnet assemblages in the amphibolite schist can be explained from the fact that the garnet formed during the moderate pressure first recrystallization and cummingtonite formed during the low pressure third recrystallization.

The combined information from the third assemblage implies that conditions of metamorphism were low pressure with a significant amount of shear stress and moderate temperatures in the epidote-amphibolite facies.

Synthesis of Structure and Petrology

Table XVIII contains a synthesis of structures and petrology at Big Falls in the order of occurrence. A fault between the banded amphibolite gneiss and the amphibolite schist has been placed early in the third deformational phase. The reasons for the fault include: 1) Composition of the hornblendes from the banded amphibolite gneiss have iron greater than magnesium in the structural formula while hornblende from the amphibolite schist are magnesium greater than iron. Whole rock chemical analysis of the banded amphibolite gneiss indicate iron increasing toward the amphibolite schist. 2) Although the contact is not visible local float is strongly deformed as though associated with a major fault. 3) Plunge of folds formed during the second deformation are opposite in the banded amphibolite gneiss and the amphibolite schist and evidence indicates that no other structure can explain the difference. 4) All rock units have undergone metamorphism under conditions of the epidote-amphibolite to lower amphibolite facies, suggesting that the units were juxtaposed at the time of the third recrystallization.

Table XVIII
Structure and Petrology Synthesis

Petrologic Event	Structural Event	Metamorphic Facies
	Joints develop	
	Left-lateral faults develop	
Alteration phases introduced Chlorite, pyrite, epidote and sericite	Right-lateral faults and joints develop	
Local mylonitization	Development of lenses especially in the banded amphibolite gneiss	
Third Deformational Phase and Recrystallization		
Crystallization of epidote, sphene and cummingtonite Titanium from hornblende and calcium from plag form sphene Calcium and aluminum from plagioclase form epidote		Epidote-amphibolite facies
Alteration of garnet porphyro- blasts to hornblende		
Recrystallization of hornblende, plagioclase, apatite, ilmentite, and quartz	Faint N 55^{o}W foliation developed	
	Cataclastic deformation Faulting developed between banded amphibolite gneiss and amphibolite schist Major shear zones developed	

Petrologic Event	Structural Event	Metamorphic Facies
	Second Deformational Phase and Recrystallization	
Crystallization of hbe, plag, qtz., ilmenite, locally garnet	Major folding of compositional banding Sinistral couple in banded amphibolite gneiss, plunge north Sheared folds in amphibolite schist, plunge south Compositional banding wrapped around fractured garnet porphyroblasts in the banded amphibolite gneiss Development of boudinage, schistosity and oldest lineations Braided foliation in transition gneiss Tension fractures in amphibolite schist	Amphibolite Facies
	First Deformational Phase and Recrystallization	
Garnet porphyroblasts develop in the banded amphibolite gneiss and the amphibolite schist	Foliations form in protolith of intrafolial folds	Amphibolite Facies

Emplacement and differentiation of a mafic igneous intrusive.

Relation to the Region

The gneisses and amphibolites at Big Falls are included in the "Chippewa Amphibolite Complex" (figure 1). The complex is bounded on the north by the Jump River Lineament with the "Flambeau Volcanic-Sedimentary Province" to the north, and on the south by the overlying "Black River Volcanic-Sedimentary Province" (Myers, et al., 1974). The "Chippewa Amphibolite Complex" is a mafic suite of volcanics into which the Big Falls rocks were intruded. The intrusion occurred in early or middle Precambrian times. Radiometric age dates from zircons from an intrusive one mile east of Big Falls yields dates of 1900 m. y. (Myers, et al., 1974). The 1900 m. y. date is interpreted as representing the time that major structural features were produced in the region (second deformational phase at Big Falls). Independent work by Myers (Myers, et al., 1974), Maercklein (1974), and the author indicate at least one major deformation prior to the 1900 m.y. event, and a third deformation after the 1900 m.y. event.

General chemical trends observed in evolution of Precambrian rocks would indicate a very early age for the Big Falls amphibolite and the "Chippewa Amphibolite Complex". Engel, et al., (1974) summarized relations between the ratio of K_2O/Na_2O

less than 1 is associated with most major Archean rock complexes (>2,500 m.y.). K_2O / Na_2O ratios from whole rock chemical analyses at Big Falls yield values of 0.103 and 0.135, suggesting an Archean age of intrusion.

Conclusions

The structure and petrology of the Precambrian gneisses and schists at Big Falls indicate three deformational phases accompanied by major recrystallization.

The first recrystallization occurred under temperature-pressure conditions approximating the amphibolite facies. Structural and petrologic evidence for this phase are limited to coarse garnet porphyroblasts and rootless intrafolical folds of a compositionally banded protolith.

The second recrystallization was synchronous with folding, producing north plunging open folds in the banded amphibolite gneiss and tight south plunging folds in the amphibolite schist. Layer geometry analysis and isogon patterns of the folded layers suggests that folds in the amphibolite schist were formed by inhomogeneous compressive strain while in the banded amphibolite gneiss the folds formed as flattened flexural slip folds and later were deformed by inhomogeneous strain. Faint amphibole lineations roughly coincident with the plunge of fold axes, are found on compositional foliations surfaces. Lineations in the amphibolite schist strongly cross-cut the direction of fold axial plunge while the orientation of boundinage structures is unknown. Faulting, with apparent left-lateral displacements, occurred before final recrystallization of the rock. Plagioclase and hornblende with local garnet were the main minerals involved in the recrystallization which occurred under conditions of moderate pressures and temperatures in the amphibolite facies. The second recrystallization is thought to date at 1900 m.y. when the major structural features of the region were formed.

A major fault developed between the banded amphibolite gneiss and the amphibolite schist either between the second and third recrystallization or during the third recrystallization.

The third recrystallization was associated with cataclastic deformation and retrograde effects resulting in disequilibrium textures and incomplete mineral reactions. Conditions were typical of the epidote-amphibolite facies with low load pressures but significant shear stress and low to moderate temperatures. A cross-cutting schistosity also developed during the third recrystallization. Euhedral epidote, cummingtonite and sphene crystallized in association with hornblende and plagioclase.

Late faulting and jointing were not accompanied by major recrystallization of the rocks, however alteration is found along some fault and joint sets.

The protolith of the various units was a differentiated mafic ignous intrusive that was intruded into the "Chippewa Amphibolite Complex", formed of mafic volcanics, during early to middle Precambrian time.

Appendix I

Petrofabrics

Petrofabric analysis was undertaken to help determine the orientation of mineral grains with reference to the fold axes. A sample from the amphibolite schist, 28IY, containing a tight set of folds that plunge south 25 degrees, was oriented in the field and later three orthogonal oriented thin sections were cut. One thin section was cut perpendicular to the fold axis and contained the trough of the fold, a synform, another section was cut perpendicular to the axial plane of the fold with the third section cut parallel to the fold axis and schistosity. Modal analyses from the three sections are presented in table I.

Table I
Modal Analyses from Sample 28IY

Orientation	Hbe	Plag	Qtz	Opaque.	Apatite	Chlor	Cumm	Bio
28IY	30.6	54.6	13.9	0.7	0.1			
28IY	40.6	46.8	5.6	1.4	0.1	2.2	2.6	0.6
28IY	25.4	62.8	8.6	1.4		1.2	0.6	

Hornblende crystals are oriented in the plane of the schistosity subparallel to the fold axial plane. A faintly defined lineation of hornblende was found to plunge steeply to the north cross-cutting the fold axis. Use of the quartz wave plate under crossed polarizers fails to show a strong preferred orientation in either plagioclase or quartz. The texture of the rock indicates a recrystallized fabric that can be expected to show some degree of orientation to the prevailing stress conditions at the time of crystallization.

Quartz was used to determine if there was a preferred orientation expressed by the orientation of the optic axes of quartz grains. The orientation of the optic axes of quartz was determined by use of a 4-axis universal stage. Sixty five quartz grains in each of the three thin sections were oriented with respect to the optic axis and recorded. Data was recorded as the Z vibration direction parallel to the east-west rotation axis of the universal stage. When the optic axis of a grain was found to be perpendicular to both the east-west and north-south stage axes, the orientation of the grain was recorded after a calculated 90 degree rotation so Z would be parallel to the east-west rotation axis. When the universal stage data, recorded as parallel elements on the universal stage, are plotted by computer, the computer plots the data as normals to parallel elements (Warner, 1969).

Figures A1, A2 and A3 show the results from orientation of quartz optic axes in the three 28IY samples. In each case a strongly defined maximum steeply dipping into the plane of the thin section was recorded. The scattered points away from the center of the diagrams represent grains that were oriented so the optic axis was nearly perpendicular to the plane of the thin section. The strong maximum observed in each case is partly produced by the difficulty in obtaining universal stage data on quartz grains whose optic axis lie at an angle between 30 degrees and 70 degrees from the plane of the thin section.

Since the maxima recorded in figure 1 are from thin sections mutually perpendicular to each other, it seems apparent that the orientation of the optic axes of quartz grains are random. Ramdomness in the orientation suggests that the recrystallization of quartz was not synchronous with the applied stress system. Since strain features are not found in quart grains, apparently quarts recrystallized after the deformation that produced the folds in the analyzed sample. However without more detailed study of the fabric of quartz and other phases, conclusions must be regarded as tentative.

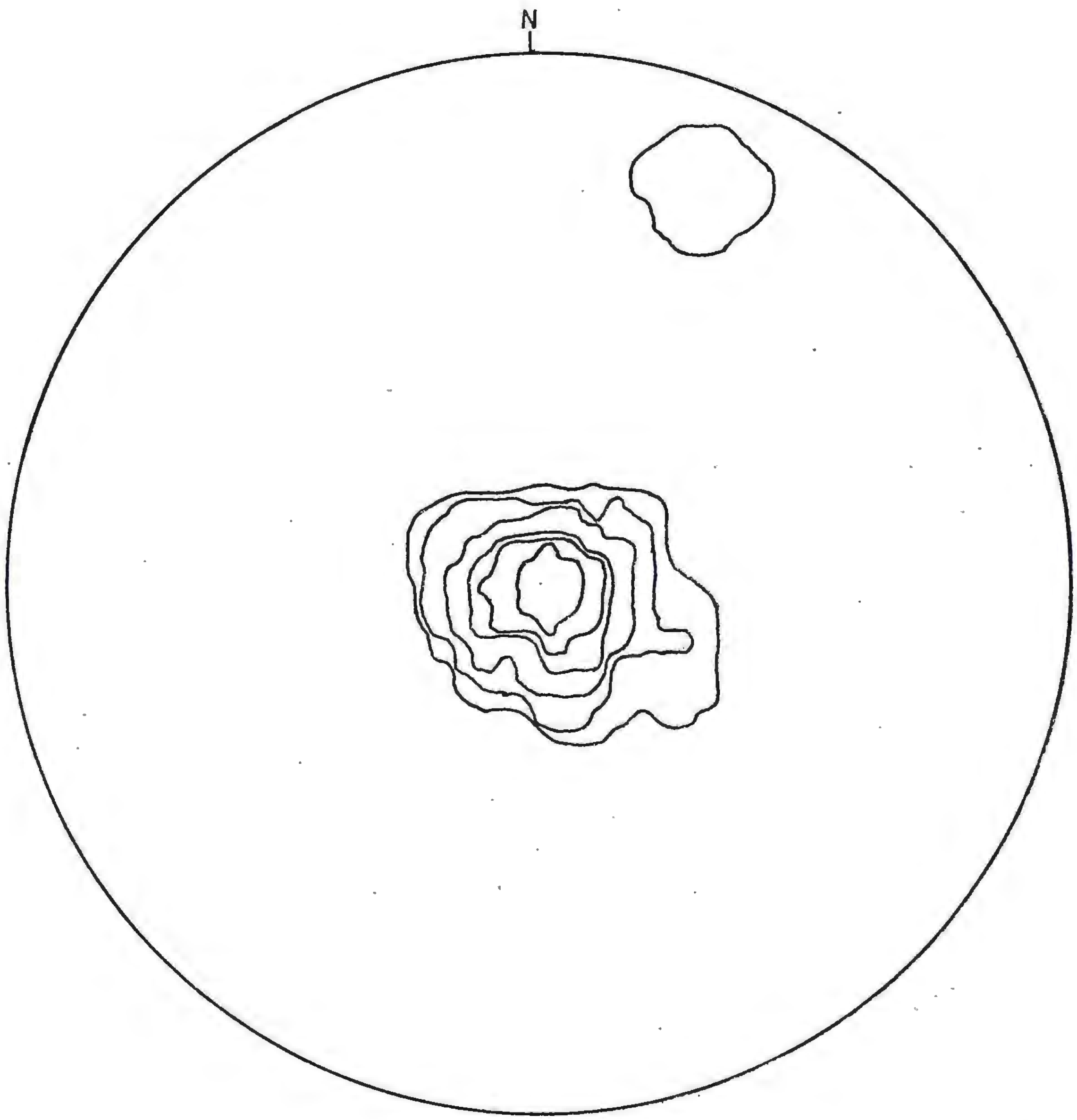

Figure A1: Equal area plot of petrofabric data from sample 28IY, contours at 1, 2, 5, 11, 15, 35 percent per 1 percent area. Based on 65 observations.

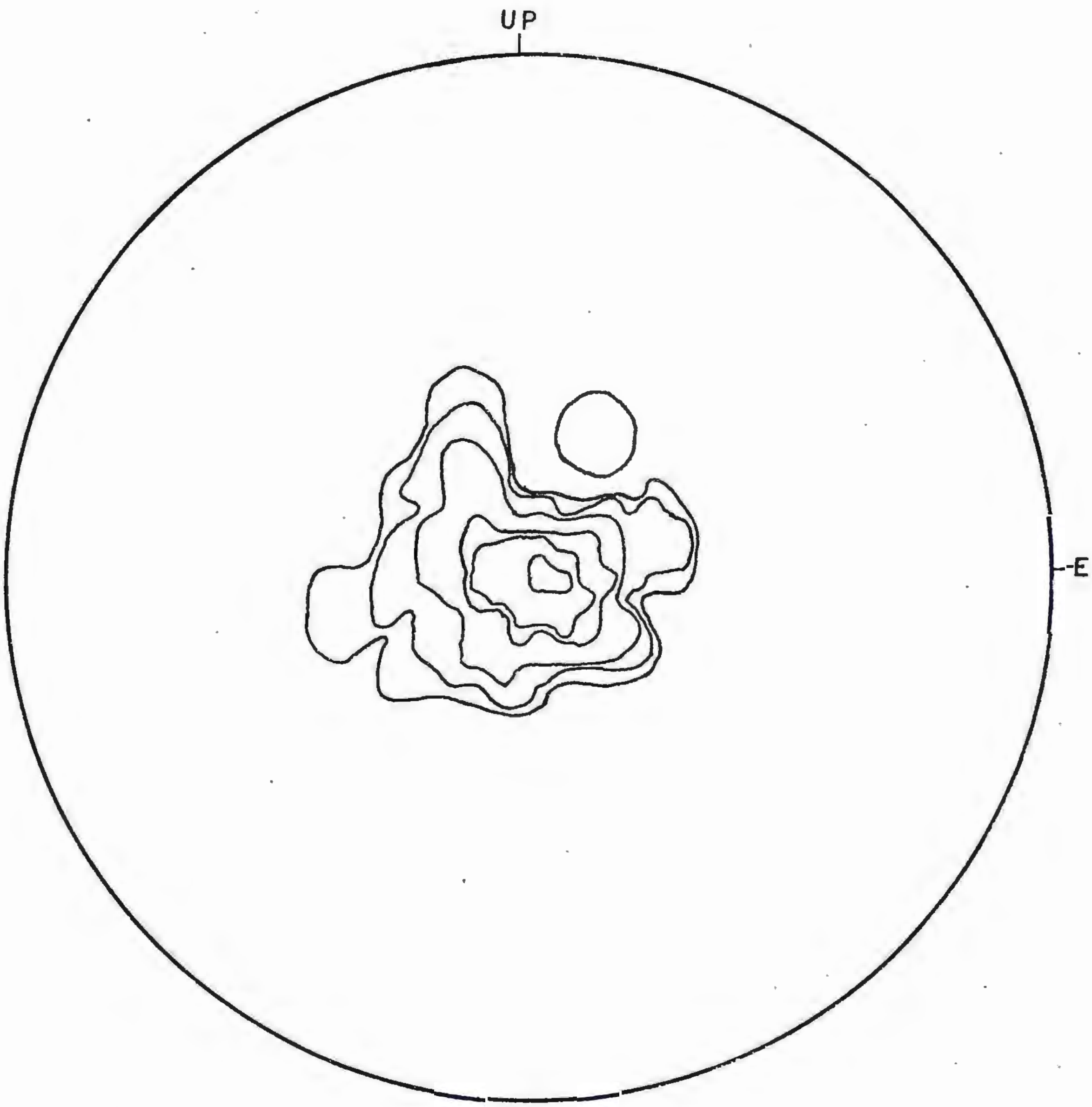

Figure A2: Equal area plot of petrofabric data from sample 28IY, contours at 1, 2, 5, 11, 15, 35 percent per 1 percent area. Based on 65 observations.

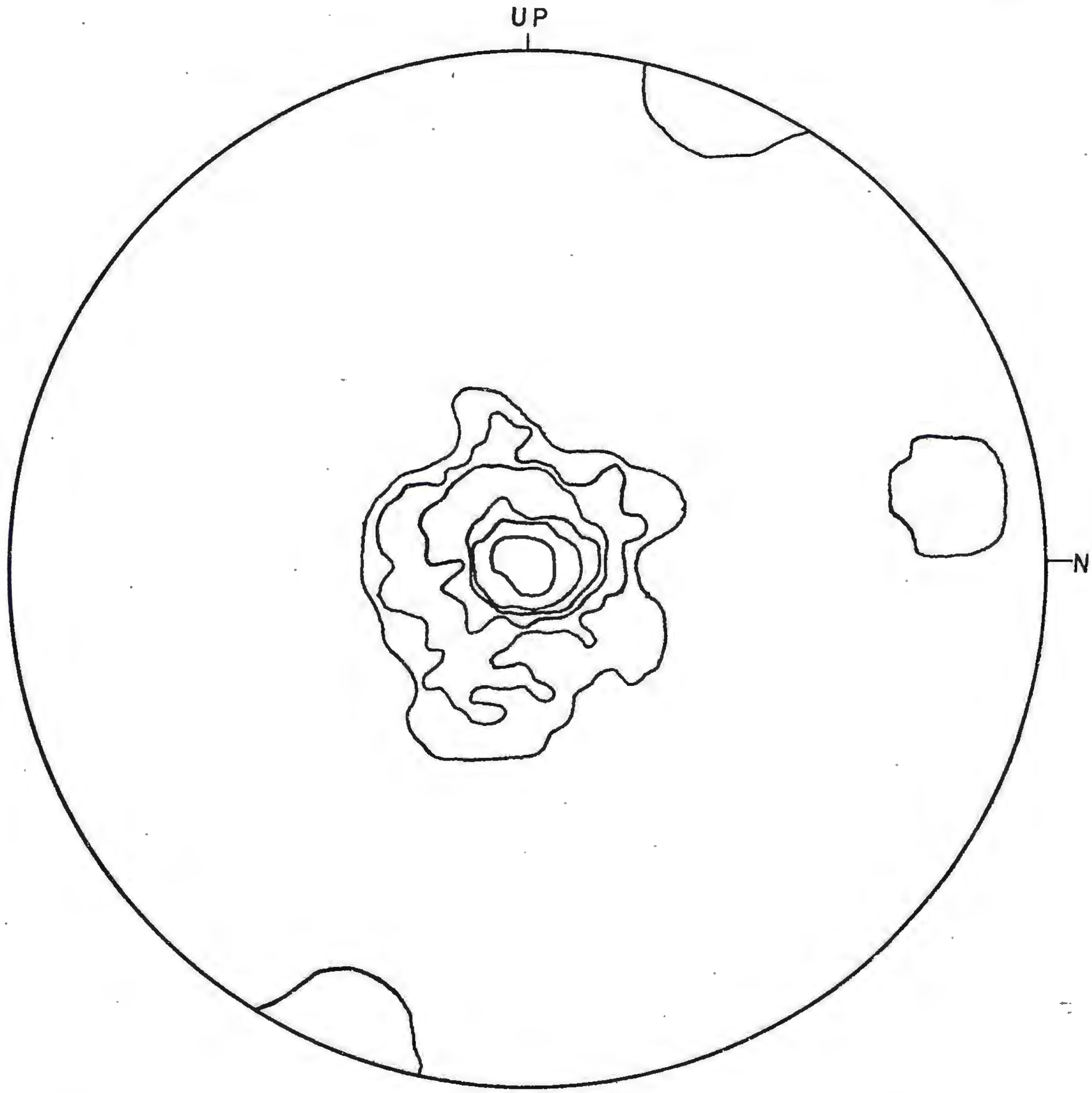

Figure A3: Equal area plot of petrofabric data from sample 28IY, contours at 1, 2, 5, 11, 15, and 35 percent per 1 percent area. Based on 65 observations.

Appendix II
Classification of Amphiboles

The classification of amphiboles from Big Falls is based on a method proposed by Shido (1958) using end members to express compositional variation.

End Members

Denotation	A	W	X + Y	Z		Name
			Structural Positions			
Tiam		Ca_2	Mg_1Ti_4	Al_8	$O_{22}(OH)_2$	Titanamphibole
Cum		Mg_2	Mg_5	Si_8	$O_{22}(OH)_2$	Cummingtonite
Ce'	Ca_4	Ca_2	Mg_5	Al_8	$O_{22}(OH)_2$	Calcium-edenite
St'	Na_2	Na_2	Mg_5	Si_8	$O_{22}(OH)_2$	Sodatrmolite
Ed'	Na_8	Ca_2	Mg_5	Al_8	$O_{22}(OH)_2$	Edenite
Gl		Na_2	Mg_3Al_2	Si_8	$O_{22}(OH)_2$	Glaucophane
Ts'		Ca_2	Al_5	Al_5Si_3	$O_{22}(OH)_2$	Tschermakite
Tr		Ca_2	Mg_5	Si_8	$O_{22}(OH)_2$	Tremolite

Ce', Ed', St' and Ts' are imaginary end members used in the calculation of the constituent molecules from the chemical analyses.

Table IB
Classification of Amphiboles

			Hornblende WP-7 Pl-1 Banded Amphibolite Gneiss							
	Ions	No. of Ions	Tiam	Cum	Ce'	St'	Ed'	Gl	Ts'	Tr
	Si	6.46		0.84					0.54	5.08
Z										
	Al	1.54	0.26		0.12		0.20		0.91	(0.05)
	Al,Fe^{+3}	0.91							0.91	
Y										
	Ti	0.13	0.13							
X	Fe^{+2},Mg,Mn	3.96	0.03	0.52	0.08		0.12			3.21
	Fe^{+2},Mg,Mn	0.21		0.21						
W	Ca	1.79	0.06		0.03		0.05		0.36	1.29
	Na									
	Na,K	0.20					0.20			
A										
	Ca	0.06			0.06					

Hornblende WP-7 P2-1 Banded Amphibolite Gneiss

	Ions	No. of Ions	Tiam	Cum	Ce'	St'	Ed'	Gl	Ts'	Tr
	Si	6.51		0.76		0.04			0.58	5.13
Z										
	Al	1.49	0.26				0.21		0.97	(0.05)
	Al,Fe^{+3}	0.97							0.97	
Y										
	Ti	0.13	0.13							
	Fe^{+2},Mg,Mn	3.90	0.03	0.47		0.02	0.13			3.25
	Fe^{+2},Mg,Mn	0.19		0.19						
W	Ca	1.80	0.06				0.05		0.39	1.30
	Na	0.01				0.01				
	Na,K	0.22				0.01	0.21			
A										
	Ca									

Hornblende 7-29-72 Banded Amphibolite Gneiss

	Ions	No. of Ions	Tiam	Cum	Ce'	St'	Ed'	Gl	Ts'	Tr
	Si	6.31		0.28		0.72		0.08	0.92	4.31
Z										
	Al	1.69	0.06						1.53	(0.10)
	Al,Fe^{+3}	1.55						0.02	1.53	
Y										
	Ti	0.03	0.03							
X	Fe^{+2},Mg,Mn	3.42	0.01	0.17		0.45		0.03		2.76
	Fe^{+2},Mg,Mn	0.07		0.07						
W	Ca	1.73	0.01						0.61	1.11
	Na	0.20				0.18		0.02		
	Na,K	0.18				0.18				
A										
	Ca									

Hornblende W-29 Amphibolite Schist

	Ions	No. of Ions	Tiam	Cum	Ce'	St'	Ed'	Gl	Ts'	Tr
	Si	6.26		2.08					0.49	3.69
Z										
	Al	1.74	0.18		0.48		0.27		0.82	
	Al, Fe^{+3}	0.82							0.82	
Y										
	Ti	0.09	0.09							
X	Fe^{+2}, Mg, Mn	4.09	0.02	1.30	0.30		0.17			2.30
	Fe^{+2}, Mg, Mn	0.52		0.52						
W	Ca	1.48	0.04		0.12		0.07		0.33	0.92
	Na									
	Na, K	0.27					0.27			
A										
	Ca	0.24			0.24					

Hornblende W-24 Amphibolite Schist

	Ions	No. of Ions	Tiam	Cum	Ce'	St'	Ed'	Gl	Ts'	Tr
	Si	6.35		2.12					0.42	3.81
Z										
	Al	1.65	0.22		0.58		0.22		0.70	(0.03)
	Al,Fe^{+3}8	0.70							0.70	
Y										
	Ti	0.11	0.11							
X	Fe^{+2},Mg,Mn	4.17	0.03	1.32	0.36		0.14			2.32
	Fe^{+2},Mg,Mn	0.53		0.53						
W	Ca	1.47	0.05		0.14		0.05		0.28	0.95
	Na									
	Na,K	0.22					0.22			
A										
8	Ca	0.29			0.29					

Hornblende W-21 Amphibolite Schist

	Ions	No. of Ions	Tiam	Cum	Ce'	St'	Ed'	Gl	Ts'	Tr	
	Si	6.96		5.64					0.22	1.10	
Z											
	Al	1.04	0.10		0.48		0.21		0.37		*
	Al, Fe^{+3}	0.37							0.37		
Y											
	Ti	0.05	0.05								
X	Fe^{+2}, Mg, Mn	4.54	0.01	3.52	0.30		0.13		0.57		
	Fe^{+2}, Mg, Mn	1.41		1.41							
W	Ca	0.59	0.02		0.12		0.05		0.15	0.23	
	Na										
	Na, K	0.22					0.22				
A											
	Ca	0.24			0.24						

Cummingtonite W-21 Amphibolite Schist

	Ions	No. of Ions	Tiam	Cum	Ce'	St'	Ed'	Gl	Ts'	Tr	
	Si	7.96		7.72					0.08	0.08	
Z											
	Al	0.04			0.02				0.14		*
	Al,Fe^{+3}	0.14							0.14		
Y											
	Ti										
X	Fe^{+2},Mg,Mn	4.86		4.82	0.01					0.05	
	Fe^{+2},Mg,Mn	1.93		1.93							
W	Ca	0.07			Tr				0.05	0.02	
	Na										
	Na,K										
A											
	Ca	0.01			0.01						

Compilation of Amphibole Recalculations

	P1-1 WP-7	P2-1 WP-7	7-29-72	W-29	W-24	W-21 Hbe	W-21 Cum
Tiam	0.26	0.26	0.06	0.18	0.22	0.10	
Cum	0.84	0.76	0.28	2.08	2.12	5.64	7.72
Ts'	1.45	1.55	2.45	1.31	1.12	0.59	0.22
Ce'	0.12			0.48	0.58	0.48	0.02
St'		0.04	0.72				
Ed'	0.20	0.21		0.27	0.22	0.21	
Tr	5.08	5.13	4.31	3.69	3.81	1.10	0.08
Cl			0.08				

Recalculation of Chemical Compositions

Hornblende compositions have been recalculated on the basis of 23 oxygen atoms instead of the 24 oxygen atoms defined by the structural formula, $A_{0-1}X_2Y_5Z_8O_{22}(OH,F)_2$ for the half-cell. Twenty-three oxygen atoms are used because water, chlorine, and fluorine in hornblende cannot be easily analyzed by microprobe. The lack of data for water and fluorine or error in values obtained for these components concentrates error in the "A" site which may be avoided by recalculation of results using 23 oxygen atoms (Binns, 1965).

The structural formula indicates the number of cations that enter the various sites of the hornblende lattice. A combination of 8.0 ions of silicon and aluminum enter the Z or tetrahedral site with any excess aluminum entering the Y sites. The Y sites are six-fold coordination sites designated M(1), M(2) and M(3). A total of 5.0 cations enter the Y structural sites and may include aluminum, magnesium, titanium and iron (+2, +3). Titanium in the Y sites requires the coupled substitution $Ti^{VI} \cdot Al_2^{IV}$ for $Mg \cdot Si_2$. The X positions are occupied by 2 cations in eight-fold coordination and are referred to as the M(4) sites. In the calcic amphiboles the typical ion in the M(4) site is calcium. If the amount of calcium is not sufficient to fill the M(4) site sodium will make up the difference. The A site can contain 0 to 1 cation which is usually either sodium or potassium in ten-fold coordination. The structural sites of particular interest in hornblende, and amphiboles in general, are the M sites in six-fold coordination and the M(4) sites in 6 and 8 fold coordination. An excess in the number of cations that normally enter the 6-fold coordinated M sites results in the entry of Fe^{+2} into the M(4) site (Shido, 1958) known as the cummingtonite substitution. The distribution of iron and magnesium in the various M sites has been found to be ordered, with Fe^{+2} strongly preferred in the M(4) site, and Mg in the M(2) site. The rest of the Mg and Fe are randomly distributed over the M(1) and M(3) sites (Kisch and Warnaars, 1969). If enough Fe enters the M(4) site in the cummingtonite substitution, calcium may be forced into the A site. When calcium enters the A site aluminum must replace silicon in the tetrahedral site to maintain electrical neutrality (Shido, 1958).

The ideal structural formula for garnet is $X_6Y_4Si_6O_{24}$ with X being the bivalent cation sites and Y the trivalent cation sites. Recalculation of garnets is contained in Table II B.

The structural formula for epidote is $X_2Y_3Si_3O_{12}(OH)$ with X and Y as bivalent and trivalent sites respectively. Table IIIB contains recalculations of epidote for all iron as ferrous and all iron as ferric.

Plagioclase compositions from probe data and recalculated data were used in calculation of structural formulas based on 32 oxygen atoms.

Table IIB
Ions Per Formula Unit for Hornblendes from the Banded Amphibolite Gneiss, Based on 23 Oxygen

Ion	WP-7 P1-1		WP-7 P2-1		7-29-72	
Si	6.46	8.00	6.51	8.00	6.31	8.00
	1.54		1.49		1.69	
Al	2.45		2.46		3.24	
	0.91		0.97		1.55	
Ti	0.13		0.13		0.03	
Fe^{+2}	2.28	5.21	2.34	5.19	1.91	5.07
Mg	1.83		1.70		1.52	
Mn	0.06		0.05		0.06	
Ca	1.85	1.98	1.80	1.97	1.73	1.90
Na	0.13		0.17		0.17	
K	0.07	0.07	0.06	0.06	0.21	0.21

All Fe as Fe^{+2}

Table IIB Continued: Ions Per Formulat Unit for Hornblendes from the Amphibolite Schist, Based on 23 Oxygen.

Ions	Hbe W-29			Hbe W-24			Hbe W-21		
Si	6.26			6.35			6.96		
			8.00			8.00			8.00
		1.74			1.65			1.04	
Al	2.56			2.35			1.41		
		0.82			0.70			0.37	
Ti	0.09			0.11			0.05		
Fe^{+2}	2.05			2.16			2.65		
			5.52			5.53			6.41
Mg	2.52			2.48			3.25		
Mn	0.04			0.06			0.05		
Ca	1.72			1.76			0.83		
			1.92			1.94			1.05
Na	0.20			0.18			0.22		
K	0.07			0.04					

Ions per Formula Unit for Cummingtonite

Ion	W-21		
Si	7.96		
			8.00
		0.04	
Al	0.18		
		0.14	
Ti	0.00		
Fe^{+2}	2.94		
			6.93
Mg	3.79		
Mn	0.06		
Ca	0.08		
			0.08
Na			
K			

Table IIIB: Garnet Recalculations for the Banded Amphibolite Gneiss and Amphibolite Schist

Ion	7-29-72		W-21	
Si	6.11		6.26	
Al	3.81		3.78	
		$\Sigma Y^{+3}=3.82$		$\Sigma Y^{+3}=3.78$
Ti	0.01			
Fe^{+2}	3.45		4.05	
Mg	0.85		0.66	
		$\Sigma X^{+2}=5.98$		$\Sigma X^{+2}=5.75$
Mn	0.23		0.40	
Ca	1.45		0.64	

Table IVB
Ions Per Formula Unit for Epidote WP-7 P2-4

Ions	All Ferrous	All Ferric
Si	3.18	2.98
Al	2.35	2.20
	$\Sigma Y=2.37$	
Ti	0.02	0.02 $\Sigma Y=3.05$
Fe^{+3}		0.83
Fe^{+2}	0.66	
Ca	2.03 $\Sigma X=2.70$	1.90 $\Sigma X=1.91$
Mn	0.01	0.01

Table VB
Ions Per Formula Unit for Plagioclase, both Probe Data and Recalculated

	WP-7P2-3		WP-7 P2-2	
Ions	Probe			Recalculated
Si	10.04	9.65	10.44	10.01
Al	5.92 $\Sigma Z=15.99$	6.32 $\Sigma Z=15.98$	5.54 $\Sigma Z=15.99$	5.96 $\Sigma Z=15.98$
Fe^{+3}	0.03	0.01	0.01	0.01
Ca	2.43	2.34	2.02	1.94
Na	0.96 $\Sigma X=3.40$	1.57 $\Sigma X=3.92$	1.35 $\Sigma X=3.38$	1.96 $\Sigma X=3.91$
K	0.01	0.01	0.01	0.01

Ions Per Formula Unit for Plagioclase from Amphibolite Schist for Recalculated Data

Ions			
Si	10.64	11.10	10.28
Al	5.44 $\Sigma Z=16.08$	5.02 $\Sigma Z=16.12$	5.75 $\Sigma Z=16.06$
Fe^{+3}	0.00	0.00	0.03
Ca	1.42	1.00	1.74
Na	2.22 $\Sigma X=3.95$	2.53 $\Sigma X=3.54$	2.02 $\Sigma X=3.77$
K	0.01	0.01	0.01
Mn	0.03		

References Cited

Albee, A. L., 1962, Relationships between the mineral association, chemical composition and physical properties of the chlorite series: American Mineralogist, v. 47, p. 851-870.

Binns, R. A., 1965, The mineralogy of metamorphosed basic rocks from the Willyama Complex, Broken Hill District, New South Wales, Part I, hornblendes: Mineralogical Magazine, v. 35, p. 306-326.

Cummings, M. L., 1971, Geology of Big Falls, Wisconsin: in Guidebook, 3rd Annual Wisconsin State University Geology Field Conference, p. 13-20.

Deer, W. A., Howie, R. A., Zussman, J., 1962-1966, The rock forming minerals; 5 vol. New York: John Wiley and Sons Inc.

De Waard, D., 1970, The Anorthosite-Charnockite suite of rocks of Roaring Brook Valley in the eastern Adirondacks (Marcy Massif): American Mineralogist, v. 55, p. 2063-2075.

Engel, A. E. J., Itson, S. P., Engel, C. G., Stichney, D. M., Cray, E. J. Jr., 1974, Crustal evolution and global tectonics: A petrogenic view: Geological Society of America Bulletin, v. 85, p. 843-858.

Eugster, H. P., Wones, D. R., 1962, Stability relations of the ferruginous biotite-annite: Journal of Petrology, v. 3, p. 82-125.

Flinn, D., 1965, On the symmetry principle and the deformation ellipsoid: Geological Magazine, v. 102, p. 36-45.

Hsu, L. C., 1968, Selected phase relationships in the system Al-Mn-Fe-Si-O-H: A model for garnet equilibria: Journal of Petrology, V. 9, p. 40-83.

Hudleston, P. J., 1973, Fold morphology and theories of fold development: Tectonophysics, v. 16, p. 1-46.

Kisch, H. J., Warnaars, F. W., 1969, Distribution of Mg and Fe in cummingtonite-hornblende and cummingtonite-actionolite pairs from metamorphic assemblages: Contributions to Mineralogy and Petrology, v. 24, p. 245-269.

Klein, Cornelis Jr., 1968, Coexisting amphiboles: Journal of Petrology, v. 9, p. 281-330.

Leake, B. E., 1968, A catalog of analyzed calciferous and subcalciferous amphiboles together with their nomenclature and associated minerals: Geological Society of America Special Paper 98, 195p.

______, 1972, Garnetiferous striped amphibolites from Connemara, Western Ireland: Mineralogical Magazine, v. 38, p. 649-665.

Maercklein, D. R., 1974, Analysis of deformation at Jim Falls, Wisconsin: unpublished M. S. Thesis, University of Wisconsin, Milwaukee.

Miyashiro, A., Seki, Y., 1958, Enlargement of the composition field of epidote and piemontite with rising temperature: American Journal of Science, v. 256, p. 423-430.

Miyashiro, A., 1973, Metamorphism and metamorphic belts: New York: John Wiley and Sons Inc., 492 p.

Muller, G., Schneider, A., 1971, Chemistry and genesis of garnets in metamorphic rocks: Contributions to Mineralogy and Petrology, v. 31, p. 178-200.

Myers, P. E., Cummings, M. L., May, E. R., Kopp, R. A., Willis, R. P., Bergstrom, J. R., 1974, Guidebook: 38th Annual Tri-State Geological Field Conference, University of Wisconsin-Eau Claire.

Phillips, R., Layton, W., 1964, The calciferous and alkali amphiboles: Mineralgocial Magazine, v. 33, p. 1097-1109.

Ramsay, J. G., 1967, Folding and fracturing of rocks: New York: McGraw-Hill Book Company, 555 p.

Reesor, J. E., 1965, Structural evolution and plutonism in Valhalla gneiss complex, British Colombia: Geological Society of Canada, Bulletin 126, 123 p.

Ruotsala, A., P., Tufford, S. P., 1965, Chemical analyses of Igneous Rocks: Minnesota Geological Survey, Information Circular 2, 87 p.

Shido, F., 1958, Plutonic and metamorphic rocks of Nakoso and Iritono districts in the Central Abukuma Plateau: Tokoyo Daigaku, Rigakubu, Journal Part II, 11, p. 131-217.

______, Miyashiro, A., 1959, Hornblendes of basic metamorphic rocks: Journal of the Faculty of Science, Imperial University of Tokoyo, Section II, v. 12, 85-102.

Spry, A., 1969, Metamorphic textures: Oxford: Pergamon Press, 350 p.

Turner, F. J., Verhoogen, J., 1960, Igneous and Metamorphic Petrology: New York: McGraw-Hill Book Company, 672 p.

Turner, F. J., Weiss, L., 1963, Structural analysis of metamorphic tectonites: New York: McGraw-Hill Book Company, p.

Wager, L. R., Brown, G. M., 1967, Layered Igneous Rocks: San Francisco: W. H. Freeman and Company, 588 p.

Warner, Jeffrey, 1969, Fortran IV program for construction of PI diagrams with the Univac 1108 computer: State Geologic Survey, Kansas, Computer Contribution 33, 138 p.

Weiss, L., 1972, The minor structures of deformed rocks: New York: Springer-Verlag, 431 p.